2014

Novel Regulators in the Germline Stem Cell Niche of Drosophila Testis

Qi Zheng
University of Pennsylvania, zhqi777@gmail.com

www.manaraa.com

Novel Regulators in the Germline Stem Cell Niche of Drosophila Testis

Abstract

Stem cells are powerful and promising tools in regenerative medicine. Understanding how stem cells are maintained in vivo is crucial for their clinical application. Studies on various stem cell systems have demonstrated that the stem cell niche, or local tissue microenvironment, provides important extracellular cues to guide stem cell behaviors. The Drosophila male germline system has emerged as an exemplary model for studying stem cell-niche biology. The apically located hub cells function as a shared niche for two stem cell populations: germline stem cells (GSCs) and cyst stem cells (CySCs). A dominant model in the field describes hub cells as the single niche for GSCs via promoting JAK-STAT signaling. However, recent work from our lab has demonstrated that BMP signaling is the primary pathway leading to GSC self-renewal. We have also revealed that CySCs function as a second niche to govern GSC maintenance. In this thesis, we identify Magu as a novel regulator controlling GSC self-renewal. We show that Magu is expressed from hub cells, and specifically required for GSC maintenance. We also show that Magu acts as an extracellular BMP modulator through interaction with Dally-like, a heparan sulfate proteoglycan. Our characterization of Magu further emphasizes the importance of BMP signaling in male GSC maintenance.

Zfh1 is a transcription factor expressed in CySCs. Zfh1 is required for CySC maintenance, and can also induce ectopic GSCs non-autonomously. Thus, Zfh1 exerts an impact on two stem cell lineages, matching with our recent notion that CySCs function as both a stem cell and a niche for GSCs. To dissect out how Zfh1 controls stem cell self-renewal, we attempt to identify target genes of Zfh1 using two genome-wide approaches: ChIP-Seq and a genetic modifier screen. Preliminary results show that eya and shg may be direct targets of Zfh1, and CtBP is required for Zfh1 function. This ongoing project will further elucidate the dual role of CySCs, and advance our understanding of the complex niche signals regulating stem cells.

Degree Type
Dissertation

Degree Name
Doctor of Philosophy (PhD)

Graduate Group
Biology

First Advisor
Stephen DiNardo

Keywords
Drosophila testis, stem cell, stem cell niche

Subject Categories
Biology

NOVEL REGULATORS IN THE GERMLINE STEM CELL

NICHE OF *DROSOPHILA* TESTIS

Qi Zheng

A DISSERTATION

in

Biology

Presented to the Faculties of the University of Pennsylvania

in

Partial Fulfillment of the Requirements for the

Degree of Doctor of Philosophy

2014

Supervisor of Dissertation

_____

Stephen DiNardo, Ph.D., Professor of Cell and Developmental Biology

Graduate Group Chairperson

_____

Doris Wagner, Ph.D., Professor of Biology

Dissertation Committee

Erfei Bi, Ph.D., Professor of Cell and Developmental Biology
George Cotsarelis, M.D., Milton Bixler Hartzell Professor of Dermatology
Michael Granato, Ph.D., Professor of Cell and Developmental Biology
Scott Poethig, Ph.D., Patricia M. Williams Professor of Biology

ACKNOWLEDGMENT

First of all, I would like to thank my PhD advisor Dr. Stephen DiNardo, who is absolutely a phenomenal scientist and mentor. Without his patient guidance, continuous support, and tremendous understanding, this thesis cannot come to completion. His strong enthusiasm to science and dedication to his students always inspire everyone in the lab. I deeply appreciate his willingness to push me to be my best, and to spend time teaching me how to accomplish task on which I do not have expertise.

I am also very grateful to have an excellent thesis committee: Dr. Erfei Bi, Dr. George Cotsarelis, Dr. Michael Granato, and Dr. Scott Poethig. Their critical input and insightful suggestions promote me to become a better thinker and perform better science.

I feel quite fortunate to have a wonderful group of labmates. The interaction with each of them makes my time as a graduate student truly unforgettable. It is my great pleasure to be friends with all these lovely people, and I thank them for making my studying abroad life so pleasant and meaningful.

I want to thank Ms. Colleen Gasiorowski, the coordinator of the Biology Graduate Group. She is like an American mom for me at Penn. Her very caring personality and constant help support me to stay strong and keep my dream alive.

I also feel very lucky to get to know many other people at Penn. The senior Chinese researchers on the 12th floor of Biomedical Research Building always care about me, and I thank these aunts and uncles in the United States. My four lovely roommates have accompanied me well during the past six years. I thank them for living with me and sharing their life experiences with me. Many fellow graduate students have also become my invaluable friends. I thank them for the continuous concern and encouragement.

Last but not least, I want to thank my mom and dad, who are definitely the number one parents on the earth. They always believe in me and support me in every way they can. I owe a great deal to them. I want to say that if reincarnation does exist, I will not hesitate at all to be their daughter again!

ABSTRACT

NOVEL REGULATORS IN THE GERMLINE STEM CELL

NICHE OF *DROSOPHILA* TESTIS

Qi Zheng

Stephen DiNardo

Stem cells are powerful and promising tools in regenerative medicine. Understanding how stem cells are maintained in vivo is crucial for their clinical application. Studies on various stem cell systems have demonstrated that the stem cell niche, or local tissue microenvironment, provides important extracellular cues to guide stem cell behaviors. The Drosophila male germline system has emerged as an exemplary model for studying stem cell-niche biology. The apically located hub cells function as a shared niche for two stem cell populations: germline stem cells (GSCs) and cyst stem cells (CySCs). A dominant model in the field describes hub cells as the single niche for GSCs via promoting JAK-STAT signaling. However, recent work from our lab has demonstrated that BMP signaling is the primary pathway leading to GSC self-renewal. We have also revealed that CySCs function as a second niche to govern GSC maintenance. In this thesis, we identify Magu as a novel regulator controlling GSC self-renewal. We show that Magu is expressed from hub cells, and specifically required for GSC maintenance. We also show that Magu acts as an extracellular BMP modulator through interaction with Dally-like, a heparan sulfate proteoglycan. Our characterization of Magu further emphasizes the importance of BMP signaling in male GSC maintenance.

Zfh1 is a transcription factor expressed in CySCs. Zfh1 is required for CySC maintenance, and can also induce ectopic GSCs non-autonomously. Thus, Zfh1 exerts an impact on two stem cell lineages, matching with our recent notion that CySCs function as both a stem cell and a niche for GSCs. To dissect out how Zfh1 controls stem cell self-renewal, we attempt to identify target genes of Zfh1 using two genome-wide approaches: ChIP-Seq and a genetic modifier screen. Preliminary results show that eya and shg may be direct targets of Zfh1, and CtBP is required for

Zfh1 function. This ongoing project will further elucidate the dual role of CySCs, and advance our understanding of the complex niche signals regulating stem cells.

iv

TABLE OF CONTENTS

LIST OF TABLES

LIST OF FIGURES

CHAPTER ONE

CHAPTER TWO

CHAPTER THREE

CHAPTER FIVE

CHAPTER SIX

CHAPTER 1

General Introduction

Stem cells

Stem cells exist throughout development and adulthood. The hallmarks of stem cells comprise both self-renewal and differentiation (1). The characteristic of self-renewal allows stem cells to perpetuate themselves by proliferation, even after long periods of inactivity. Their ability to produce differentiated cells makes stem cells produce specialized progeny for the tissue, responding to either physiological disturbance or tissue damage.

Based on the differentiation potential, stem cells can be categorized into three types. The totipotent stem cell often refers to zygote, which has the ability to give rise to all cells of an organism (2). The power of totipotent stem cell is enormous, as an individual human zygote can develop into an adult with 37.2 trillion cells (3). A pluripotent stem cell is an embryonic stem cell, derived from the inner cell mass of an embryo (2). Embryonic stem cells can produce all cells of an embryo, but not extra-embryonic tissues (2). The last type of stem cell is the adult stem cell, which only generates the specialized cell types for the tissue it resides in. Adult stem cells are maintained throughout life, and have been identified in many body parts, including skin, gut, brain, liver, bone marrow, skeletal muscle, and testis (1). I will focus on adult stem cells for the rest of my discussion.

The first difficulty in studying stem cells is identifying that stem cells exist for a tissue, and determining where they reside. Genetic lineage tracing has become the gold standard of identifying stem cells (1). Cells in a living tissue are labeled with molecular markers, and the identity of differentiated cells generated by cell division is characterized. Alternatively, cells removed from a living animal are labeled in cell culture, and transplanted into another animal to examine whether their tissue of origin can be reformed *in vivo*.

The unique power of stem cells is the potential that they can be harnessed to repair damaged tissues or organs. However, a profound hurdle in such regenerative medicine is how to maintain and grow sufficient amount of stem cells *in vitro* efficiently. Thus, understanding how adult stem cells are maintained *in vivo* can provide us important clues to better manipulate them in cell culture.

Various models of stem cell maintenance have been identified. Historically, asymmetric cell division has been supposed as the key mechanism (4). This model argues that the division of stem cell is polarized as stemness determinants are distributed to the mother cell but not inherited by the differentiating daughter. A classical example of asymmetric cell division is *Drosophila* neuroblast (1). A series of proteins have been well characterized to explain how the polarity is established, the mitotic spindle is oriented, and the ultimate cell fate is determined (5). Asymmetric cell division has also been observed in several mammalian systems, but its mechanism and influence in stem cell maintenance is less well understood (5, 6). Recently, the dynein-binding protein Lis1 was implicated in regulating asymmetric division in hematopoietic stem cells. Loss of Lis1

causes defective spindle positioning and impaired inheritance of cell fate determinants, accelerating cell differentiation (7).

In recent years, accumulating evidence has demonstrated that symmetric division can play an important role in stem cell maintenance. Contrary to asymmetric division, symmetric renewal gives rise to two stem cells. In *Drosophila* testis, using live imaging and lineage tracing, two groups have independently reported symmetric division for germline stem cells (GSC) (8, 9). During steady state, the rate of symmetric division is very low, however, the frequency increases when GSC depletion is genetically induced or a cell adhesion molecule is ectopically expressed (8, 9). Thus, symmetric renewal is not prevalent under physiological condition, but becomes critical when tissue homeostasis is disturbed experimentally. In contrast to the fly testis, symmetric division occurs more frequently in mammalian systems under normal tissue turnover. These systems are often constantly cycling, including the mouse hair follicle, intestine, and testis (10-13). Symmetric division is usually combined with the model "neutral drift", which argues that stem cell maintenance is stochastic, and when a stem cell is lost, its neighboring stem cell can replenish the pool by producing two stem daughter cells (4, 5, 14). The identification of symmetric division reveals the dynamic nature of stem cell maintenance, and modifies the traditional view of invariant asymmetric renewal.

Whether tissue stem cells renew using mostly asymmetric or symmetric divisions, identifying the mechanisms at work is essential if we are to achieve the goal of better manipulating them in cell culture. Tissue maintenance by stem cells is even more complex. For example, the maintenance of stem cells is also contributed by their differentiating daughters via a process coined dedifferentiation (15). The cellular plasticity of the daughter cells allows them to be converted back to stem cells when necessary. In *Drosophila* testes and ovaries, when the original pool of GSCs was removed by transiently driving the differentiation factor Bam, differentiating germ cells can revert to GSCs (8, 16). The process of dedifferentiation has also been observed in mouse testis and intestine (10, 17). A most recent study also shows that committed epithelial cells lining mouse airway can regain stemness *in vivo* after airway basal stem cells are ablated (18). The mechanism by which differentiating cells can switch back into stem cells is not clear. As more studies progress, the mechanism of dedifferentiation will be further elucidated.

Stem cell niche

Regardless of the types of division used by tissue stem cells to renew the pool, one still has to identify mechanisms. Isolated stem cells often lose their capability of self-renewal outside the body. This suggests that tissues surrounding stem cells are also required for stem cell maintenance. Studies from many systems have demonstrated that the stem cell niche, or the local tissue microenvironment, provides important extracellular cues to guide stem cell behavior. There are two basic types of niche: the stromal niche

3

and the epithelial niche (1). Stromal niche consists of specialized cells. A canonical example of stromal niche is the post-mitotic distal tip cell for germline stem cells (GSCs) in *C. elegans* (19). Removal of distal tip cell by laser microsurgery causes all GSCs to differentiate (20). In contrast to niches composed of dedicated cells, an epithelial niche often lacks a dedicated set of support cells. Rather the niche is formed by basement membrane, which is composed of extracellular matrix located at the basal side of epithelial tissue. For example, in the *Drosophila* ovary, the basement membrane directly contacts somatic follicle stem cells, and controls stem cell behavior through integrin-mediated interaction
(21, 22). Due to complicated anatomical structure, the composition of mammalian stem cell niche often appears exceedingly complex and incompletely defined, even though the gross niche location is known (1). Take the best understood hematopoietic stem cell (HSC) niche as an example. After more than ten years of experimentation, a model of two distinct niches has been proposed: the endosteal niche houses quiescent HSCs, whereas the perivascular niche supports active HSCs. Previous studies have defined multiple niche components including sinusoidal endothelial cells, sympathetic nerve fibers, and cells of the osteoblastic lineage (23). Recent work identifies two new players: perivascular mesenchymal stem cells and macrophages, which are important to regulate the mobilization of HSCs between the two niches (23).

Niche cells often secrete cytokines, and regulate stem cells through signaling pathways (1). The focus of my thesis is how these extrinsic signals control stem cell behaviors. Thus, later in this chapter, I will discuss various signals using the *Drosophila* testis as a model. It is also interesting to point out that stem cells and their niche are often anchored to each other by adhesion molecules. In *Drosophila* ovary, E-cadherin is required for niche occupancy of the germline stem cell (GSC), and GSCs expressing more E-cadherin can outcompete wildtype stem cells (24, 25). Stem cell anchorage is crucial not only under physiological condition, but also during the trafficking of transplanted stem cells to the niche. For example, it has been demonstrated that integrin is required for transplanted hematopoietic stem cells and spermatogonial stem cells to home to the niche (26-29).

The stem cell system in *Drosophila* testis

The *Drosophila* testis has emerged as a valuable model to study adult stem cells (Fig.1). The existence and location of stem cells in the system have long been proposed since 1970s, based on electron microscopy studies and structural organization of spermatogenesis (30). However, the definitive identity of stem cells was not established until lineage tracing approach was applied. Using FLP/FRT-mediated recombination, Gönczy and DiNardo labeled individual somatic or germline cell with LacZ expression at the apex of the tubular testis. They demonstrated that the LacZ+ cell can not only remain in the presumptive stem cell location, but also produce progeny present in all stages of

4

spermatogenesis (31). Thus, there exist two stem cell populations in the testis: germline stem cells (GSCs), and accompanying cyst stem cells (CySCs). The two types of stem cells are radially arranged around the hub, a shared niche composed of post-mitotic somatic cells. Upon asymmetric division (32), GSC generates two daughter cells, one remains attached to the hub, and the other undergoes differentiation as a gonialblast (GB). GB divides mitotically four rounds with incomplete cytokinesis, giving rise to a cyst of 16 interconnected spermatogonia. Terminal differentiation is initiated in spermatogonia to produce spermatocytes, which then enter meiosis to generate 64 spermatids (33). Asymmetric division also occurs in CySCs (34), as one daughter cell stays associated with the hub and GSCs, whereas the other differentiates as a somatic cyst cell. A pair of differentiating cyst cells continues to embrace the cyst of spermatogoina. While encysted gonial cells undergo cell division, cyst cells do not divide any longer, they rather increase in size in order to accommodate the tremendous growth of germline cells.

The *Drosophila* testis has several unique advantages for studying stem cells. First, stem cell behavior can be investigated at a single cell resolution, since individual cells can be identified and genetically manipulated. In contrast, stem cell markers in mammalian systems are more ambiguous, and usually only identify a subpopulation of stem cells (1). Second, while the initial establishment of the stem cell niche is largely unknown for most vertebrate tissues, major advances have been made recently to elucidate the specification of hub cells as well as associated stem cells (35, 36). Understanding how a niche is first formed can promote new strategies of tissue engineering in regenerative medicine. Lastly, the seemingly simple fly testis share similarities with mammalian systems. The general stem cell architecture and steps of spermatogenesis are parallel between fly and mouse (37, 38). The recent finding that CySCs serve as an additional niche for GSCs, demonstrate the complex but elegant regulation in the system, similar to discoveries in mouse bone marrow and bulge of the hair follicle (39).

Signaling pathways function in *Drosophila* testis stem cell-niche system

As stated before, the niche provides crucial extrinsic signals to control stem cell behavior. The neatly defined testis system and the mature genetic manipulation methods in *Drosophila* have allowed the clear identification of cells either sending or receiving signals. The overarching goal of my thesis is to investigate how GSCs are maintained by signals emanated from the two distinct niche systems: the hub and CySCs. Therefore, below I will describe several signaling pathways identified in the field. Recent advances have uncovered the complexity in the testis, especially the importance of BMP signal and the niche function of CySCs (40-43). However, we are still at the beginning in deciphering cross-regulation among different cell types and relationship of different signaling pathways to each other.

- **The JAK-STAT pathway**

Two seminal papers identified the JAK-STAT pathway as a key for stem cell maintenance in the fly testis (44, 45). The secreted ligand Upd is expressed selectively from hub cells. The binding of Upd to its receptor Domeless on adjacent cells activates JAK and phosphorylates STAT (Fig.2A). The subsequent translocation of STAT to the nucleus activates target gene expression. The requirement of JAK-STAT for stem cell self-renewal was demonstrated by generating STAT mutant clones using mitotic recombination. STAT null GSCs lose stemness, and leave the hub to differentiate (44, 45). Direct target genes of STAT have not been reported. But effectors downstream of JAK-STAT have been identified in CySCs, and one of them is Zfh1, a zinc finger homeodomain transcription factor (to be discussed in more detail below) (42). Cells with sustained JAK-STAT activation also have high and sustained expression of Zfh1 (42).

JAK-STAT was thought to be required for the self-renewal of both GSCs and CySCs . This conclusion came from the fact that testes with STAT depletion in all cells lose both stem cell populations (44, 45). However, recent study has further dissected out the distinct roles of JAK-STAT on CySCs and GSCs. When STAT activity was restored specifically in the cyst lineage of *stat* mutant testes, functional GSCs were retained even though they were depleted for STAT (40). Therefore, JAK-STAT is not intrinsically required for GSC self-renewal. The rescued germ cells exhibited all the hallmarks of wildtype GSCs, except that they lost contact with the hub (40). Under wildtype conditions, E-Cadherin was enriched along the hub-GSC interface; however, E-Cadherin was delocalized in STAT-depleted GSCs prior to their loss from the hub (40). Thus, the primary role for the JAK-STAT pathway in germ cells regulates GSC anchorage to the hub.

In contrast to the germ line, CySCs do require JAK-STAT activation for self-renewal. CySCs mutated for *stat* are lost rapidly from the hub (42). JAK-STAT signaling is also sufficient to promote CySC fate, as sustained JAK-STAT activity in the cyst lineage causes ectopic CySCs (42, 46). Therefore, JAK-STAT plays different roles in the two stem cell populations: adhesion for GSCs, and self-renewal for CySCs. It is thought that Zfh1 is one downstream target of JAK-STAT, as Zfh1 can phenocopy all the functions of JAK-STAT in CySCs (42). However, whether Zfh1 is directly activated by STAT is not clear. The activation of JAK-STAT in CySCs is also fine tuned via SOC36E, an antagonist of the signaling. When SOC36E is suppressed, CySCs outcompete neighboring GSCs through stronger integrin-mediated binding to the hub (47). It has been shown recently that the active transcription of SOCS36E in CySCs is maintained by a histone demethylase dUTX (48).

JAK-STAT signaling also plays a role in dedifferentiation. By growing a temperature sensitive allele of *stat* under the restrictive temperature, Brawley and Matunis created a condition in which no stem cells existed (49). However, after shifting these stem cell-depleted testes to the permissive temperature to allow STAT restoration, stem cells reappeared adjacent to the hub (49). It has been shown that the restored stem cells are

6

derived from dedifferentiated spermatogoina (49). Although it is not understood how the differentiating cells find their way back to the hub, it is likely that with restored STAT activity, the capacity for adhesion to the niche is reestablished among these dedifferentiating gonial cells. Note that the study of dedifferentiation has been restricted so far to the effects on germline cells for technical reasons. Thus, we know little about how somatic cells (that are encysting the germline cells) dedifferentiate into new CySCs.

- **The BMP pathway**

The evolutionarily conserved BMP pathway is the second pathway identified in the field. The BMP ligands *dpp* and *gbb* are produced by hub cells and CySCs, and the pathway is activated in GSCs (50-52) (Fig.2B). Loss of BMP pathway components in GSCs causes premature differentiation (50-52). The direct targets of BMP pathway in GSCs are unknown, but Bam, a differentiation factor, is shown to be suppressed by BMP activation (50-52). As a consequence of this repression, Bam only becomes expressed in daughter cells of GSCs, and Bam function is necessary in these cells for their continued differentiation through the gonial amplification into spermatocyte development.

For a long time, the importance of BMP was disregarded compared to JAK-STAT. However, recent study has shown that BMP is the primary pathway controlling GSC self-renewal (40). As mentioned before, STAT-depleted GSCs can be retained if JAK-STAT signaling is activated normally in the cyst lineage. However, the cell non-autonomous effect of the cyst lineage JAK-STAT activation cannot be achieved if BMP activity was blocked by misexpressing extracellular BMP antagonist (40). Thus, BMP acts downstream of JAK-STAT to guide GSC maintenance.

- **The Hedgehog pathway**

Hedgehog signaling is another major developmental pathway, and it is also active in the testis. Similar to BMP, the requirement of Hedgehog is lineage-specific. Two labs have independently shown that the hub-generated ligand Hh is necessary for CySC maintenance, as cells mutant for pathway transduction fail to self-renew (46, 53) (Fig.2C). Ectopic Hh expression leads to a moderate increase of CySC number, but the extra CySCs are confined to the testis tip, and the differentiation in cyst lineage appears normal (46, 53). Therefore, sustained Hh promotes CySC proliferation, but not unlimited renewal (as STAT activation would). The relationship between Hh and JAK-STAT in CySCs has also been investigated. Cells that cannot transduce either Hh or JAK-STAT can still activate the other pathway normally (46), thus Hh and JAK-STAT act independently for CySC self-renewal, with the STAT pathway playing a more robust role.

- **The EGFR pathway**

Studies on EGFR signaling have demonstrated cross-talk between the two stem cell populations. The ligand Spitz is expressed from the germline cells, and as a consequence

the EGFR pathway is activated in the cyst lineage (54-56) (Fig.2D). In testes depleted for EGFR receptor function or mutated for Spitz, there are more GSCs present (54-56). By staining GSCs with markers for either M- or S-phase mitotsis, Parrot *et al.* discovered that GSCs were dividing more rapidly in *spitz* mutants (57). For example, when flies were fed with food containing DNA analogue BrdU, it took a shorter time for *spitz* mutants to have all GSCs labeled by BrdU (57). Thus, Parrot *et al.*concluded that GSCs in *spitz* mutants divided faster, causing the increased GSC number. This observation is specific to EGFR, as pertubation of other pathways does not result in increased division frequency (57). EGFR actiavtion normally occurs in the encysting cyst cells. Thus, the inreased proliferation among GSCs was due to something missing from the mutant somatic cells. The factor(s) has not been identified, but it might be that direct contact from somatic cells is necessary for normal developemnt. The enclosure of germ cells by somatic cells also appears abnormal when the EGFR pathway is defective in somatic cells. Depending on the mutant conditinon, the germ cells either lack associated cyst cells or are surrounded by multiple somatic cells (55, 58).

Additonally, the requirement for EGFR activiation in somatic cells further extends to transit amplifying spermatognial cells, as these cells continue to proliferate rather than undergo differentiation in EGFR mutant testes (54-56).

- **Questions that are going to be addressed in this thesis**

Taking what we have learned about niche signals for GSC maintenance, two important questions need to be addressed. One is about BMP signaling. It is clear that BMP is the primary pathway for GSC self-renewal, but we do not know how the signal is regulated extracullularly. To address this question, I characterized the role of a novel BMP modulator named Magu in the system. The other pressing issue in the field is how CySCs, the second niche for GSCs, control GSC behavior. Work from several labs including ours has identified four transcription factors (STAT, Zfh1, Chinmo, and Ken) that are expressed in CySCs and control GSC self-renewal non-autonomously. Understanding effectors downstream of these transcription factors can be breakthroughs in elucidating the molecular mechanism of CySC function. However, no target genes of any of these transcription factors have been reported. Therefore, I attempted to identify targets of Zfh1.

The *Drosophila* testis niche

hub= shared niche cells
GSC= Germline Stem Cell
CySC= Cyst Stem Cell= Somatic Stem Cell
Gb= Gonialblast, the daughter of GSC initiating differentiation
Cyst Cell= the daughter of CySC initiating differentiation
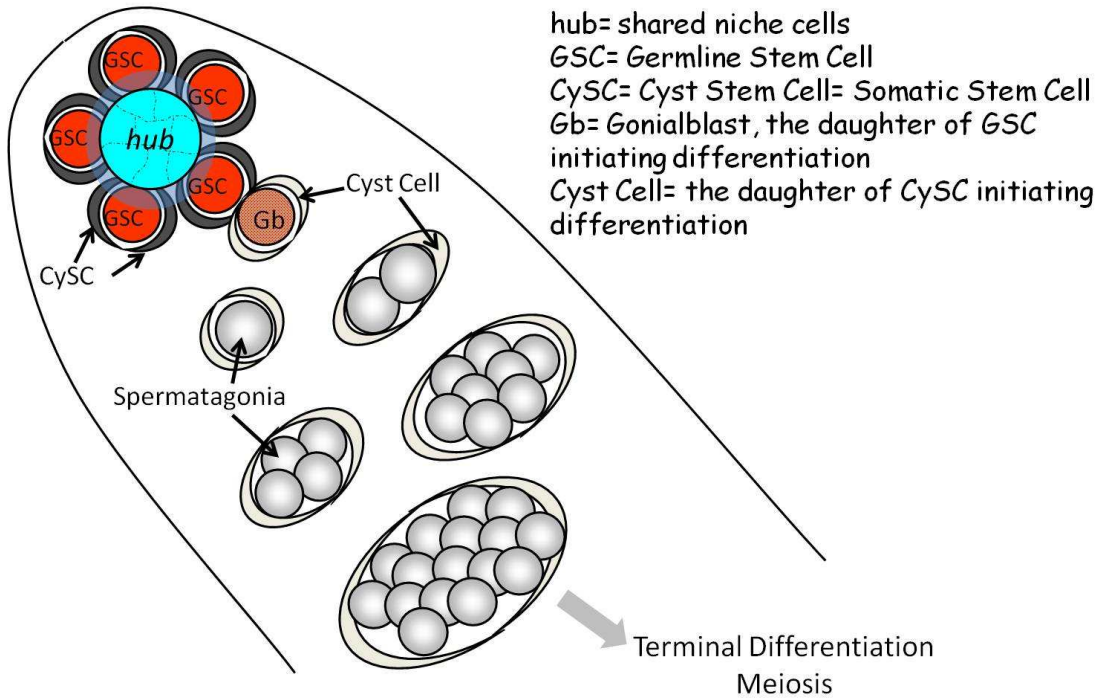
Figure 1. The stem cell system in *Drosophila* testis.
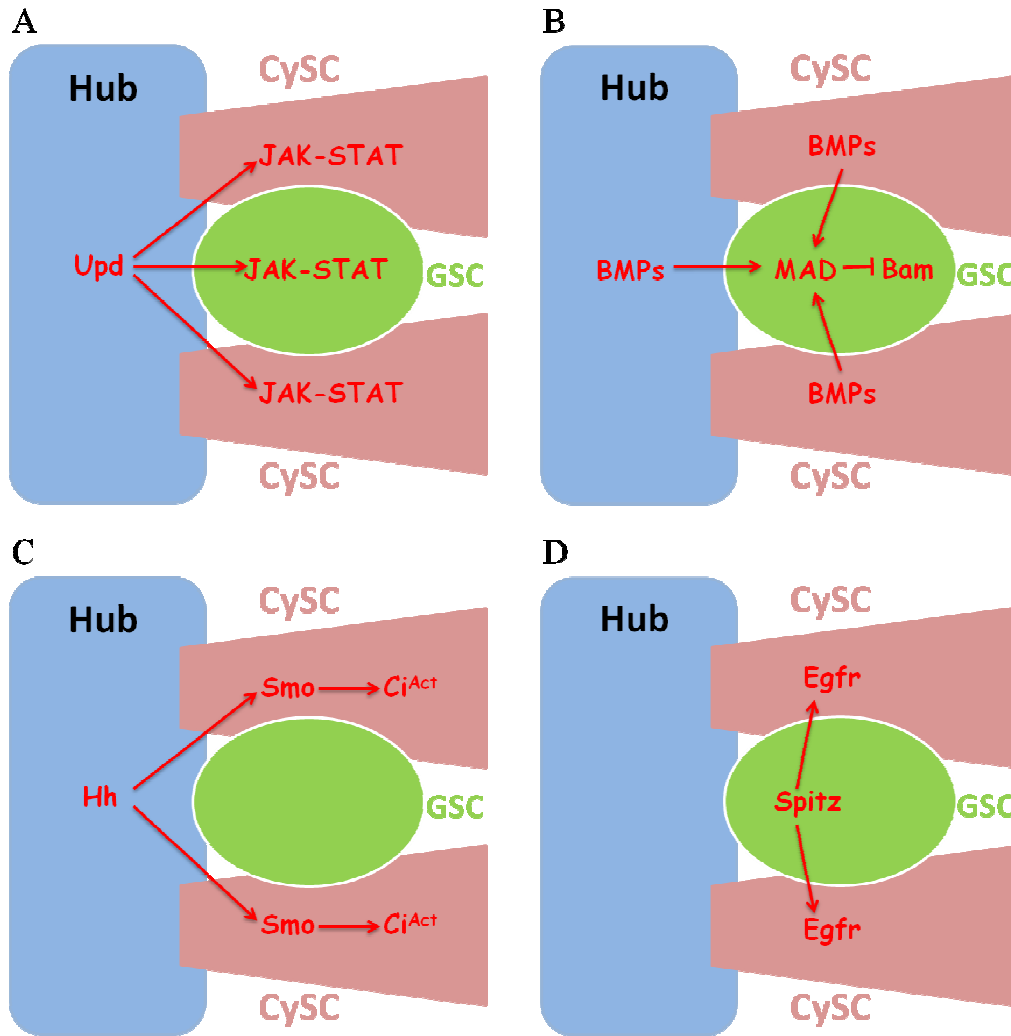
Figure 2. Signaling pathways function in *Drosophila* testis stem cell-niche system. (A) JAK-STAT (B) BMP (C) Hedgehog (D) EGFR. See text for details.

CHAPTER 2

magu is required for germline stem cell self-renewal through BMP signaling in the *Drosophila* testis*

Summary

Understanding how stem cells are maintained in their microenvironment (the niche) is vital for their application in regenerative medicine. Studies of *Drosophila* male germline stem cells (GSCs) have served as a paradigm in niche-stem cell biology. It is known that the BMP and JAK-STAT pathways are necessary for the maintenance of GSCs in the testis (44, 45, 50-52). However, our recent work strongly suggests that BMP signaling is the primary pathway leading to GSC self-renewal (40). Here we show that *magu* controls GSC maintenance by modulating the BMP pathway. We found that *magu* was specifically expressed from hub cells, and accumulated at the testis tip. Testes from *magu* mutants exhibited a reduced number of GSCs, yet maintained a normal population of somatic stem cells and hub cells. Additionally, BMP pathway activity was reduced, whereas JAK-STAT activation was retained in mutant testes. Finally, GSC loss caused by the *magu* mutation could be suppressed by overactivating the BMP pathway in the germline. Preliminary data suggests that Magu may modulate BMP signaling through interaction with Dlp, a heparan sulfate proteoglycan.

Introduction

Adult stem cells contribute a steady source of new cells to maintain many tissues, including skin, blood, intestine and the germline. A key hallmark of these cells is their ability to generate new stem cells as well as differentiating progeny. Maintaining a balance between self-renewal and differentiation is thereby crucial for tissue homeostasis. Studies on diverse stem cell systems have demonstrated that the stem cell niche, or the local tissue microenvironment, provides important extracellular cues for controlling this balance (59). Understanding the modulation of these cues and the signaling pathways they act upon is central focus of current research.

The *Drosophila* male germline system has emerged as an exemplary model for studying the biology of adult stem cells (60). Cells that comprise the niche have been conclusively identified, as have several niche signals that serve to maintain the stem cell pool (44-46, 50-53). The apical tip of the testis is occupied by a group of tightly packed, terminally differentiated somatic cells, called hub cells (30). Radially arranged around the hub are two intermingled sets of stem cells. One is a population of germline stem cells (GSCs), and the other is a population of somatic stem cells, called cyst stem cells (CySCs).

Generally, each GSC division is oriented (32), such that one daughter remains adjacent to the hub and to CySCs, thereby retaining stem cell character, while the other is pushed away, and will initiate differentiation as a gonialblast (Gb). After four rounds of mitosis, the Gb generates a cyst of sixteen spermatogonia, which then undergo differentiation into spermatocytes. The division of each CySC is also oriented (34), such that one daughter cell remains attached to the hub, and likely retains stem cell identity, while the other daughter, displaced away from the hub, becomes a differentiating cyst

12

cell. The cyst cell daughters withdraw from the cell cycle, and they continue to provide regulatory input to the encysted differentiating germ cells throughout spermatogenesis (61, 62).

Both hub cells and CySCs serve as a niche for GSCs (40, 42). It has been shown that BMP ligands are expressed from these two types of niche cells, and that they activate the BMP pathway in GSCs (50, 52). One output of pathway activation is repression of *bag of marbles* (*bam*) in GSCs, which would otherwise drive differentiation (50-52). Loss of BMP receptors or signal transducers in the GSCs causes de-repression of *bam* and precocious differentiation (50-52). Recently, Michel *et al.* develops a fluorescent reporter for the activation of BMP type I receptor Thickvein (63). Using this tool, they have demonstrated that BMP signals from the hub are specifically received at the hub-GSC interface, where adherens junctions locate (63).

The second signaling pathway active in the stem cell niche is the JAK-STAT pathway. Unlike BMPs, Unpaired (Upd), the JAK-STAT ligand, is only expressed from hub cells (44, 45). Upd activates the pathway not only in GSCs, but also in CySCs (40, 42, 44, 45). JAK-STAT activation appears important for adhesion of both GSCs and CySCs to the hub, but is only crucial for self-renewal of the CySCs (40, 42).

Although BMP signaling is required for GSC maintenance, research has heavily focused on JAK-STAT in stem cell self-renewal over the last several years. Part of the reason may be because induction of ectopic GSCs can be achieved by overactivating the JAK-STAT pathway, but not the BMP pathway (44, 45, 50-52). However, recent work from our lab demonstrates that the expansion of GSCs is not directly due to activation of JAK-STAT in GSCs, but rather due to JAK-STAT activation in CySCs, and the consequent enhanced expression of BMP ligands from CySCs (40). Therefore, it now appears that BMP is the primary pathway leading to GSC self-renewal, and it is imperative to dissect out the mechanism by which BMP signaling maintains GSCs.

In a previous microarray experiment performed by our lab, *CG2264* was identified as a gene exhibiting transcriptional enrichment in cells near the testis tip (64). Subsequently, Li and Tower reported that global ectopic expression of *CG2264*, which they named *magu*, led to an increased life span in both sexes and an increase in the fecundity of older females (65). Vuilleumier et al. have also identified *CG2264*, naming it *pentagone* (*pent*), and demonstrated, through loss- and gain-of-function experiments, that it was required for the proper graded activation of the BMP pathway during wing patterning (66). Interestingly, the Xenopus homologue of CG2264 has been shown to block BMP signaling during early dorso-ventral patterning of embryos (67).

Here, we will use *magu* as the name for *CG2264*. We report that *magu* is expressed from hub cells, and functions as a BMP modulator that specifically affects the GSC population. Our work emphasizes the importance of BMP signaling in male GSC maintenance.

13

Results

magu is expressed from hub cells

Using in situ hybridization, we visualized magu mRNA in the hub cells (Fig.1A). In our hands, *in situ* hybridization in testes did not have the resolution and reproducibility usually afforded in other tissues. We always observed signals among small cells clustered at tip (Fig.1A, arrowheads), and we concluded that these were hub cells. Due to the technical limitations, we could not rule out the possibility that *magu* is expressed in some somatic cells near the hub (in some CySCs). However, we have not observed any evidence of expression in large-profile cells surrounding the hub. Thus, we are confident that *magu* is not expressed in germline cells. Interestingly, *in situ* hybridization sometimes suggested that *magu* was expressed only from some hub cells, or to higher degree from some hub cells (Fig.1A, arrowheads).

To more definitively identify which cells express *magu*, we made use of a LacZ reporter line of *magu* (66). This reporter utilizes a 2 kilobase fragment that recapitulates *magu* expression in the developing wing disc (66). In the testis, we observed that *magu* expression was restricted to hub cells as shown by double-labeling with E-Cadherin (Fig.1B). Interestingly, the reporter was not expressed in all hub cells. It remains possible that some other regulatory region at *magu* drives expression in the remaining hub cells. However, since some of our *in situ* preparations also suggested non-homogenous expression from hub cells, perhaps *magu* is under temporal or spatial control, and under repression by BMP signaling (66). Indeed, mutation of Mad/Medea/Schnurri binding sites within the reporter fragment led to expression in most hub cells (Fig.1C). Collectively, our data suggest strongly that *magu* is expressed from hub cells, but potentially not from all hub cells equally.

magu encodes a putative matricellular protein, which is defined as a secreted protein that could regulate cell-matrix interactions. To investigate the localization of Magu, we raised antibodies against an N-terminal portion of Magu (Yiwen Wang). Sera from immunized rabbits showed specific immuno-reactivity on western blots to bacterially expressed, His-tagged Magu protein (Yiwen Wang, data not shown). After preabsorption using wildtype testes (see Materials and Methods), we observed an enriched pattern of puncta in the hub region (Fig.1D, D'). Magu accumulated along the interfaces among hub cells (Fig.1D upper inset), similar to FascIII. In addition, it was present along the interface between hub cells and stem cells (Fig.1D lower inset, arrowheads). Since this serum was effective only sporadically, we also explored the accumulation of Magu by using a second antibody, raised against a C-terminal peptide (66). This antiserum reproducibly exhibited an extended distribution of Magu relative to the hub, with strongly staining puncta appearing among stem cells and their daughters (Fig.1E, and insets; E', bracket). In addition, there was a more subtle enrichment in a ring along the hub cell-stem cell interface (Fig.1E lower inset and E', arrowhead), reminiscent of that obtained with the N-terminal antisera. These patterns were reduced significantly in testes bearing

14

mutations in *magu* (Fig.1F, F'). Since Magu is predicted to be a secreted protein, we attempted to visualize Magu under conditions where the antibody could only detect extracellular proteins (see Materials and Methods). Using the C-terminal antiserum (but not the N-terminal antiserum) a strong punctuate signal was observed only in optical sections above the hub (Fig. 1G), and this pattern disappeared in the *magu* mutant (Fig.1H). We do not know if the differences in accumulation pattern comparing the two antisera reflect differing distributions or availabilities of their respective epitopes. Nevertheless, these data are consistent with the model whereby *magu* is transcribed in hub cells, and its encoded protein secreted and accumulates in the vicinity of neighboring cells.

Generating *magu* mutants

In order to investigate the function of *magu*, we identified mutations among transposon insertion lines and generated null mutations by manipulating those lines (see Materials and Methods). Two insertions, KG02847b (KG) and d00269, were homozygous viable and exhibited no detectable phenotype. These insertions were mapped upstream of exon 3 of *magu* (Fig.2A). However, flies homozygous for the insertion e00439, or heteroallelic combinations of e00439 and f02256 were viable and exhibited both a wing vein defect (Fig3.B, C) and a testis phenotype. These PiggyBac insertions each mapped near the 3' end of exon 3 (Fig.2). To obtain potentially stronger mutant alleles, we generated deletions encompassing some or all of the genomic region containing *magu* (Yiwen Wang). Deletion mutant I lacked exon 3, which contained the *magu* translational start codon (Fig.2). More extensive deletions were generated from the KG insertion. Individual deletions removed the whole *magu* region downstream of KG, and extended from 15 to 374 kilobases downstream of *magu* (Fig.2). By comparing the strength of both the wing vein and testis phenotypes, we established that e00439 and deletion I behave as null alleles of *magu*, while f02256 is a strong loss-of-function allele.

Below I will first characterize the testis phenotype, and then touch on the wing vein defect in the later part of the Results section.

Magu is required for maintenance of GSCs

Compared with wildtype, *magu* mutant testes appeared thinner, containing fewer germ cells (data not shown). Since *magu* was expressed from hub cells, we tested whether a GSC defect might account for this phenotype. We scored GSCs by counting individual small-size germ cells attached to the hub. In one mutant condition, $magu^{e00439}/magu^{f02256}$, the median GSC number per testis was only 3, whereas the sibling control carried a median of 9 GSCs (Fig.4A, B; Table 1). Moreover, *magu* mutant testes displayed germ cells with branched fusomes next to the hub (Fig.4D arrowhead), indicating they were differentiated and no longer *bona fide* stem cells. We found a similarly dramatic reduction in the median number of GSCs for other *magu* mutant combinations (Table 1). We also noticed that there was variation in phenotypic strength.

15

For a given allele, or allele combination, some mutant testes were devoid of all GSCs, while others retained some GSCs. As a measure of this, we also calculated the percentage of testes with GSCs for each genotype. That fraction depended on the genotype and growth condition used in a particular experiment (Table 1).

We took two approaches to confirm that the defect in GSC maintenance indeed resulted from mutation of *magu*. First, the transposon insertion, e00439, was remobilized to establish a revertant line (Yiwen Wang). We found that GSCs were substantially restored in flies carrying this revertant chromosome placed over the f02256 mutant (Table 1). While there remained a slight difference in the median number of GSCs retained in the revertants compared to controls, all revertant testes now retained GSCs. Second, we attempted to rescue the GSC defect by restoring *magu* expression in the mutant background. To accomplish this, we used the hub cell driver *upd*-Gal4 to express *magu* containing either an N-terminal (V5) (66) or C-terminal (Myc) epitope tag. To promote continued and robust expression using the Gal4-UAS system, young adults were aged at 29°C for either 3 days or 12 days before analysis. We scored both median GSC number, and the fraction of testes maintaining GSCs. Using both measures, we obtained statistically significant, but incomplete rescue. Among mutant siblings from these crosses, it was common that more than half of the testes contained no GSCs. When either N-terminal V5- or C-terminal Myc-tagged *magu* was expressed in the mutants, the fraction of testes with GSCs increased to more than 50%, and sometimes approached or equaled 100% (Table 1) Restoration of V5-*magu* also increased the median number of GSCs for both younger and older flies (Fig.4E; Table 1). But restoration of *magu*-Myc only led to an increase in median GSC number for older flies (Table 1). This was the case using several different UAS-*magu*-Myc or GFP transgenic insertion lines (data not shown). Thus, the slightly different behavior of N-terminal versus C-terminal rescuing construct might be due to a difference in inherent activity of the proteins produced. We observed a similar difference in rescuing ability for the wing vein defect of *magu* mutants (Fig.3D, E). In spite of the difference in transgene effectiveness, collectively, the data demonstrate that Magu is required for normal GSC number in the adult testis.

The loss of GSCs was also observed in *magu* mutant gonads from the 3rd instar larvae (Table 1). But the phenotype in gonads was much less severe than in adult testes, because the median GSC number per mutant gonad was much higher, and all mutant gonads still retained some GSCs (Table 1). This suggested that Magu plays a dominant role in adult GSC maintenance. To test this hypothesis, we conducted a so-called cohort experiment, in which GSC numbers were counted in *magu* mutants at different developmental stages. Animals dissected at a later stage were siblings of those processed earlier. We hoped to minimize any phenotype variation by conducting the experiment in this controlled way. We found that GSC number was normal in 1st instar larvae gonads of *magu* mutants, but progressively reduced in 3rd instar larvae gonads and testes (Table 2). This demonstrated that Magu does not affect GSC establishment, even though it was

16

expressed in embryonic gonads (data not shown). It also confirmed that Magu functions during larva development, and it is possible that the more severe phenotype observed in mutant testes is an accumulation effect due to continuous loss of Magu since an earlier stage.

To further dissect out from which larva stage Magu starts to play a role in GSC maintenance, we designed an experiment called larva shift experiment. We wanted to compare the rescue extent in *magu* mutants, for which ectopic Magu expression was turned on at different time points during larvae development. We hypothesized that if the function of Magu begins right after GSC specification, then mutant cohorts with Magu activation started earlier would have a higher GSC number compared to those started later. To achieve this, *magu* mutants were initially grown at 25°C. One cohort containing 1st and 2nd instar larvae (early shift), and another cohort with 3rd instar larvae and early pupae (late shift), were moved to 29°C to allow the maximum expression of ectopic Magu by Gal4-UAS system. Eclosed young adult flies were further aged at 29°C for 3 more days before analysis. It turned out that the rescue efficiency was not statistically different in the two cohorts (Table 3). This suggested that Magu may not function until the late stage of larval development. However, there was a caveat for this conclusion. Since the GSC number in sibling control testes was also lower than normal (Table 3), we suspected that the presence of the transgene *upd-Gal4* could result in GSC reduction at 29°C for unknown reason (we also noticed this in *magu* RNAi experiments, data not shown). This may add a complexity to the larva shift experiment, as the longer animals with *upd-Gal4* were aged at 29°C, the more likely their GSC numbers would get reduced.

Magu does not affect CySC or hub cell number

In the normal testis, GSC self-renewal depends on CySCs and hub cells (40, 42). Thus the loss of GSCs that we observed in *magu* mutant testes could be a secondary effect attributed to either CySCs or hub cells. To determine whether there are any defects among CySCs in the *magu* mutants, we analyzed the number of CySCs by staining for Zfh1, an essential CySC marker (42). In contrast to the GSCs, significant numbers of Zfh1-expressing cells were still present in the mutant (Fig.5B; Table 4). These cells were arranged more compactly around the hub, presumably because they now occupied the space vacated by the loss of GSCs (Fig.5A, B). To investigate whether CySCs in the mutants function properly, we marked cycling cells by S phase labeling using Edu. The ratio of Edu and Zfh1 double positive cell number to Zfh1 single positive cell number in the mutants was indistinguishable from that in the sibling controls (Fig.5C, D arrowhead; Table 4), indicating that the mutant CySCs cycle properly. To further confirm the undifferentiated state of CySCs in mutant testes, we examined Eya expression as a marker for cyst cell differentiation (Fig.6). The small-sized cyst cells close to hub did not express Eya (Fig.6B, B'). We occasionally noted some Eya positive cyst cells near the hub in *magu* mutants (Fig.6C arrowhead, C'). But these cells were much larger,

17

suggesting they were late-stage cyst cells, associated with spermatocytes, that had failed to be pushed away from the hub due to the reduced production of germ cells. Thus, taken together with their expression of Zfh1 and cell cycling behavior, we conclude that these cells were *bona fide* CySCs.

To test whether Magu affects the maintenance of the hub, we counted hub cell numbers using the cell biological hub marker FascIII (Fig.5E, F). We found *magu* mutants contained a similar number of hub cells compared to sibling controls (Table 4). To determine whether these hub cells were capable of functioning properly, we asked whether they expressed a key niche signal, *upd*. Indeed, *upd* was expressed normally in *magu* mutant testes, and there was no difference in the number of *upd* positive hub cells comparing mutants and sibling controls (Fig.5G, H; Table 4). Thus we conclude that the loss of GSCs in *magu* mutants is not secondary to depletion or defect of either of the essential niche cell types, the CySCs or hub cells.

What pathways might Magu use to control GSC maintenance?

At the time of this work, the major signaling network in the establishment and maintenance of GSCs involved the JAK-STAT pathway (44, 45, 68). As shown in Fig.4H, *magu* mutants did not affect the expression of Upd, a key JAK/STAT-activating ligand expressed from hub cells. To test whether *magu* mutants affect activation of the STAT pathway, we analyzed the accumulation of STAT protein. In control testes, STAT accumulated among the first tier of cells surrounding the hub (Fig.7A). This represented STAT accumulation in both nearby germ cells and somatic cells (the GSCs and CySCs). In *magu* mutants, which have a normal complement of CySCs and occasionally have some remaining GSCs, STAT accumulated in cells surrounding the hub in a similar pattern to wildtype (Fig.7B). Therefore Magu does not appear to affect STAT pathway activation.

Once we ruled out involvement in JAK-STAT signaling, we sought clues for Magu function by further analyzing its role during wing patterning.

Magu also affects the specification of the 5th longitudinal wing vein L5

The wing vein defect in *magu* mutants was predominantly a failure in the patterning of L5, the 5th longitudinal wing vein (Fig.3B, C, arrowhead). Since so much is known about the patterning of wing veins, we thought clues for the function of Magu in testes might come from also investigating its role in vein development.

The development of *Drosophila* wing veins starts on wing imaginal discs during larval stages. The primordial longitudinal veins (L1 to L5) are already specified and identifiable on the 3rd instar larval wing blade (Fig.8A, copied from Fig.1A Blair 2007). To investigate whether *magu* is expressed during wing vein specification, we performed an *in situ* hybridization experiment. The expression of *magu* was mainly visualized in peripheral cells on wing blade, including regions around L5 (Fig.8B, arrow). *magu*

18

expression also appeared in the notum region of the wing disc (Fig.8B, arrowhead). To further test whether Magu affects the specification of L5, we examined the vein patterning on *magu* mutant wing discs. Delta is a marker for three longitudinal veins L3 to L5, whereas DSRF marks all intervein cells. For sibling control wing discs, L5 was scorable in all 9 samples by Delta staining (Fig.8C, arrow), and 7 out of 11 samples by DSRF (Fig.8D, arrow). In contrast, we observed that L5 could only be unambiguously identified in about 3 out of 20 *magu* mutant discs by either Delta or DSRF staining (Fig.8D, F, arrow). Therefore, we concluded that Magu affected the specification of L5.

It has been shown that the BMP signaling pathway is required for L5 specification. Interestingly, the mutant phenotype of the BMP ligand *gbb* resembles that seen in *magu* mutants (69-71). Thus we hypothesized that Magu also affects BMP signals in the wing. The most straight-forward way to test this hypothesis was to examine BMP activation on *magu* mutant discs. However, we had difficulty achieving high enough signal-to-noise pMad staining on wildtype discs initially. Therefore, we decided to test the expression of Abrupt, a L5 organizer that functions downstream of BMP activation (72). In sibling control testes, the staining of Abrupt nicely marked L5 (Fig.8G, arrow), in a pattern sharply complementary to that of DSRF (data not shown). However, in *magu* mutant discs, the staining of Abrupt was less clear (Fig.8H, arrow), showing an overlap with DSRF (data not shown). This result supported the idea that Magu might affect BMP pathway in L5 patterning.

We were interested to know whether Magu plays a role on the BMP signal-sending or receiving side. To investigate this, we induced *magu* mutant clones in heterozygous wing discs. The idea was that if Magu functions on the signal-receiving side and acts only locally, a defect in L5 region would be observed when the mutant clones cover the responding cells. While we could successfully generate *magu* mutant clones, we could not detect L5 defect by either DSRF or Abrupt staining (data not shown). This is consistent with the fact that Magu is predicted to be a secreted protein. Surrounding wildtype cells would supply Magu to the mutants.

We aborted our further analysis of wing patterning with publication of the Vuilleumier *et al*. paper in which the role of Magu in wing vein patterning was characterized nicely. They showed that Magu is necessary for proper transport of the BMP ligands; without Magu, BMPs cannot properly reach the disk region for L5 specification (see Discussion).

Magu affects GSC maintenance through the BMP signaling pathway

Our preliminary data on wing vein patterning suggested that Magu may be involved in BMP signaling. In fact, the BMP pathway has been shown to that is required for GSC maintenance is BMP (40, 50-52). To test whether Magu affects this pathway, we examined the activation of Mad, a transducer of BMP signaling. In several tissues, the accumulation of phosphorylated Mad (pMad) can be used as a read-out of BMP pathway

activation. We never observed pMad staining among germ cells surrounding the hub in *magu* mutant testes (Fig.7D). However, we could not conclude that BMP pathway activation was compromised because we found it difficult to observe pMad staining consistently in the GSCs of control and wildtype testes. In our hands, only occasionally would control testes present with pMad accumulation among the tier of germ cells surrounding the hub (Fig.7C). In contrast to that inconsistency in testes, gonads from 3rd instar larvae reproducibly showed pMad staining (Fig.7E). In gonads from *magu* mutants, we never observed pMad accumulation in germ cells surrounding the hub (Fig.7F), suggesting strongly that BMP pathway activation was compromised in *magu* mutants. In passing, we noted two characteristics of pMad accumulation in control larval gonads. First, in some gonads, not all the GSCs were positive (data not shown). Second, we often observed pMad accumulation in the second tier germ cells (Fig.7E, arrowheads), likely gonialblast progeny of the GSCs. This suggests occasional, more broad BMP pathway activation than previously reported.

To confirm the apparent diminution of BMP signaling in *magu* mutants, we examined a presumed target of BMP activation, the *bam* gene, whose expression is repressed in BMP-signaled cells. We used a *bam* promoter-GFP transgene (*bam*-GFP) (73) as a read-out for pMad activity. Consistent with a defect in BMP activation in *magu* mutants, *bam*-GFP was enriched in some germ cells attached to the hub (Fig.7H, arrowhead), while it was expressed only in amplifying gonial cells in control testes (Fig.7G). This data supports the hypothesis that Magu affects BMP signaling.

To further demonstrate the involvement of Magu in BMP signaling pathway, we conducted a genetic interaction experiment to test whether transheterozygotes of *magu* and *gbb* would have a reduced number of GSC. Gbb is a BMP ligand in *Drosophila*. It has been shown that Gbb plays an essential role for male GSC maintenance in testes, and *gbb[1]* is a null allele of *gbb*. As shown in Table 5, the reduction in GSCs was observed in younger flies of *magu[f02256]*/+; *gbb[1]*/+, as well as older flies of *magu[e00439]*/+; *gbb[1]*/+.

If *magu* was indeed required for proper BMP activation in germ cells, constitutive activation of the BMP pathway in the germline could bypass the requirement for *magu*. To accomplish this, we expressed an activated form of BMP type I receptor Thickvein (TkvA) using the germ cell driver, *nanos*-Gal4:VP16. Indeed, this raised the fraction of testes with GSCs from 63% to 100% (Table 1). The median GSC number also doubled compared to that observed in mutants (Fig.7J; Table 1). Thus intrinsic activation of the BMP pathway in germ cells can bypass the need for *magu*. This result is consistent with a simple model that GSCs are lost because BMP activation is compromised in *magu* mutants.

magu encodes a secreted protein, expressed selectively from hub cells, and accumulating among cells nearby. Our data suggests that Magu is necessary for proper BMP activation within adjacent germ cells. BMP ligands appear to be produced by both hub cells and CySCs, but not by germ cells (50, 52). To test whether *magu* must be co-

expressed with BMP ligands for its proper function, we attempted to rescue the GSC defect using the germ cell driver *nanos*-Gal4:VP16. Indeed, we observed a statistically significant increase in median GSC number in such testes (Fig.4F; Table 1). This suggests that *magu* does not need to be co-expressed with BMP ligands to be effective, and likely acts in the extracellular environment.

Magu may interact with Dlp in testes

Vuilleumier *et al*. also suggested that Magu interacts directly with Dally, a HSPG (heparan sulfate proteoglycan) (66). Interestingly, Dally and its homologue Dally-like (Dlp) are also important for male GSC maintenance (74, 75). Furthermore, it had been reported that Dlp was specifically expressed in hub cells, consistent with a major role for GSC maintenance ((75), Fig.9E, E'). I undertook extensive effort to verify the expression pattern of Dlp. I never observed selective accumulation of Dlp among hub cells. For example, Dlp appeared at low levels among all cells at the tip of the testes (Fig.9A, B), and not restricted to hub cells (Fig.9A', B'; white). I even stained fruit fly testes from different genetic backgrounds, including the one used in the Hayashi *et al.* paper (Oregon R, Fig.9B, B'). We communicated these (negative) observations to the authors, and they, too, cannot confirm their published description.

While expression enrichment was not observed, the previous authors' genetic analysis still stood. Since *dlp* and *dally* were required for GSC maintenance, we took two approaches to test the possible interaction of Magu and HSPG in testes. The first involved genetic interaction experiments between *magu* and *dally*, *dlp* or two other genes needed for HSPG biosynthesis. However, we did not observe any difference in GSC numbers between heterozygous *magu* mutants and transheterozygotes of *magu* and HSPG mutants (Table 6).

The other attempt was to rescue *magu* mutants by overexpressing Dlp. When ectopic Dlp was expressed in germ cells using *nanos-Gal4 UAS-dlp-GFP*, the fraction of testes retaining GSCs among *magu* mutants was indeed increased (Table 7). However, the expression pattern of ectopic Dlp appeared different in control and mutant. Dlp-GFP accumulation as visualized by GFP staining was enriched only at the hub cell-GSC interface in sibling control testes (Fig.10A', arrow). In contrast, Dlp protein appeared more diffused in *magu* mutant testes, in a punctate distribution, and often surrounding GSCs (Fig.10B', arrow). This suggested that the location of Dlp is Magu-dependent.

Since Magu was expressed from hub cells, to further confirm the diffused location of Dlp in *magu* mutant, we overexpressed *dlp-GFP* from hub cells using *hh-Gal4*. Because Magu was an extracellular protein, we also chose to examine extracellular Dlp proteins by staining non-permeabilized testes. In sibling control testes, Dlp was mainly enriched along hub-GSC interfaces (Fig.11A', arrow). In *magu* mutant testes, the accumulation of Dlp was not restricted to the hub-GSC interface, but also accumulated among hub cells (Fig.11B', arrow). Interestingly, in some mutant testes, the extracellular Dlp staining

21

extended beyond hub cells, and appeared to embrace somatic cells next to the hub (Fig.11C, arrow). Since there was no extracellular Magu protein present in the mutants (Fig.1H), these results suggest that extracellular Magu may be functional in the testis, regulating the localization of secreted Dlp.

Magu may not interact with Perlecan, Type IV Collagen, and Integrin

Because Magu was predicted to be a matricellular protein, we wanted to know whether Magu could interact with other extracellular matrix (ECM) proteins. To visualize the ECM, we stained testes using antibodies against either Perlecan or Type IV Collagen, two major components of basal lamina. We observed that both proteins accumulated under the sheath of testes (Fig.12A, C). Occasionally, they also exhibited as a hazy staining or two layers at the tip of testes (Fig.12A, C, arrow). This was expected, as EM micrographs have shown that the hub is anchored to the tip through a convoluted layer of basal lamina (Hardy, 1979). In most *magu* mutant testes, we did not observe a defect of basal lamina (data not shown). But sometimes, the Perlecan staining appeared thicker in mutants. In the most severe case, the sheath of testes seemed delaminated, and the ECM arced further into the testes (Fig.12B, arrow). We did not think this phenotype was a primary defect in *magu* mutants. The protruding ECM could be layers of muscle and pigment cells from the sheath of testes. These layers were usually as prominent in wildtype testes, as they were tightly pressed to each other with basal lamina by the plentiful cells inside testes. Since *magu* mutants had fewer germ cells, the testes might not be stretched as much, thus the different layers of the sheath became more distinguishable. To further test the possible interaction of Magu and ECM proteins, we co-stained extracellular Magu and Type IV Collagen in wildtype testes, but did not observe an overlap (Fig.12D). Thus we concluded that Magu does not interact with basal lamina proteins.

Another possible role of an ECM protein is that it regulates signal transduction pathways through interactions with cell-surface receptors like Integrin. To test this possibility for Magu, we examined the location of βPS-Integrin in sibling control and *magu* mutant testes. The staining appeared in somatic cells in both genotypes (Fig. 12E, E'). Since Magu specifically affects GSC maintenance, we concluded it unlikely that Magu acts through Integrin.

A *magu* RNA

WT

B LacZ

*magu*frgII-LacZ

C LacZ

*magu*frgIIΔS-LacZ

D

WT

E

magu/+

F

magu

D' anti-Magu-N-term

E' anti-Magu-C-term

F' anti-Magu-C-term

G anti-Magu-C-term (extracellular)

magu/+

H anti-Magu-C-term (extracellular)
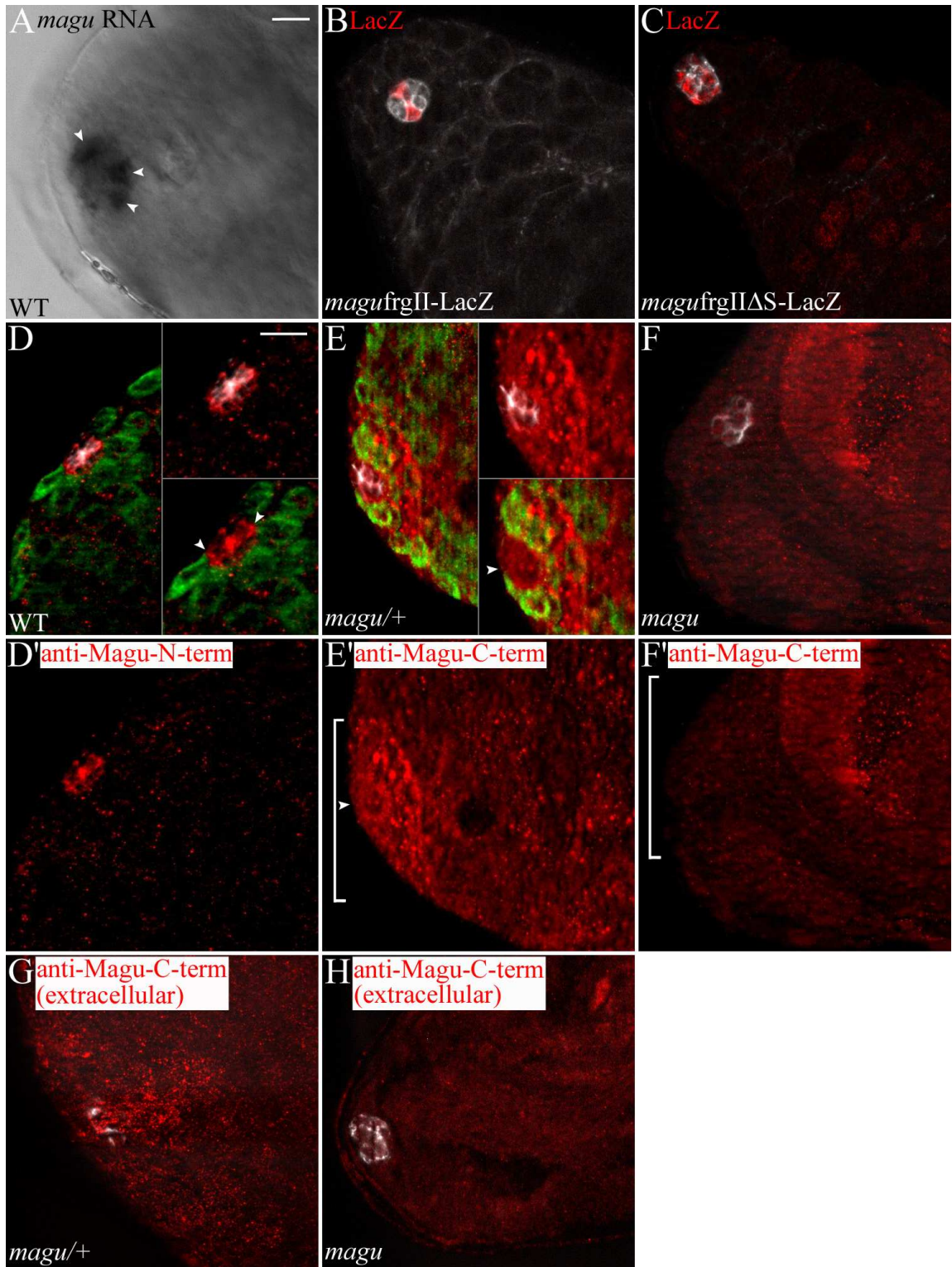
magu

Figure 1. *magu* is expressed from hub cells. The genotype for WT is *w1118*, for *magu/+* is *magu*^{deletionI}/*CyOKrGFP*, and for mutant is *magu*^{deletionI}/*magu*^{deletionI}. Hub (E-Cadherin in B and C, FascIII in other panels, white); germ cells (Vasa, green). (A) *In situ* hybridization revealing *magu* RNA in hub cells. RNA was enriched toward the portion of hub cells that faces the stem cell tier (arrowheads). (B and C) The lacZ expression (LacZ, red) in flies transgenic for *magu* reporter line frgII-lacZ (66) revealed the expression of *magu* in a few hub cells (B), whereas expression driven by a mutated version of frgII-lacZ (frgIIΔS-lacZ) (66) was expanded into almost all hub cells (C). This suggests that BMP pathway is active in these cells. The expression in spermatogonia far away from the testis tip in C was spurious. (D and D') *magu* protein exhibited an accumulation in the hub region, as visualized by anti-Magu-N-term (D and D', red). The expression was not only in the interface between hub cells (D upper inset), but also presented along the hub cell-germ cell interface (D lower inset, arrowheads). (E-F') Using another antibody (anti-Magu-C-term, (66)), Magu accumulated in a broader domain around the hub (E upper inset, and E' red inside the bracket). The expression appeared to be a circle along the interface of hub cell and germ cells (E lower inset and E', arrowheads). The accumulation was highly reduced in magu mutant testes (F, and F' red inside the bracket). The signal also presented in late stage spermatogonia and cyst cells in both sibling control and *magu* mutant testes (data not shown). Thus it must be due to cross-reaction with non-Magu epitopes. (G and H) The extracellular Magu, visualized by applying anti-Magu-C-term (66) prior to fixation, exhibited an enriched punctate pattern in areas near the hub (G, red). This dotted staining disappeared in the *magu* mutant (H).
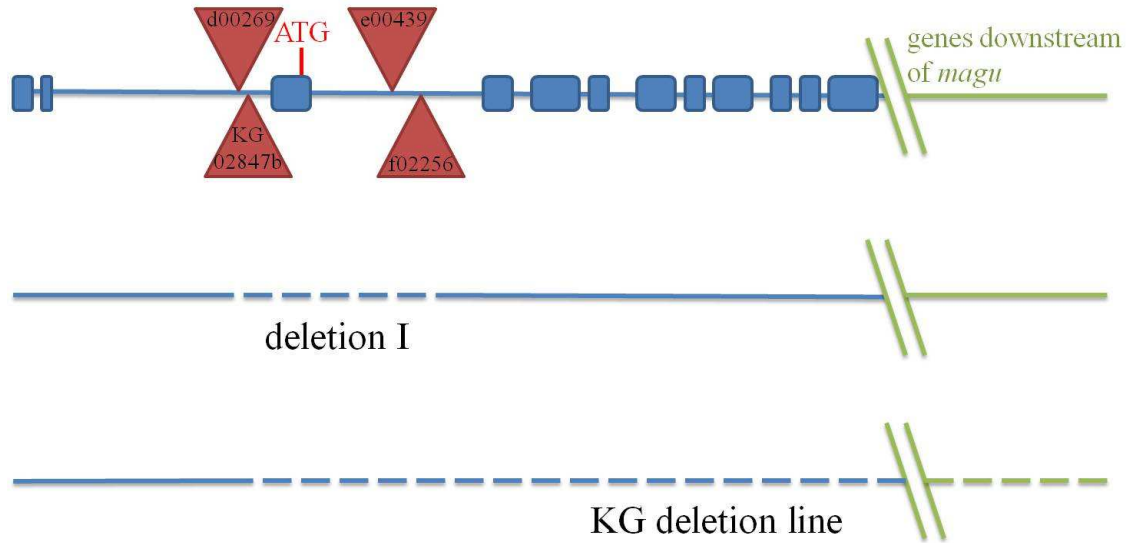
Figure 2. *magu* gene structure and mutants. The map of *magu* is shown in blue with exons denoted by rectangles, and genes downstream of *magu* are represented in green. Positions of transposable elements used to create deletion mutants are denoted by red triangles. The deleted sequences are indicated by dashed lines. Deletion I lacks the sequence between the PiggyBac insertions d00269 and f02256, which contains exon 3 and the translational start codon. Extent of deletions in KG deletion line begins from KG02847b to at least 15 kilobases downstream of *magu*.
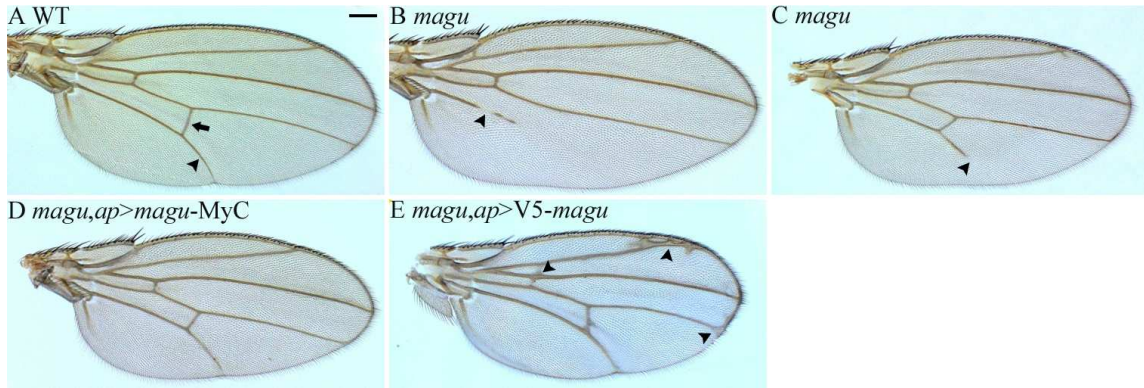
Figure 3. *magu* mutants also exhibit wing phenotypes. The genotype for mutant is *magu*[e00439]/*magu*[f02256]. (A-C) Compared with *w1118* (A, arrow and arrowhead), the *magu* mutants exhibited a truncated 5th longitudinal vein (B and C, arrowhead), and loss of posterior crossvein (B). The wing size was also reduced in *magu* mutants (C). (D and E) The wing vein defects were restored when Magu was ectopically expressed in the dorsal domain of wing discs. The genotypes were *magu*[e00439]/*magu*[f02256]*ap*-Gal4;UAS-Magu-Myc(D), and *magu*[e00439]/*magu*[f02256]*ap*-Gal4;UAS-V5-Magu (E). Notice overexpressing V5-Magu also caused some gain-of-function phenotypes, for instance the excess veins (E, arrowheads), indicating this transgene is stronger than UAS-Magu-MyC.
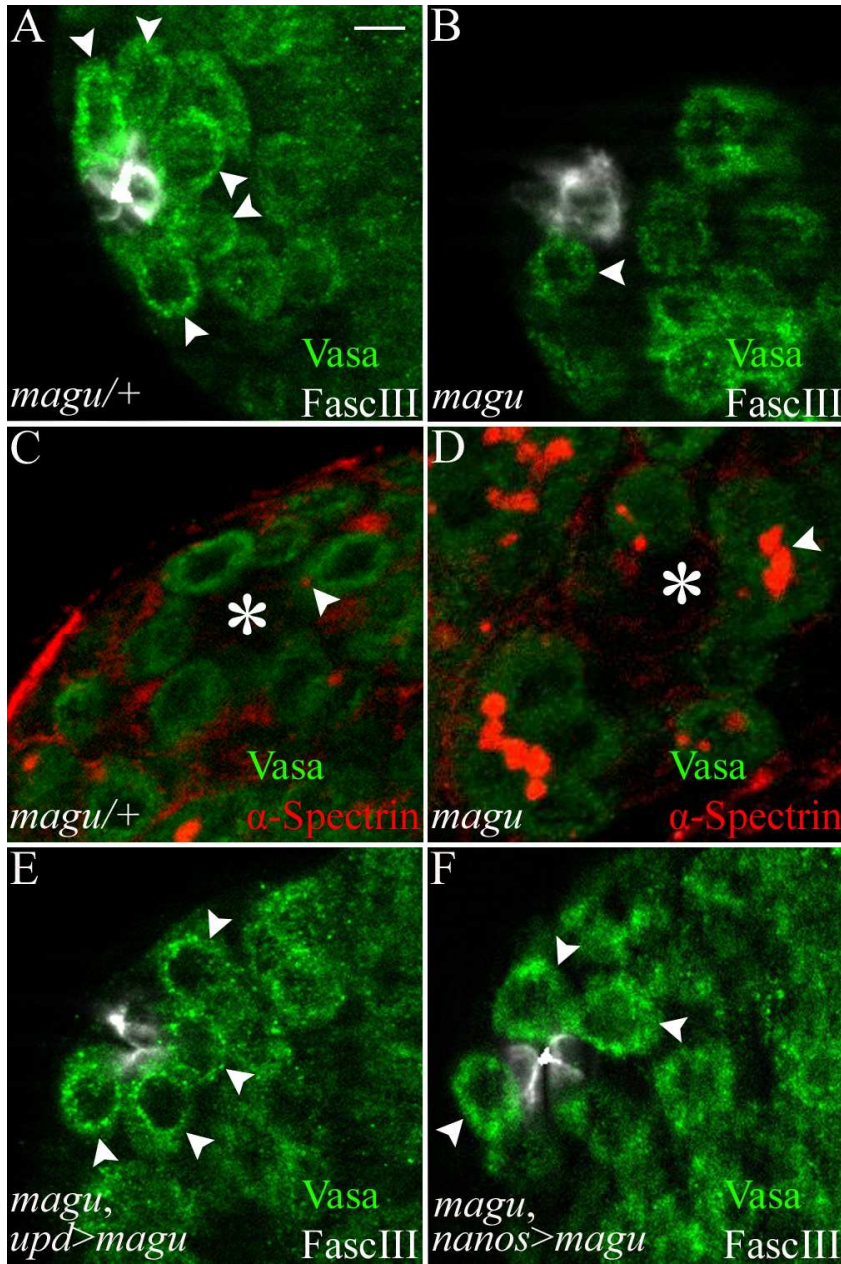
Figure 4. GSCs are lost in *magu* mutants. The genotype for *magu/+* is *magu*[e00439] or *magu*[f02256]/ *CyOkr-Gal4UAS-GFP*, and for mutant is *magu*[e00439]/*magu*[f02256]. Hub (FascIII or asterisk, white); germ cells (Vasa, green); fusome (α-Spectrin, red). (A and B) A control testis tip exhibited five GSCs attached to the hub (A, arrowheads), while the tip of a *magu* mutant testis carried one remaining GSC (B, arrowhead). (C and D) The dotted fusome, unique to GSCs, was present in an individual germ cell adjacent to the hub in a *magu/+* testis (C, arrowhead), whereas branched fusomes, a character of differentiated cells, were located in a cyst of germ cells directly contacted to the hub in a *magu* mutant (D, arrowhead). (E and F) Overexpression of Magu in either hub cells (E) or germline (F) resulted in ectopic GSCs next to the hub in the mutants.

27

Table 1. *magu* affects GSC maintenance

Condition	Genotype [a]	Median GSC #	IQR [b]	Min - Max [c]	P value [d]	% of Testes w/GSCs	P value [e]
0-3 days, 25°C (unless noted)	*magu*[e] or [f] /*CyO* [f]	8 (19) [g]	8 - 10	6 -13		100	
	magu[e] /*magu*[f]	3 (21)	2 - 4	0 - 7	<0.01	76	NA [h]
	magu[e] or [delI] /*CyO*	7 (10)	7 - 7.8	6 - 9		100	
	magu[e] /*magu*[delI]	0 (10)	0 -1.5	0 - 6	<0.01	30	NA
	magu[KG delI] or [f] /*CyO*	10 (10)	9.3 - 11	8 - 12		100	
	magu[KG delI] /*magu*[f]	2.5 (10)	0 - 4	0 - 5	<0.01	60	NA
	magu[delI] /*CyO* [i]	9 (13)	7 - 10	6 - 13		100	
	magu[delI] / *magu*[delI] [i]	6 (10)	5.3 - 7.8	4 - 9	<0.01	100	NA
	magu[eREV] or [f] /*CyO*	9 (8)	8 - 9	5 - 10		100	
	magu[eREV] /*magu*[f]	7 (10)	6 - 8	4 - 9	<0.05	100	NA
aged at 29°C for 3 days [j]	*upd-Gal4*; *magu*[e] /*magu*[f] ; *MKRS*	0 (23)	0 - 3.5	0 - 6		43	
	upd-Gal4; *magu*[e] /*magu*[f] ; *UAS-V5-magu*	4 (21)	3 - 5	1 - 7	<0.01	100	<0.01
	upd-Gal4; *magu*[e] /*magu*[f] ; *MKRS*	0 (27)	0 - 3	0 - 6		44	
	upd-Gal4; *magu*[e] /*magu*[f] ; *UAS-magu-Myc*	3 (25)	0 - 4	0 - 8	>0.1	64	<0.01
aged at 29°C for 12 days [j]	*upd-Gal4*; *magu*[e] /*magu*[f] ; *MKRS*	0 (12)	0 - 0.3	0 - 3		25	
	upd-Gal4; *magu*[e] /*magu*[f] ; *UAS-V5-magu*	4 (12)	2.8 - 4	2 - 5	<0.01	100	<0.05
	upd-Gal4; *magu*[e] /*magu*[f] ; *MKRS*	0 (11)	0 - 0	0 - 0		0	
	upd-Gal4; *magu*[e] /*magu*[f] ; *UAS-magu-Myc*	3 (17)	2 - 4	0 - 5	<0.01	94	NA
0-5 days, 25°C	*magu*[e] /*magu*[f] ; *MKRS*	3 (18)	2 - 4	0 - 6		83	

28

	magu[e] /*magu*[f] ; *nanos-Gal4/UAS-magu-Myc*	4 (15)	3 - 5	2 - 7	<0.05	100	>0.05
	magu[e] /*magu*[f] ; *MKRS*	2 (13)	0 - 4	0 - 5		62	
	magu[e] /*magu*[f] ; *nanos-Gal4/UAS-magu-GFP*	4 (17)	3 - 4	2 - 6	<0.05	100	<0.01
0-3 days, 25°C	*magu*[e] /*magu*[f] ; *MKRS*	2.5 (16)	0 - 4	0 - 6		63	
	magu[e] /*magu*[f] ; *nanos-Gal4/UAS-tkvA*	5 (25)	3 - 6	1 - 8	<0.01	100	<0.01

[a] Alleles used: [e]=[e00439]; [f]=[f02256]; [eREV]= [revertant of e]; [del I]=[deletionI]; [KG del]=[KG deletion].

[b] interquartile range = Quartile 3 - Quartile 1 (Q[3] - Q[1]), Q[3] = the 75th percentile, Q[1] = the 25th percentile.

[c] Minimum - Maximum, representing the spread of GSC numbers observed

[d] Calculated by Mann-Whitney test.

[e] Calculated by Chi-square test.

[f] *CyOkr-Gal4UAS-GFP*

[g] Number of testes scored in parentheses

[h] Not Applicable

[i] GSC number scored in gonads from 3rd instar larvae.

[j] Animals (0-3 days of age) raised at 25°C were shifted to 29°C for 3 or 12 days.

29

Table 2. Cohort Experiment

Condition	Genotype [a]	Median GSC #	IQR [b]	Min - Max [c]	P value [d]
1st instar larvae	*magu*[delI] / *CyOGFP*	7 (11) [e]	6 - 9	5 - 9	
	magu[delI] / *magu*[delI]	7 (17)	6 - 8	5 - 9	>0.05
3rd instar larvae	*magu*[delI] / *CyOGFP*	12.5 (6)	11.3 - 13	10 - 13	
	magu[delI] / *magu*[delI]	6 (12)	5 - 7	5 - 8	<0.01
0-6 days adult flies	*magu*[delI] / *CyOGFP*	11 (15)	10 – 11.5	9 - 12	
	magu[delI] / *magu*[delI]	0 (17)	0 - 0	0 - 8	<0.01

[a] Allele used: [del I]=[deletionI].
[b] interquartile range = Quartile 3 - Quartile 1 (Q[3] - Q[1]), Q[3] = the 75th percentile, Q[1] = the 25th percentile.
[c] Minimum - Maximum, representing the spread of GSC numbers observed
[d] Calculated by Mann-Whitney test.
[e] Number of testes scored in parentheses

Table 3. Larva Shift Experiment

Condition	Genotype [a]	Median GSC #	IQR [b]	Min - Max [c]	P value [d]	P value [e]
early shift[g]	*upd-Gal4; magu[e] /magu[f]; MKRS*	2 (7) [f]	1.5 - 2.5	0 - 5		
	upd-Gal4; magu[e] /magu[f]; UAS-V5-magu	4 (12)	2.3 - 5	2 - 6	<0.05	
	upd-Gal4; magu[e] or [f]/CyO; MKRS	4 (8)	0 - 4	0 - 5		
	upd-Gal4; magu[e] or [f] /CyO; UAS-V5-magu	5.5 (10)	5 - 7	4 - 8	<0.01	
late shift[g]	*upd-Gal4; magu[e] /magu[f]; MKRS*	1 (5)	1 - 2	0 - 2		0.46
	upd-Gal4; magu[e] /magu[f]; UAS-V5-magu	3.5 (10)	3 - 6	2 - 6	<0.01	
	upd-Gal4; magu[e] or [f]/CyO; MKRS	4 (9)	3 - 4	2 - 5		
	upd-Gal4; magu[e] or [f] /CyO; UAS-V5-magu	5 (9)	5 - 6	2 - 8	<0.05	

[a] Alleles used: [e]=[e00439]; [f]=[f02256].

[b] interquartile range = Quartile 3 - Quartile 1 (Q[3] - Q[1]), Q[3] = the 75th percentile, Q[1] = the 25th percentile.

[c] Minimum - Maximum, representing the spread of GSC numbers observed

[d] Calculated by Mann-Whitney test.

[e] Calculated for early and late shift rescue samples.

[f] Number of testes scored in parentheses

[g] 1st and 2nd instar larvae (early shift) or 3rd instar larvae and early pupae (late shift) raised at 25°C were moved to 29°C until eclosion. Adult flies (0-3 days of age) continued grown at 29°C for 3 days.
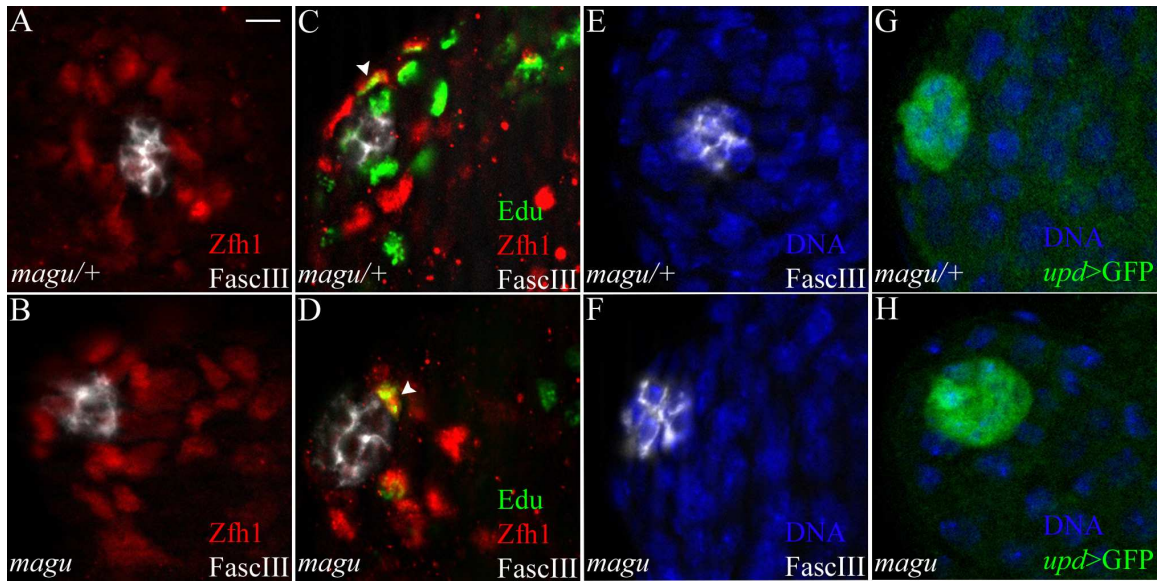
Figure 5. CySCs and hub cells are maintained in *magu* mutants. The genotype for *magu/+* is *magu*[e00439] or *magu*[f02256]/*CyOkr-Gal4UAS-GFP*, and for mutant is *magu*[e00439]/*magu*[f02256]. Hub (FascIII, white); CySCs (Zfh1, red); cycling cells (Edu in B and F, green); DNA (Hoechest, blue). (A and B) The number of CySCs in *magu/+* (A) and mutant (B) testes was similar. (C and D) *magu* mutant CySCs (D, arrowhead) divided normally as *magu/+* (C, arrowhead). (E and F) Visualized by FascIII and DNA stainings, the number of hub cells appeared similar in *magu/+* (E) and mutant (F) testes. (G and H) Using another marker (*upd*>GFP, green), the hub cell number in *magu/+* (G) and mutant (H) was also similar.

Table 4. magu does not affect CySCs or hub cells

	Genotype [a]		P value
	magu[e]/*magu*[f]	Sibling Control	(Student's T-Test)
Average CySC number [b]	21.7 ± 1.0 (16) [c]	21.9 ± 1.0 (14)	>0.5
S-phase index for CySCs [d]	0.2 ± 0.03 (10)	0.2 ± 0.01 (10)	>0.5
Average hub cell number [e]	9.6 ± 0.4 (20)	9.9 ± 0.5 (17)	>0.5
Average hub cell number [f]	7.8 ± 0.5 (19)	8.0 ± 0.5 (20)	>0.5

[a] Alleles used: [e]=[e00439]; [f]=[f02256]; Sibling control=*magu*[e] or [f]/*CyOkr-Gal4UAS-GFP*

[b] CySC number was scored in 0-4 day adults at 25°C.

[c] Number of testes scored in parentheses

[d] The fraction of EdU+ Zfh1+ cells to total Zfh1+ cells, in 1-4 day adults at 25 degree.

[e] Hub cell number was scored using FascIII and DNA staining, in 0-3 day adults at 25°C.

[f] Hub cell number was scored using Upd-Gal4 UAS-GFP and DNA staining, in 0-3 day adults grown at 25°C and aged at 29°C for 3 days.
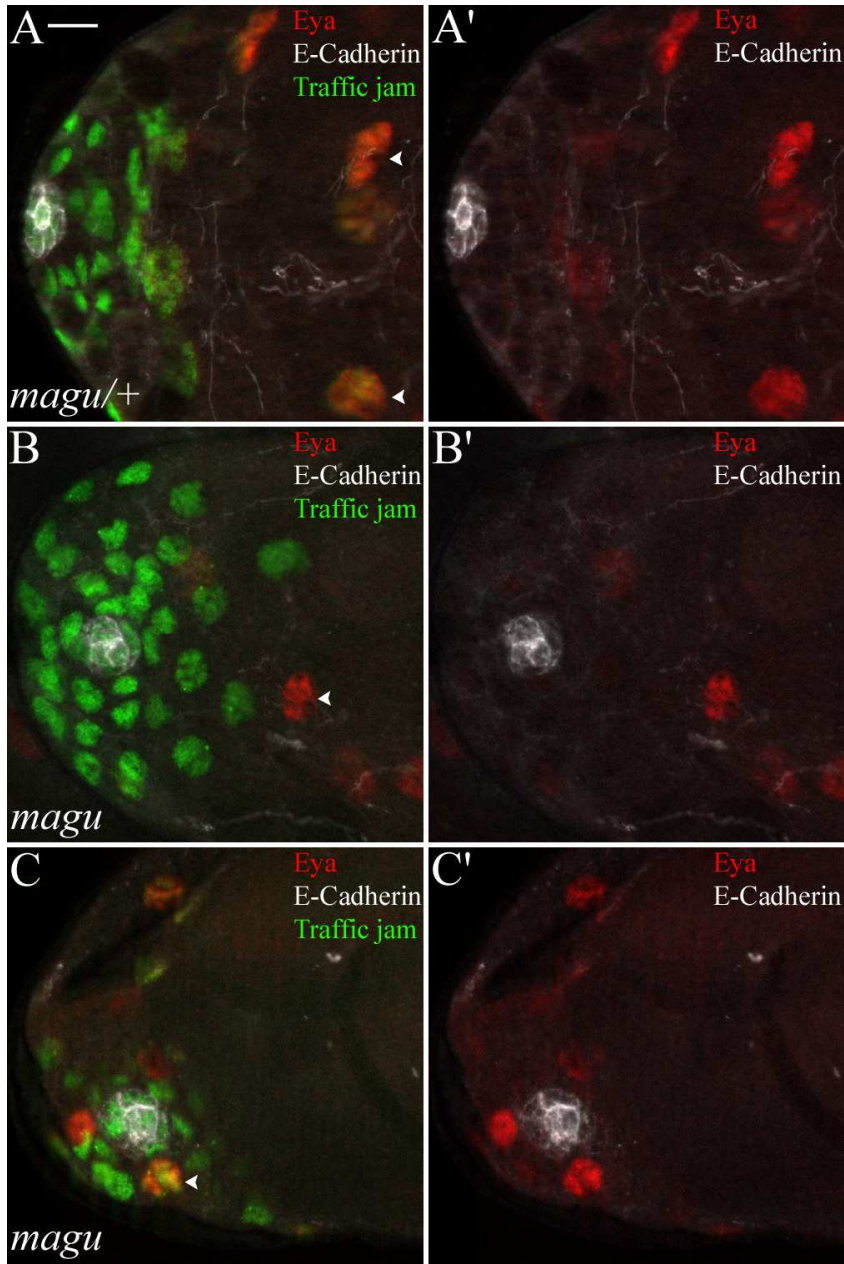
Figure 6. The CySCs in *magu* mutants are not differentiated. The genotype for *magu/+* is *magu*deletionI/*CyOKrGFP*, and for mutant is *magu*deletionI/*magu*deletionI. Hub (FascIII, white); somatic cells (Traffic jam, green); and differentiated cyst cells (Eya, green). (A-B') Similar to *magu/+* (A' arrowheads), the differentiated cyst cells in mutant testes presented far away from the hub (B', arrowhead). The somatic cells close to the hub, including CySCs, were not differentiated (A and B, green). Notice the differentiated cells had a larger size than undifferentiated somatic cells. (C and C') The larger-sized differentiated cells occasionally appreared next to hub cells in *magu* mutants (C', arrowhead)
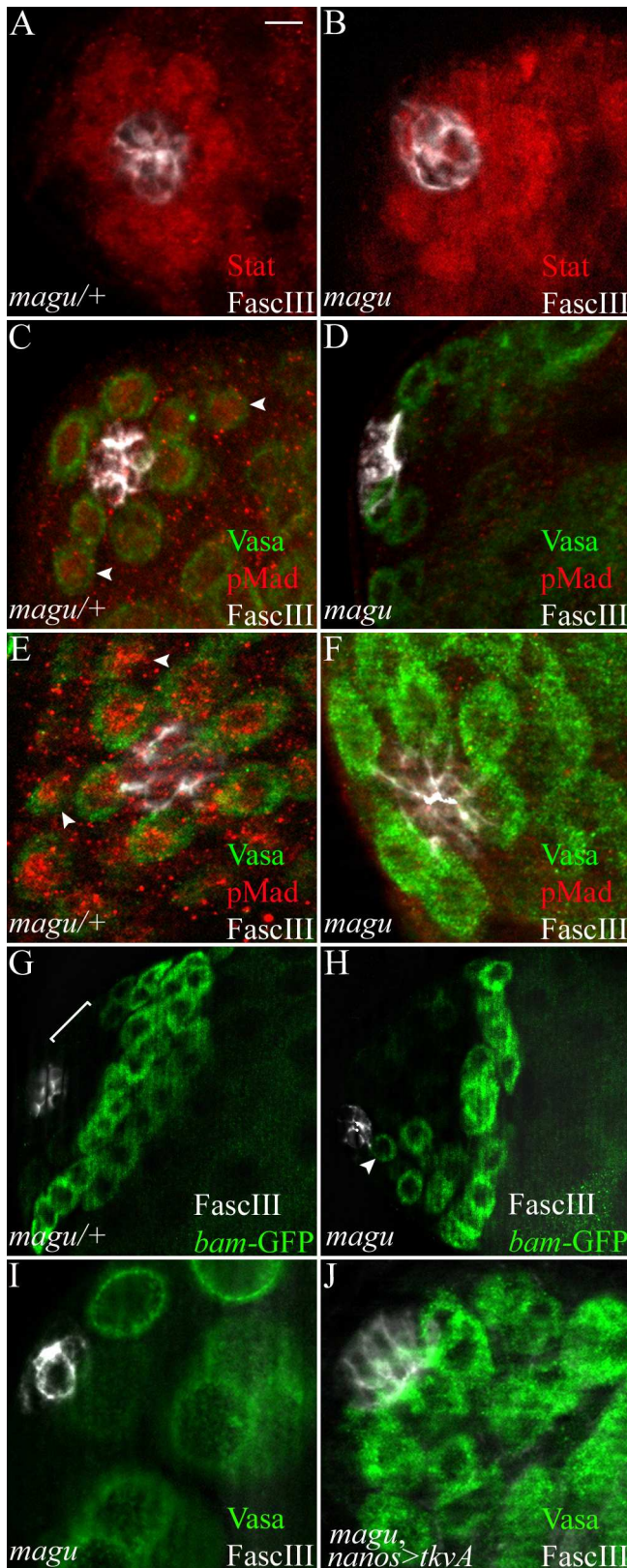
Figure 7. BMP signaling is impaired in *magu* mutants. The genotype for *magu/+* is *magu*deletionI/ *CyOKrGFP* in A and E, *magu*e00439 or *magu*f02256/*CyOKrGFP* in C, and *magu*e00439*bam-GFP*/*CyOKrGFP* in G. Correspondingly, the genotype for mutant is *magu*deletionI/*magu*deletionI in B and F, *magu*e00439/*magu*f02256 in D, and *magu*e00439*bam-GFP*/*magu*f02256 in H. Hub (FascIII or E-Cadherin, white); germ cells (Vasa, green). (A and B) The activation of JAK-STAT signaling (Stat, red) remained unchanged in mutant testes (B) compared to *magu/+* (A). (C-F) The activation of BMP pathway (pMad, red) was reduced in *magu* mutant GSCs (D and F) as compared to *magu/+* (C and E). C and D were adult testes, and E and F were gonads from 3rd instar larvae. Notice the BMP signal was not restricted to GSCs, but also appeared in gonialblasts (C and E, arrowheads). (G and H) The tip of a *magu/+* testis exhibited high *bam* expression in spermatogonia away from the hub (G), whereas a *magu* mutant testis tip showed *bam* expression in the germ cell adjacent to the hub (H, arrowhead). (I and J) GSCs were restored in *magu* mutants when BMP signaling was overactivated in the germline (J).

A — 3rd Instar LarvaWing Disc / Wing blade

B — *magu* RNA

C — *magu*/+ — Delta (vein) — L3, L4, L5

D — *magu* — L3

E — *magu*/+ — DSRF (intervein) — L4, L5

F — *magu* — L4, L5?

G — *magu*/+ — Abrupt (L5) — L5

H — *magu* — L5?
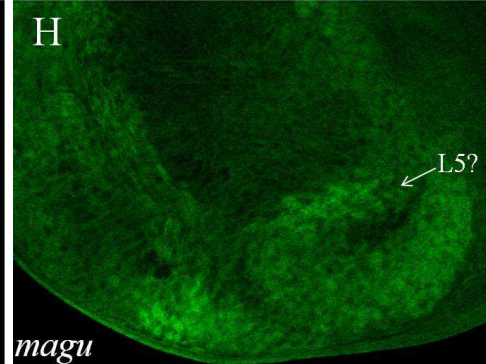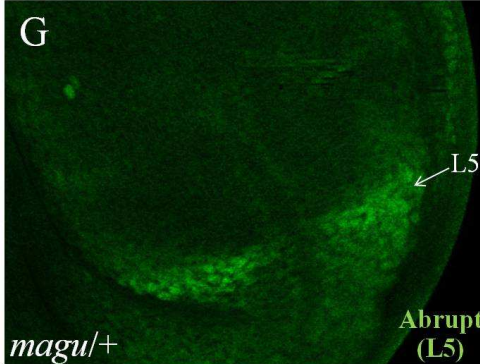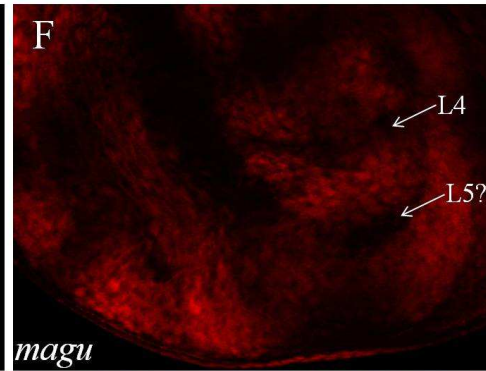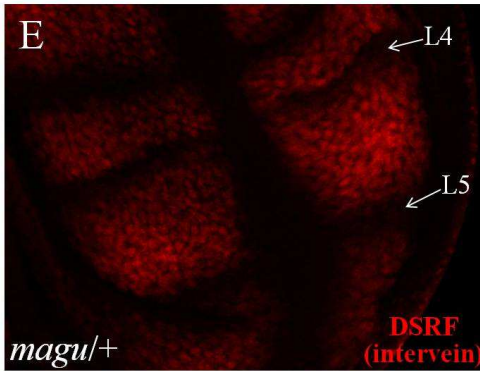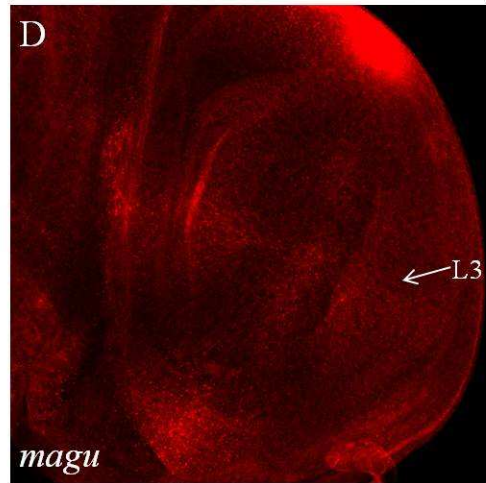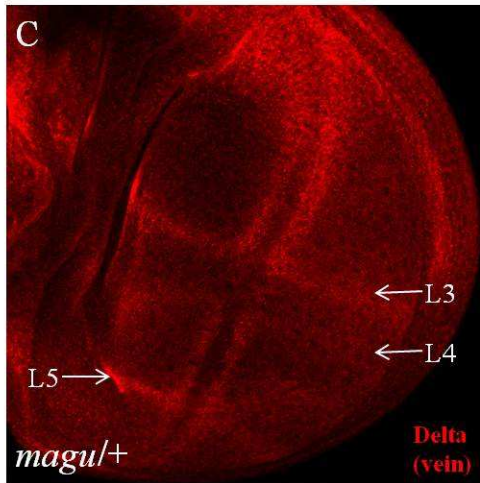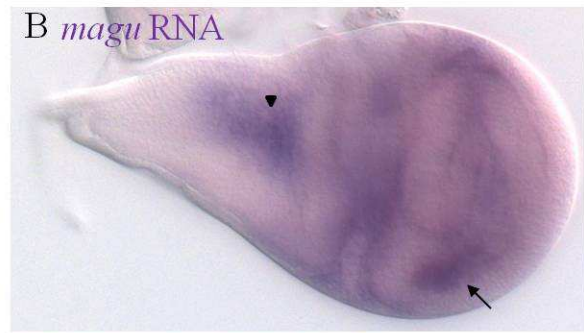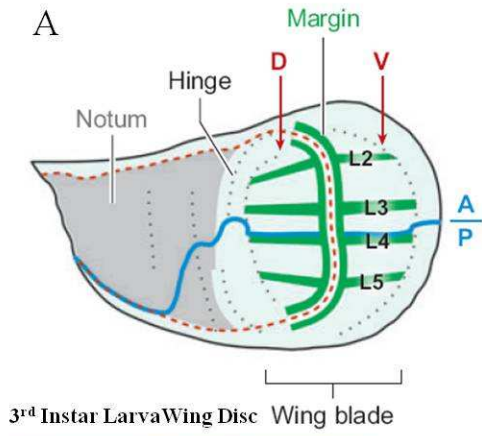
Figure 8. *magu* affects L5 specification. (A) Positions of primordial longitudinal veins (L2-L5) in late 3rd instar wing disc. The boundary between anterior (A) and posterior (P) compartments and that between dorsal (D) and ventral (V) compartments are shown as a blue and a dotted red line, respectively (copied from Fig.1A in ref (76)). In following panels, anterior is up, dorsal is left. (B) *In situ* hybridization in wildtype 3rd instar wing disc revealing *magu* RNA mainly in periphery cells on wing blade (arrow). The expression of *magu* also appeared in the notum region of wing disc (arrowhead). (C) *magu/+*. Anti-Delta revealed L3-L5 (arrows) on the wing blade. The staining for L4 was often much weaker than L3 and L5. (D) *magu*^{e00439}/*magu*^{deletionI}. In mutants, only L3 was visible by anti-Delta (arrow). The fact that L4 was not detectable on this particular wing disc was likely due to the variability of anti-Delta to mark L4. (E-H) Only the posterior compartment is shown. (E) *magu/+*. Anti-DSRF marked intervein cells. L4 and L5 were revealed as gaps between interveins (arrows). (F) *magu*^{e00439}/*magu*^{deletionI}. The region of interveins appeared narrower and disorganized in mutants. L4 could be determined based on anti-DSRF staining, but the periphery position of L5 made it harder to be identified unambiguously (arrows). (G) *magu/+*. Antibody against Abrupt, a L5 organizer downstream of BMP activation, revealed L5 on the sibling control wing discs. (H) *magu*^{e00439}/*magu*^{deletionI}. Anti-Abrupt staining was present in the presumptive L5 region, but the signal appeared weak, and the pattern was not as discrete compared to *magu* heterozygotes.

37

Table 5. The genetic interaction between *magu* mutant alleles and *gbb[1]*

Condition	Genotype [a]	Median GSC #	IQR [b]	Min - Max [c]	P value [d]
0-3 days, 25°C	*magu*[e] /*SM6a* or *gbb[1]/CyO*	7 (10) [e]	6 - 7	5 - 9	
	magu[e] / *gbb[1]*	6 (10)	5 - 6	5 - 7	>0.05
	magu[f] /*SM6a* or *gbb[1]/CyO*	7 (10)	6 - 7.8	5 - 8	
	magu[f] / *gbb[1]*	5.5 (8)	4 - 6	3 - 6	<0.01
13-16 days, 25°C [f]	*magu*[e] /*SM6a* or *gbb[1]/CyO*	8 (15)	5 - 9	3 -10	
	magu[e] / *gbb[1]*	4 (16)	3 - 5	2 - 9	<0.01
	magu[f] /*SM6a* or *gbb[1]/CyO*	4 (18)	4 - 6	4 - 10	
	magu[f] / *gbb[1]*	4 (19)	3.5 - 5	2 - 7	>0.05

[a] Alleles used: [e]=[e00439]; [f]=[f02256].

[b] interquartile range = Quartile 3 - Quartile 1 (Q[3] - Q[1]), Q[3] = the 75th percentile, Q[1] = the 25th percentile.

[c] Minimum - Maximum, representing the spread of GSC numbers observed

[d] Calculated by Mann-Whitney test.

[e] Number of testes scored in parentheses

[f] Animals (0-3 days of age) raised at 25°C were aged at 25°C for 13 days.
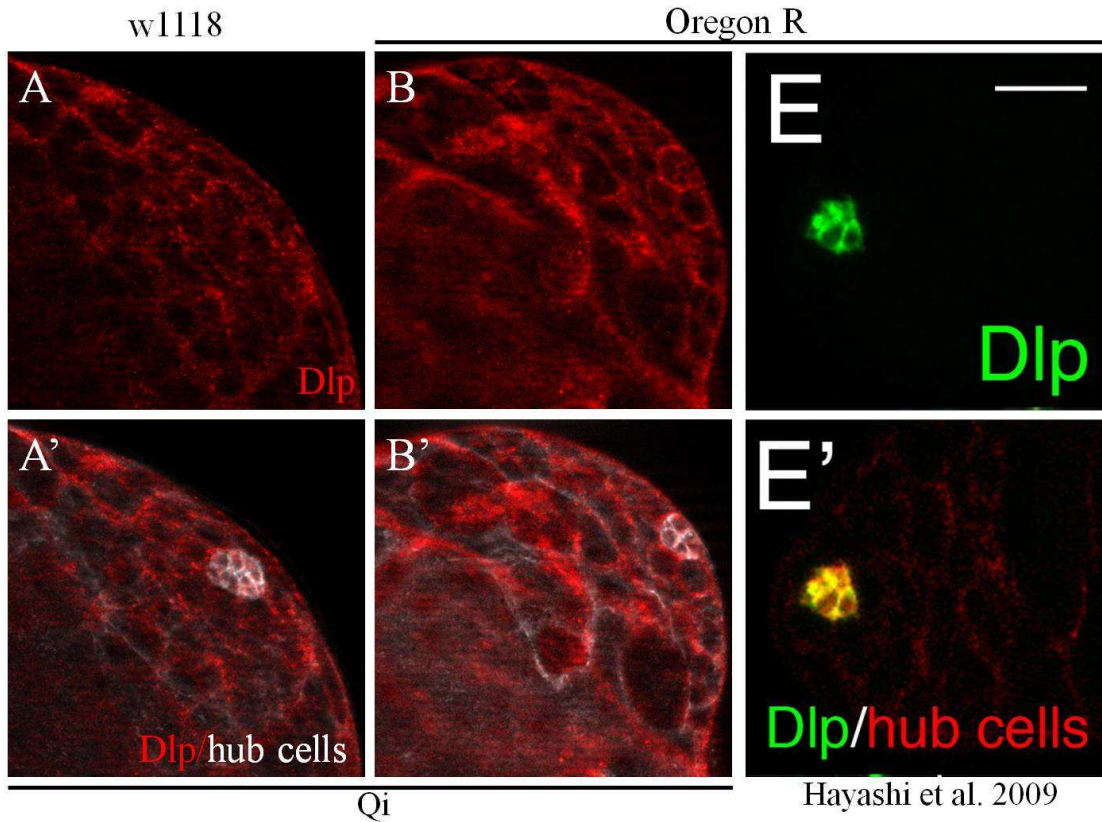
Figure 9. Dlp is expressed ubiquitously in testis. (A and B) Using two different wildtype fly lines (w1118, A; Oregon R, B), the expression of Dlp (red) appeared among many cells at the testis tip, and was never restricted to the hub (A', B', white). (E) In contrast, Dlp (green) was reported previously to specifically accumulate at hub cells in the Oregon R background (E', red; copied from Fig.4E in ref (75)).

Table 6. The genetic interaction between *magu* mutant allele and HSPG

Condition	Genotype [a]	Median GSC #	IQR [b]	Min - Max [c]	P value [d]
0-3 days, 25°C	*magu*[delI]; *TM6b, Hu, Tb*	8 (5) [e]	7 - 9	6 – 9	
	magu[delI]; *dally[80]dlp[A187]*	9 (5)	9 - 10	9 - 11	>0.05
12-15 days, 25°C [f]	*magu*[delI]; *TM6b, Hu, Tb*	5 (5)	3 - 6	3 - 6	
	magu[delI]; *dally[80]dlp[A187]*	5 (5)	5 - 5	4 - 9	>0.05
	magu[delI]; *TM6b, Hu, Tb*	5.5 (14)	4.3 - 6.8	3 - 9	
	magu[delI]; *dlp[A187]*	7 (18)	5 - 8	4 - 11	>0.05
	magu[delI]; *TM6b, Hu, Tb*	5 (9)	4 - 5	4 - 8	
	magu[delI]; *sfl[9B4]*	7 (9)	6 - 7	4 - 9	0.042
	magu[delI]/*CyO*	7 (9)	6 - 8	3 - 11	
	magu[delI]/*ttv[63]*	6 (10)	5.3 - 7	4 - 8	>0.05

[a] Allele used: [del I]=[deletionI].

[b] interquartile range = Quartile 3 - Quartile 1 (Q[3] - Q[1]), Q[3] = the 75th percentile, Q[1] = the 25th percentile.

[c] Minimum - Maximum, representing the spread of GSC numbers observed

[d] Calculated by Mann-Whitney test.

[e] Number of testes scored in parentheses

[f] Animals (0-3 days of age) raised at 25°C were aged at 25°C for 12 days.

Table 7. Ectopic expression of Dlp can rescue *magu* mutant.

Condition	Genotype [a]	Median GSC #	IQR [b]	Min - Max [c]	P value [d]	% of Testes w/GSCs	P value [e]
0-3 days, 25°C	*UAS-dlp-GFP* or fM7; *magu*[e] /*magu*[f]; MKRS	0 (19)	0 - 0	0 - 6		21	
	UAS-dlp-GFP; *magu*[e] /*magu*[f]; *nanos-Gal4*	2 (21)	0 - 4	0 - 9	0.06	57	<0.01
12-15 days, 25°C[g]	*UAS-dlp-GFP* or fM7; *magu*[e] /*magu*[f]; MKRS	0 (15)	0 - 0.5	0 - 5		27	
	UAS-dlp-GFP; *magu*[e] /*magu*[f]; *nanos-Gal4*	2 (17)	0 - 3	0 - 4	0.15	59	<0.01

[a] Alleles used: [e]=[e00439]; [f]=[f02256].

[b] interquartile range = Quartile 3 - Quartile 1 (Q[3] - Q[1]), Q[3] = the 75th percentile, Q[1] = the 25th percentile.

[c] Minimum - Maximum, representing the spread of GSC numbers observed

[d] Calculated by Mann-Whitney test.

[e] Calculated by Chi-square test.

[f] Number of testes scored in parentheses

[g] Animals (0-3 days of age) raised at 25°C were aged at 25°C for 12 days.
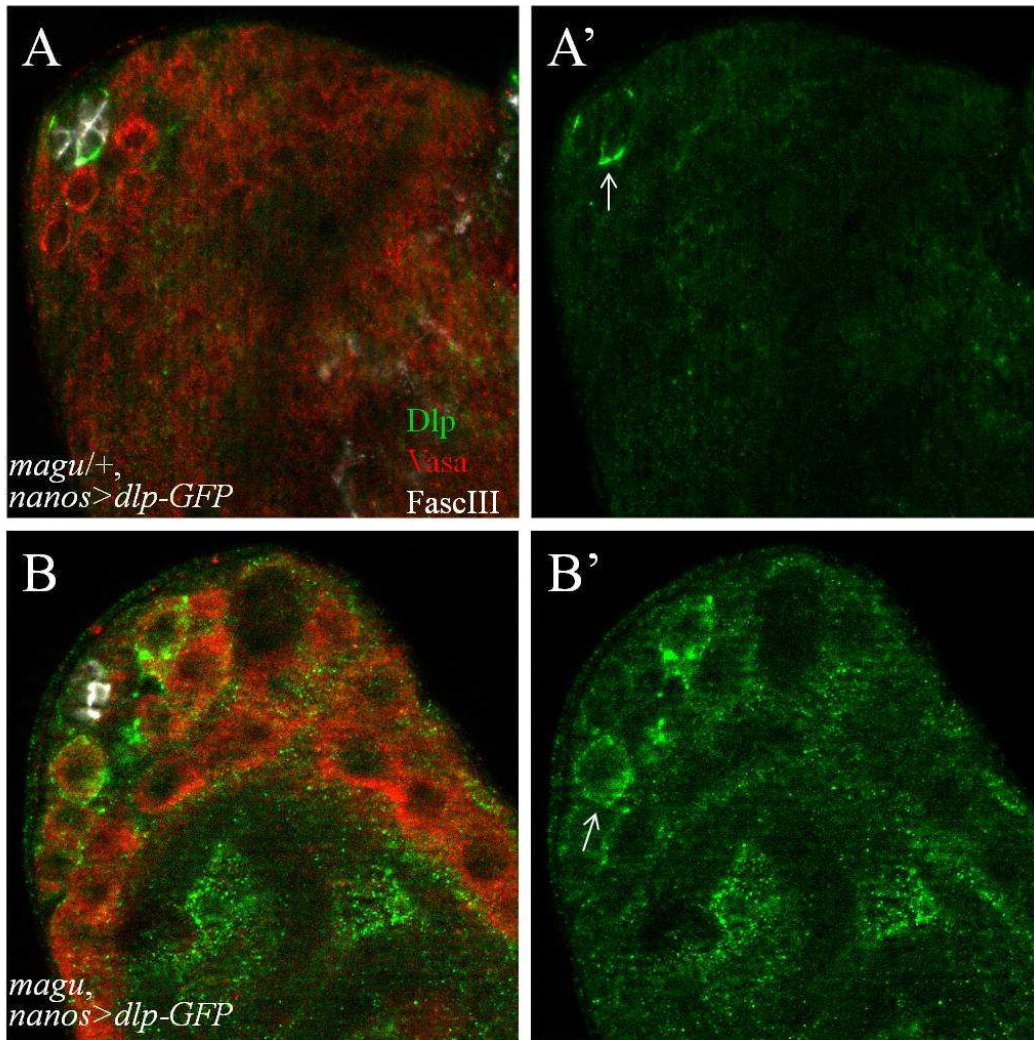
Figure 10. Magu controls the localization of ectopic Dlp expressed in germ cells. UAS-*dlp-GFP* was driven selectively in germ cells by *nanos*-Gal4. (A) *magu/+; nanos>dlp-GFP*. In sibling control testes, anti-GFP (green) revealed ectopic Dlp proteins accumulated along the interface between hub cells (FascIII, white) and GSCs (Vasa, red) (A', arrow). (B) *magu*[e00439]/*magu*[deletionI]; *nanos>dlp-GFP*. In magu mutants, Dlp (green) was not restricted to the hub-GSC interface; rather, it exhibited a punctate staining in and surrounding GSCs (B', arrow).
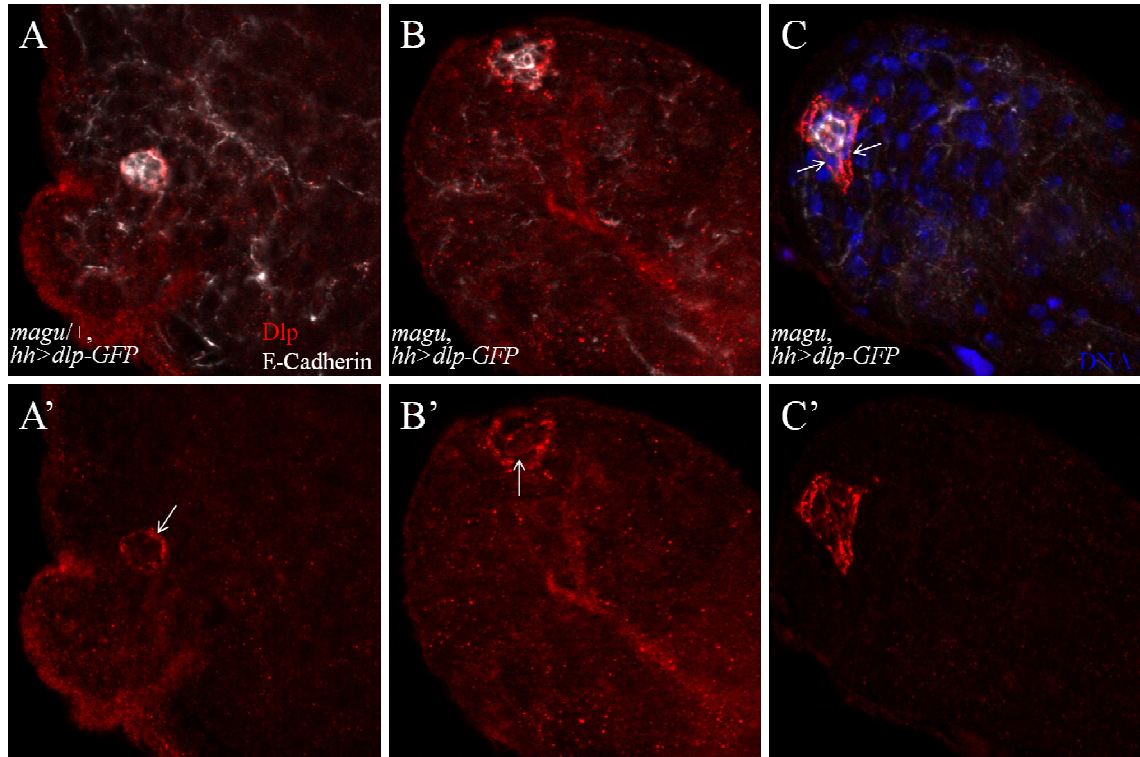
Figure 11. Ectopic Dlp expressed from hub cells (*hh*-Gal4) exhibits abnormal localization in *magu* mutant. The extracellular Dlp was visualized by staining non-permeablized testes. (A) *magu/+; hh>dlp-GFP*. Anti-GFP (red) revealed that Dlp was enriched on the outer layer of the hub (E-Cadherin, white), along the interface between hub cells and GSCs (A', arrow). (B) *magu*[e00439]/*magu*[deletionI]*; hh>dlp-GFP*. In mutant testes, extracellular Dlp exhibited a punctate staining along the hub-GSC interface. The accumulation of Dlp was also observed inside the hub (B', arrow). (C) *magu*[e00439]/*magu*[deletionI]*; hh>dlp-GFP*. In some mutant testes, the shape of Dlp expression region appeared polygonal, rather than rounded like the hub. The membrane-bound Dlp extended beyond hub cells expressing E-Cadherin (white), and embraced somatic cells next to the hub (arrow).
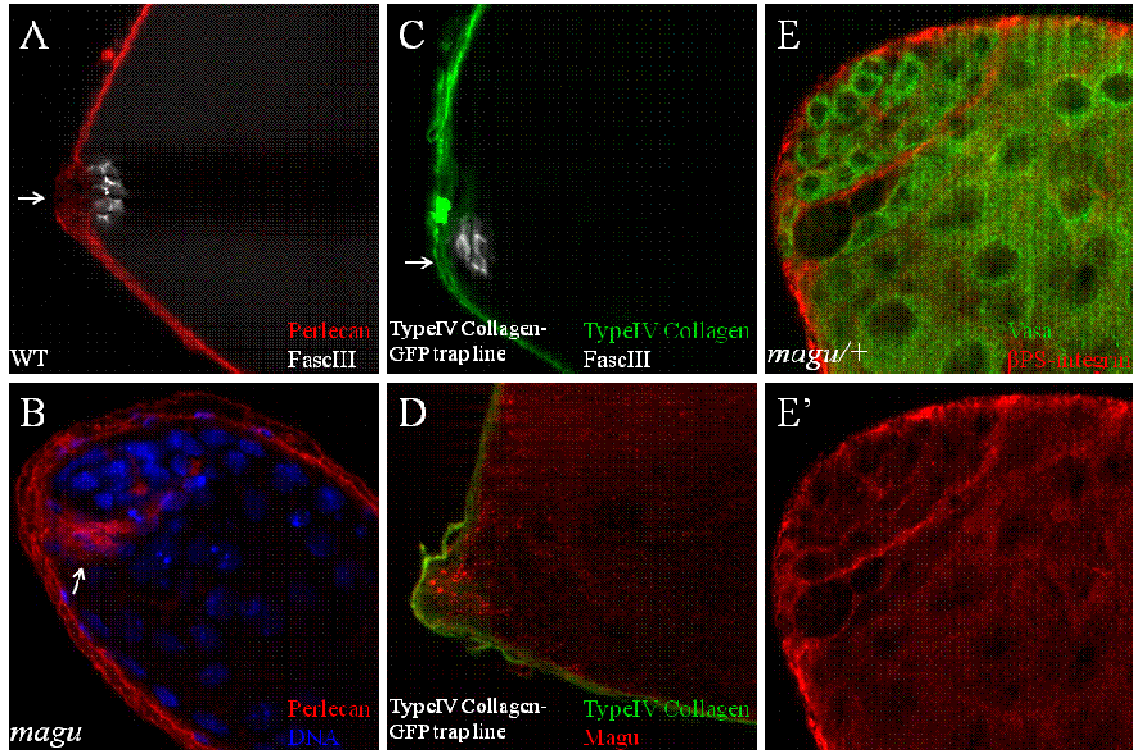
Figure 12. Magu may not interact with several ECM-associated proteins. (A) WT. Anti-Perlecan (red) revealed basal lamina under the sheath of testis. A hazy staining was also observed near the hub (FascIII, white), suggesting an ECM enrichment in that region (arrow). (B) $magu^{deletionI}$/ $magu^{deletionI}$. Perlecan appeared normal in most mutant testes (data not shown). But in some mutants, the Perlecan staining exhibited multiple layers along the testis sheath. Occasionally, basal lamina revealed by anti-Perlecan arced further into the testis (arrow). We did not think this was a primary defect in mutants (see text for details). (C) TypeIV Collagen-GFP trap line. Similar to Perlecan staining, anti-GFP (green) revealed basal lamina under the testis sheath. Two layers of Collagen near the hub (arrow) also suggested an accumulation of basal lamina. (D) TypeIV Collagen-GFP trap line. Location of extracellular Magu (red) did not overlap with Collagen (GFP) in wildtype condition. (E) $magu/+$. Integrin (red) was expressed ubiquitously in testis tip, in somatic cells (Vasa negative) and along the testis sheath.

Discussion

Here, by following up on a previous microarray approach that identified transcripts enriched at the testis tip, we show that *magu* plays an important role in GSC maintenance. We also provide strong evidence that it does so by modulating BMP activation in germ cells. *magu* encodes a secreted protein of the SPARC/BM-40/osteonectin family, shown to ensure the proper activity gradient for the BMP morphogen, Dpp, across the developing wing epithelium (66). More recently, two groups further showed that Magu functions as an important mediator of scaling Dpp signaling activity with wing disc size (77, 78). The role we have characterized for Magu in the testis niche exhibits some similarities as well as differences to that proposed for the wing.

Magu serves as a BMP modulator to maintain GSCs in adult testes

It has been shown that the BMP pathway is activated and required in GSCs, whereas the JAK-STAT pathway is activated and required in both GSCs and CySCs (40, 42, 44, 45, 47, 50-52). Our data shows that *magu* is required for maintenance of GSCs, but not CySCs, and that BMP activation was impaired in germ cells adjacent to the hub in *magu* mutants. We also found that forcing activation of the BMP pathway in germ cells substantively rescued the *magu* phenotype. Thus, we conclude that the primary role of *magu* in the testis niche is to modulate BMP signaling and thereby maintain GSCs.

Superficially, our results suggest that Magu works in a manner similar to that described in the wing epithelium, where Magu facilitates the transport of BMP ligands to establish the proper signaling gradient. However, in our view, the role of Magu in BMP signaling is tissue-dependent: it serves as a facilitator for ligand distribution in the wing, but a signaling co-receptor in the testis. Our evidence is elaborated upon next.

The most obvious difference between testis and wing is that to control wing patterning, BMP signaling is graded and must be effective over a long range. Thus, Dpp is expressed from a stripe of cells in the center of the wing disc, while the region where BMP activation is modulated by Magu is located far laterally, many tens of cells away from the ligand source (66). In striking contrast to this situation, BMP ligands are produced in hub cells and CySCs of testes, which are directly adjacent to GSCs, where pathway activation is required (50, 52). In the testis, there is no documented graded requirement, and, if anything, it is likely that pathway activation must be restricted to cells near the niche to ensure that few cells take on stem cell character. Therefore, while Magu is thought to assist the movement of Dpp over a long range in the wing (66), there is no need for long-range transport for GSC maintenance in the testis. This distinction between the two systems suggests that key mechanistic differences remain to be uncovered for how Magu affects BMP signaling.

One way that Magu supports robust signaling far from the BMP ligand source in the wing is that *magu* gene expression is engaged by a feedback circuit in order to be used as a positive modulator of signaling. Thus, *magu* expression is repressed in areas of

45

relatively high signaling, and that repression is relieved in regions of low signaling. Its action in the low signaling region is to promote signaling even though these areas are far from the ligand source (66). In fact, expressing *magu* ectopically in the area of high signaling serves to dampen signaling there, while it enhances signal at a distance, presumably by promoting movement or stabilization of the ligand. In the testis niche, we do have some evidence for feedback regulation. We found that a reporter construct of Magu, containing pMad/Medea/Schnurri complex binding sites (66) is expressed in hub cells, as one would expect. However, when these binding sites are mutated, the reporter is expressed more robustly, and in more hub cells. This suggests that feedback exists in the testis system also. However, in contrast to the wing, we have no evidence that this negative feedback regulation is necessary in the testis niche, as overexpression of *magu* did not result in fewer GSCs (data not shown).

One other potential difference between the wing and testis niche is that the BMP ligands acted on by Magu might differ in the two systems. Vuilleumier *et al.* have addressed the function of Magu with respect to Dpp, the principal BMP ligand used globally for wing patterning. However, the major BMP ligand for male GSC maintenance appears to be the related molecule, Gbb (50, 52). This difference could have consequences for the mechanism by which Magu influences BMP signaling comparing the two systems. For example, although Dpp does not interact directly with Magu (66), the potential remains that Magu might bind to Gbb for GSC maintenance. In this regard, it is worth noting that *gbb* is expressed throughout the wing (69), and that compromising *gbb* function does generate a wing vein phenotype similar to *magu* mutants (70, 71). Thus, in the wing, even though the focus has been on Dpp, perhaps there is an effect also on Gbb signaling that has yet to be characterized. Thus, further investigation of the modulation of BMP signaling by Magu in both the wing and testis niche should be revealing.

How might Magu modulate BMP signaling in the testis niche?

The fact that overexpressing a constitutively active form of BMP type I receptor in the germline can rescue the GSC phenotype suggests that Magu acts upstream of receptor binding. This is in agreement with its proposed role in the wing and also preliminary analysis in zebrafish (66). There are a number of membrane-associated and secreted factors that Magu might influence to modulate BMP signaling.

In the wing, Magu interacts directly with Dally, a HSPG (heparan sulfate proteoglycan) (66). Interestingly, Dally and its homologue Dally-like (Dlp) are also important for male GSC maintenance (74, 75). While we have not observed genetic interactions between *magu* and *dally*, *dlp* or other genes needed for HSPG biosynthesis, some preliminary data indicate that overexpressing *dlp* in the germ cells can increase the fraction of testes retaining GSCs among *magu* mutants. Preliminary data also showed that ectopically expressing *dlp* from germ cells led to an enrichment of Dlp along the hub-

46

GSC interface, and that this enrichment was Magu-dependent. This suggests a hypothesized model of how Magu regulates BMP activation. Studies from other tissues have demonstrated that Dlp acts as a BMP co-receptor to recruit ligands and facilitate ligand-receptor binding (79). Thus, Magu may concentrate Dlp to the hub-GSC interface, and thereby activate the BMP signaling robustly in the specific region (Fig.13A). Without the presence of Magu, Dlp proteins are not enriched along the hub-GSC interface. Consequently, fewer BMP ligands can be recruited, and BMP activation is diminished (Fig.13B). Although this simple model is consistent with our data, it is worth noticing that Dlp is expressed ubiquitously in testes, therefore, further experiments are needed to examine the role of endogenous Dlp with respect to Magu. In addition, the location of another HSPG, Dally, is also reported to be hub specific, thus we can verify the specific expression pattern of Dally, and further test its interaction with Magu in GSC maintenance (74, 75)

Given that Magu is secreted from hub cells, its localization could have suggested a more specific hypothesis for its action in the testis niche. However, *magu* protein localization among cells of the niche appears complex. An antibody we raised against an N-terminal portion of Magu exhibits punctate signal restricted among hub cells, and at the hub-GSC interface, but this serum was effective only sporadically. A second serum directed against a C-terminal peptide (66) robustly exhibits the same punctate pattern among hub cells, but also reveals a slightly extended distribution among stem cells and their daughter cells near the hub. Additionally, this serum revealed strong punctate signal likely among the extracellular matrix (ECM) near the hub. It is not possible at this time to distinguish whether the pool of Magu associated with ECM or the more generally distributed pool is active for GSC maintenance.

However, considering the close proximity of hub cells to GSCs, it is simplest to envision that Magu acts along the hub cell-germline stem cell interface. In fact, the BMP signals from the hub are received at the hub-GSC interface, as visualized by a fluorescent reporter of BMP type I receptor Thickvein (63). It is possible that Magu facilitates interactions between BMPs and their receptors via formation of ternary ligand/Magu/receptor complex. Such a ternary complex has been shown for Crossveinless 2 (Cv2), an extracellular BMP modulator engaged for crossvein patterning in the wing (80). Although Cv2 and Magu do not encode similar proteins, perhaps some lessons can be learned from the role of Cv2. This protein can also bind to Dally, and the Cv2-HSPG interaction is important for normal BMP signaling in crossvein patterning (80). Magu and its vertebrate orthologues SMOC1/2 have two Thyroglobulin type-1 repeats. It has been shown that proteins with such repeats can inhibit extracellular proteases (81). Thus, although Cv2 appears to have no effect on the function of Tolkin, the protease promoting BMP signaling in crossvein patterning (80), it is reasonable to speculate that Magu may function as a protease inhibitor to protect BMP ligands from being degraded by other extracellular proteases.

47

Alternatively, the enrichment we observed among the ECM is interesting. Thus, we explored possible roles and interactions extracellular matrix components may have with Magu. First, among the family of proteins to which Magu belongs, SPARC interacts with type IV Collagen, a component of basement membrane (82), and SMOC1/2 are associated with basement membrane (83, 84). Interestingly, Viking (Vkg), the type IV collagen in *Drosophila*, is involved in female GSC maintenance. However, its role is to restrict BMP signaling in the germarium (85), and this would be opposite to the phenotype expected for a Magu interactor in the testis niche. In addition, we did not observe a defect of type IV collagen in *magu* mutants, or co-localization of type IV collagen and extracellular Magu in wildtype testes. Second, we tested another ECM component, Perlecan, but this also appeared to accumulate normally in *magu* mutant testes. Finally, since SMOC2 depends on intergrins to modulate the attachment of epidermal cells and for angiogenesis (86, 87), we also investigated the possible interaction of Magu and integrins in testes. But we did not observe a defect of βPS-Integrin in *magu* mutants.

Speculation about other roles Magu may play in adult testes

The extended staining pattern at the testis tip as visualized by antibodies against C-terminal Magu is interesting. BMP ligands are expressed by hub cells and CySCs, and pMAD accumulation can often be detected in the second tier germ cells, even though these cells are not GSCs. Perhaps Magu is assisting in BMP signaling at these extended distances, playing a role more similar to that in wing as a ligand transporter. While we have no direct data that Magu plays such a role in the testis, a mild extension of BMP activation could act in dedifferentiation. For example, it may confer a stronger tendency for dedifferentiation on daughter germ cells near the hub. In fact, it has been shown that early rather than late stage spermatogonia are more likely to restore the GSC population (49).

Finally, punctate Magu staining can be observed in regions of testes far away from the hub, as shown by both antibodies against Magu. We do not know whether these signals are real, but it is worth noting that BMP signaling plays a role in later stage cyst cells where this pathway must be activated (62). It is possible that Magu may facilitate the distribution of BMP ligands from the hub region down to the area where spermatogoina are located. To demonstrate this hypothesis, live imaging of ligand transportation using epitope tagged Dpp/Gbb and Magu are needed.

Does Magu play a role in GSCs in larval gonads?

It has been shown that JAK-STAT pathway is required for both GSC and CySC establishment during *Drosophila* embryogenesis (68, 88). Male GSCs are established during the embryo-larval transition (68). Although no experiments have been reported to directly test the requirement of BMP in GSC establishment, a consistent pMad staining

in early germ cells is not detectable until 4hrs after larva hatching (89). We have found that GSC number is normal in 1ˢᵗ instar larva gonads mutant for *magu*. Thus we conclude Magu does not affect GSC establishment. Therefore, it is likely that BMP pathway is not involved in GSC establishment.

Nevertheless, once GSCs are established, Magu starts to act in their maintenance. This conclusion is based on the observation that 3ʳᵈ instar larva gonads mutant for *magu* have a significantly lower number of GSCs compared to sibling controls. We have noticed that there is normally an increase in GSC number from 1ˢᵗ to 3ʳᵈ instar. This observation is supported when comparing data reported by two other groups (68, 89). However, Magu mutants do not show such an increase, thus BMP signaling must be necessary for this increase.

Evidence for dynamic BMP signaling in *Drosophila* male GSCs during development

The requirement of BMP signaling for GSC maintenance has been well established. In adult testes, GSC clones mutant for components in BMP signal transduction are not maintained, but instead differentiate (50-52). This suggests strongly that the BMP pathway is active in adult GSCs. However, in contrast to earlier reports (50), we have difficulty detecting BMP activation in wildtype testes using either pMAD or reporter gene assays. While this might imply that the level of BMP pathway activity is below the threshold of our detection, positive pMAD staining can be always nicely observed in 3ʳᵈ instar larva gonads. Furthermore, a recent paper from the Fuller lab fully supports our observation (89). Chang *et al.* go on to show that the response to BMP signaling in GSCs is downregulated during development as demonstrated by pMAD and *dad*-LacZ stainings. This downregulation is mediated by Smurf, an ubiquitin protein ligase for MAD degradation. In *smurf* mutant adult testes, high levels of pMAD and *dad*-LacZ expression are observed in GSCs and early germ cells. Smurf also controls GSC numbers. In wildtype situation, the average GSC number in testes is significantly lower in adult compared to pupa. However, this difference is abolished in *smurf* mutants. These data are consistent with the observation in our cohort experiment that GSC number in 3ʳᵈ instar larva gonads is slightly higher than that in adult testes (Table 2). Taken together, the data suggest strongly that there is indeed a temporal regulation of BMP signaling in GSCs during testis development.

Is BMP signaling activated in hub cells of adult testes?

It has not been reported before that BMP activation occurs in hub cells. However, Magu is a target gene of BMP pathway (66), and is expressed in hub cells. In addition, antibody staining against Medea and expression of dad-LacZ also suggest BMP activation in hub cells. Therefore, we think BMP signaling is activated in hub cells. Considering the heterogeneous pattern of *magu* and *dad* reporter lines (Fig.1B; Addendum Fig.1B, B'), we also conclude that the activation of BMP pathway in hub

49

cells is spatially regulated. We do not know the importance of BMP activation at the hub, besides stimulating *magu* expression. It is intriguing to think that the non-uniform activation may indicate functional heterogeneity among hub cells. Further evidence would be needed to test this speculation. But, this idea may be supported by the fact that hub cells derive from two groups of somatic gonad precursors during embryonic development: one from parasegment 10, and the other from parasegment 11.
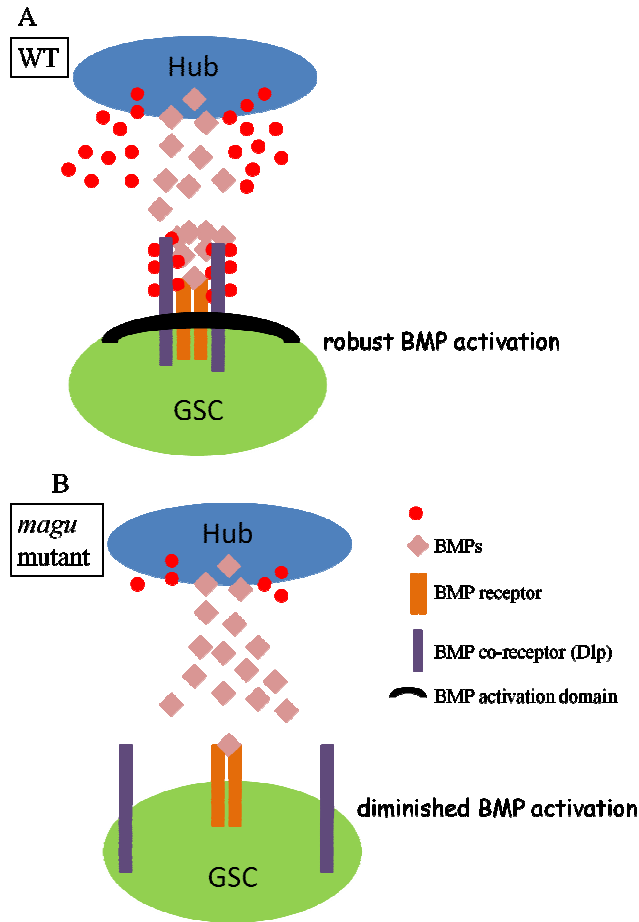
Figure 13. A hypothesized model of how Magu regulates BMP activation. (A) In wildtype testis, Magu concentrates Dlp to the hub-GSC interface. The enriched Dlp proteins recruit BMP ligands to the surface of BMP receptors, thereby facilitate the activation of BMP signaling. (B) In *magu* mutant testis, Dlp proteins are diffused around the GSC membrane surface, thus BMP ligands are not concentrated along the hub-GSC interface, and BMP activation is diminished.

Material and methods
Fly strains

Fly lines used were: *magu*frgII-LacZ, *magu*frgIIΔS-LacZ, and UAS-V5-*magu* (George Pyrowolakis, University of Freiburg, Germany), *nanos*-Gal4:VP16 (Erica Selva, University of Delaware, USA), *upd*-Gal4 (Erika Matunis, John Hopkins University, USA), *upd*-Gal4 UAS-GFP (Erika Bach, New York University, USA), *bam*-GFP (Dennis McKearin, UT Southwestern, USA), UAS-*tkv*A (Kristi Wharton, Brown University, USA). All stocks related to HSPG came from Xinhua Lin, Cincinnati Children's Hospital Medical Center. The following transposable insertion lines were from the Exelixis Collection at Harvard Medical School: *magu*[d00269] (FBti0053977), *magu*[e00439] (FBti0046433), and *magu*[f02256] (FBti0050490). All other stocks including *magu*[KG02847b] (FBti0023111) were provided by the Bloomington Stock Center or generated in this study. Flies were grown at 25ºC unless noted.

Generation of magu mutants

A precise excision of *magu*[e00439] was isolated as described to generate a revertant, while deletion I was made using FRT/FLP-mediated hybrid element insertion starting with the PiggyBac insertions *magu*[d00269] and *magu*[f02256] (90). The resulting lines were verified by PCR. Some of the same mutant alleles were independently made and reported previously (66). To obtain mutants with potentially larger deletions, the P-element transposon KG02847b was remobilized, and new lines exhibiting a wing vein phenotype over the *magu*[e00439] allele were selected out. Inverse PCR was used to identify the endpoints of the resulting deletions. The deletions begin in the KG element, and extend to genomic coordinate 5966K for line 76 (reported in Table 1), 5987K for line 123, 6325K for line 166, 5988K for line 862 (Flybase, release before Feb. 2010).

Generation of an anti-Magu antibody

A 6xHis epitope tag (Qiagen pQE vector) was fused N-terminally to residues 36-213 of Magu. The resulting protein was purified from soluble whole bacterial extracts, using Ni-NTA beads (Qiagen), and injected into rabbits. The crude sera were preabsorbed 1:5000 against fixed *w1118* testes at 4ºC for 24 hrs. Titration of this antibody revealed that the preabsorbed 1:5000 dilution gave the best signal-to-noise ratio.

Plasmids

magu sequence was amplified via PCR from BDGP cDNA LD30894, and cloned using Gateway recombination methods (Invitrogen) into either a pUAST-Myc or pUAST-GFP destination vector (developed by Terence Murphy, DGRC). Transgenic flies were produced using standard germline transformation techniques.

In situ hybridization

In situ hybridization on testes and wing imaginal discs using digoxigenin-labeled antisense RNA probes was performed as previously described (64).

Immunostaining

Immunostaining for gonads, adult testes, and wing imaginal discs was performed as previously described except 1×PBS was substituted for Buffer B (40). The following antibodies were used: mouse anti-lacZ (1:10,000, Promega), rat anti-E-Cadherin (1:20, DSHB), rabbit anti-Magu (1:5000), rabbit anti-Magu (1:15,000, George Pyrowolakis, University of Freiburg, Germany), goat anti-Vasa (1:400, Santa Cruz), mouse anti-FascIII (1:50, DSHB), rabbit anti-α-Spectrin (1:200, DSHB), rabbit anti-Zfh1 (1:5,000, Ruth Lehmann, New York University, USA), chick anti-GFP (1:1000, Molecular Probes), rabbit anti-Stat (1:5000, Erika Bach, New York University, USA), mouse anti-pMad (1:1000, Carl-Henrik Heldin, Ludwig Institute for Cancer Research, Sweden), mouse anti-Eya (1:20, DSHB), guinea pig anti-Traffic jam (1:10,000, Dorothea Godt, University of Toronto, Canada), mouse anti-Dlp (1:50, DSHB), mouse anti-Delta (1:3000), mouse anti-DSRF (1:200), and rabbit anti-Abrupt (1:1000). Attempts to visualize pMad in adult testes using anti-pMad generally failed. In one experiment, several testes exhibited clearly positive signals. The example in Fig 5C is from this experiment.

For extracellular staining, testes were dissected in cold Ringer's solution, and incubated for 2 to 3 hrs in cold Ringer's solution containing 2% normal donkey serum and 1:15,000 rabbit anti-Magu (developed by George Pyrowolakis), and washed for 3×20 min in cold Ringer's solution, followed by the standard fixation and immunostaining protocol.

Imaging and imaging analysis

Images were captured with a Zeiss Axioplan 2 equipped with an apotome. Z-series were analyzed by the AxioVision 4.6 software, except that projection images for Magu (standard staining), α-Spectrin, and pMad (for testes) were created by ImageJ (NIH) software. Various cell types were counted by stepping through optical sections. Excel (Microsoft) was used for statistical analysis. GSC number in *magu* mutants did not fall into a normal distribution, thus the Mann-Whitney test was used to calculate P-value on the VassarStats web site (http://faculty.vassar.edu/lowry/VassarStats.html).

Mounting fly wings

Wings from adult flies were dissected in methylsalicilate (Sigma, C1705) and mounted in 2:1 Canada Balsam (Sigma, M-6752): methylsalicilate.

S phase labeling

S phase labeling of testes was performed as previously described (40).

53

Acknowledgements

CHAPTER 3

Identifying target genes of the transcription factor Zfh1 in CySCs of the *Drosophila* testis

Summary

Stem cells are often situated in a special microenvironment called niche. Niche cells regulate stem cell behavior through local signals. In *Drosophila* testes, two stem cell populations, GSCs and CySCs share a common niche called the hub. Recent work from our lab has demonstrated that CySCs also function as a niche for GSCs (40). We further showed that the transcription repressor Zfh1 governs the double role of CySCs (42). Zfh1 is required for CySCs self-renewal, and also sufficient to induce excess CySCs and GSCs (42). How Zfh1 plays its role is ill-defined. Thus here we attempt to identify target genes of Zfh1 using complementary approaches. ChIP-qPCR results show that Zfh1 is enriched near the cyst cell differentiation gene encoded by *eya* and the epithelial component E-Cadherin encoded by *shg*. The complementary genetic approach suggests that Zfh1 requires co-repressor CtBP to generate ectopic stem cells.

Introduction

Niches regulate the behavior of many tissue-specific stem cells (1). The microenvironment formed by niche cells provides important extrinsic cues to guide the self-renewal of stem cells. Studies of *Drosophila* male germline stem cells have served as a paradigm in niche-stem cell biology. In the fruit fly testes, a group of tightly packed somatic cells, called hub cells, are located at the apical tip. Two intermingled stem cell populations, germline stem cells (GSCs) and cyst stem cells (CySCs), are organized around the hub. It has been known for more than ten years that JAK-STAT signals emanating from the hub are necessary and sufficient for the self-renewal of both GSCs and CySCs (44, 45). Stem cells mutant for a JAK-STAT signal transducer will lose their stemness and differentiate, leaving the hub (44, 45). When the ligand of JAK-STAT pathway is overexpressed in testes, excess GSCs and CySCs are induced, resulting in a stem cell tumor phenotype (Fig.1B) (40, 44, 45). Therefore, the hub functions as a well-established niche to control stem cell behavior through JAK-STAT signaling.

This somewhat simple model, where one niche signal is key, has modified extensively by recent work from our lab (40). We found that CySCs are also part of the niche: they act together with hub cells to renew GSCs. Furthermore, we also significantly clarified the role of JAK-STAT pathway in the function of this niche. Surprisingly, when JAK-STAT signaling is only activated in the CySCs, GSCs are still maintained even though they are not transducing a STAT signal (40). Therefore, STAT cannot be necessary for GSC renewal. Interestingly, the stat-depleted GSCs are no longer adherent to the hub (40). Thus, JAK-STAT signaling is not required for GSC self-renewal, but rather regulates GSC adhesion to hub cells (Fig.1A, copied from Fig.4E in ref (40)). Under these conditions the CySCs govern the renewal of GSCs, and thus, CySCs constitute part of the germline niche. The novel notion that hub cell and CySC function cooperatively to serve as a GSC niche may not be surprising, as hub cells and CySCs are derived from a common pool of somatic gonadal precursors (SGPs) during

56

gonadogenesis. Interestingly, the niche architecture and signaling in male gonads has been shown to be similar to our observation in adult testes (88). Further evidence supporting CySC's role as part of the niche comes from dedifferentiation studies on spermatogonia, daughter cells of GSCs that have already taken on the fate of differentiation. Brawley and Matunis have shown that GSCs can be regenerated by coaxing spermatogonia to convert back into GSCs (49). They find that the regenerated GSCs are often accompanied by CySCs. Their data also indicate that when CySCs or cyst cells are not present, spermatogoina are not able to undergo dedifferentiation. Thus, CySCs may be required to guide the dedifferentiation of gonial cells into GSCs.

The fact that CySCs were not only a stem cell population, but also comprised part of the niche has led me to focus on these special cells. From a prior microarray study in the lab, a number of genes were identified whose expression was enriched in stem or niche cells (64). Among these was the zinc finger homeodomain protein Zfh1. We discovered that Zfh1 was highly expressed in CySCs, but downregulated in hub cells and also downregulated in differentiating cyst cells (42). Furthermore, CySCs mutant for Zfh1 left the hub and started to differentiate (42). Therefore, Zfh1 is specifically required for CySC maintenance. More interestingly, when Zfh1 is sustained in otherwise differentiating cyst cells, we observe a stem cell tumor phenotype similar to ectopic JAK-STAT activation (42). Using various stem cell markers, we have demonstrated that the excess somatic cells and germ cells induced in Zfh1 overexpression testes are *bona fide* stem cells (42). Thus, Zfh1 is not only intrinsically sufficient for CySC self-renewal, but also regulates GSC self-renewal non-autonomously. The impact of Zfh1 on two cell lineages matches with our notion that CySCs function as both a stem cell and a niche for GSCs.

How does Zfh1 regulate stem cell behavior? We think *zfh1* is a presumptive target gene of JAK-STAT. We have shown that the function of Zfh1 is downstream of JAK-STAT activation, as ectopic STAT proteins are not accumulated in Zfh1 overexpression testes (42). Another signal that is required for GSC maintenance is BMP. We have found that when BMP signals are impaired, the effect of Zfh1 to cause excess GSCs is dampened (40). Thus, we previously proposed a model in which activation of JAK-STAT in CySCs induces Zfh1, which in turn induces the expression of BMP ligands required for GSC self-renewal (Fig.1A). However, if BMP is the key GSC renewal signal downstream of Zfh1 activation, then constitutive activation of the BMP pathway in the germline would cause excess GSCs. But this reasonable expectation is not observed in testes with ectopic BMP activation in the germline (Fig.1C) (50-52). We have also tried to co-activate both JAK-STAT and BMP in the germline, but this attempt also fails to recruit extra GSCs (Fig.1D). Thus, there must exist an unidentified GSC renewal signal(s) that is controlled by target genes of Zfh1 in the CySCs.

Zfh1 is a transcription factor with pleiotropic roles during embryogenesis (91-98). The protein contains zinc finger clusters at both the N- and C-terminals. It also has a polyQ region, a homeodomain, and a CtBP (C-terminal-binding protein) binding motif.

57

Data from *in vitro* experiments have shown that the zinc fingers of Zfh1 can bind to EBox sites in the regulatory region of a gene (91). It has also been shown that Zfh1 functions as a transcriptional repressor with the recruitment of its co-repressor CtBP (99). We have found out that Zfh1 with a mutation in CtBP binding motif fails to generate extra stem cells (42). Thus, we think Zfh1 also acts as a transcriptional repressor in the testis.

Here, to further dissect out how Zfh1 controls stem cell self-renewal, we are trying to identify target genes of Zfh1 using two genome-wide approaches: ChIP-Seq and genetic modifier screen. ChIP-qPCR results show that *eya* and *shg* may be direct targets of Zfh1. We also further demonstrate the requirement of CtBP for Zfh1 function, as lowering the gene dose of CtBP reduces the stem cell tumor phenotype generated by Zfh1 overexpression.

Results

To identify target genes of Zfh1, we have taken two approaches. One is ChIP-Seq, which combines chromatin immunoprecipitation with high throughput DNA sequencing. The other is a genetic modifier screen. ChIP-Seq allows us to identify potential direct targets of Zfh1. The gene list generated by ChIP-Seq will be long, requiring much effort in prioritization to select out a small set of targets for follow-up analysis. Thus, the genetic modifier screen serves as a complementary method to narrow down our focus. The screen approach identifies genes functioning either in parallel with or downstream of Zfh1. It is an unbiased genome-wide method, but depending on the dosage sensitivity of a particular gene, it may not fish out all the potential targets of Zfh1. Therefore, we think genes identified from both approaches have a higher chance to be a real Zfh1 target. The project is currently underway. Below I will elaborate how we have carried out each approach, how far along we are, and what will be required to finish each approach.

ChIP-Seq for Zfh1

The general procedure of ChIP-Seq is shown in Fig.2. First, cells of interest are enriched, and chromatin and protein are cross-linked using formaldehyde. Second, chromatin isolated from cell lysates are fragmented by sonication. Third, immunoprecipitation (IP) is performed on chromatin fragments using antibody-conjugated beads. Forth, pulled down chromatin-protein complexes are isolated, and the IP'ed chromatin is eluted by reversing the cross-linking. Finally, purified DNA fragments are assembled into a library and sequenced.

For the ChIP-Seq approach to be successful, we need to have three essential components in place.

1. Can we isolate enough chromatin from testes for ChIP?

58

There are only 25 *zfh1* expressing cells (CySCs) per testis. In order to have sufficient numbers of this cell type from which to isolate chromatin, we decided to significantly boost the number of cells expressing *zfh1* using the Gal4-UAS system.

2. Do we have a ChIP-grade antibody for Zfh1?

There were various antibodies against Zfh1 generated by different labs (96, 98, 100). It was unknown whether they were suitable for ChIP. Alternatively, we could use commercially available ChIP-grade antibodies against an epitope tag. In this latter case, we needed to construct an epitope tagged UAS-Zfh1.

3. Can we carry out ChIP in our lab?

In order to assess the success of ChIP, we decided to perform qPCR experiments on ChIP'ed chromatin before sequencing. We also chose to perform ChIP-qPCR on a histone mark as a positive control (trimethyl, lysine 27 on Histone H3; H3K27me3). We used IgG as a negative control. No known targets existed for Zfh1 in the testis so far, thus we selected putative positive control genes based on our genetic data and a gene list generated from Zfh1 ChIP on wildtype embryos (see details later).

Our tests for these three essential components are obviously interrelated. The reliability of satisfying the requirement for one depends on how reliably the other two components function. However, for the sake of clarity, I will summarize results for each component separately.

Can we isolate enough chromatin from testes for ChIP?

There are two ways to significantly increase the number of *zfh1* expressing cells in the testes. The first relies on the fact that *zfh1* expression is regulated by activation of the JAK-STAT pathway in CySCs. Thus inducing the JAK-STAT pathway in the cyst lineage would then activate the downstream gene *zfh1*. The second way involves overexpressing *zfh1* directly using a cyst lineage Gal4 and UAS-Zfh1. No matter which method is used, the key will be to obtain robust production of excess *zfh1* expressing CySCs. This proved trickier than we had hoped.

Since the potential exists that directly expressing artificially high levels of Zfh1 might lead to some aberrant binding and increase the false-positive rate, we initially tried activating the JAK-STAT pathway. To do this, we expressed either the ligand (Upd), or an activated form of the kinase, JAK[Act]. However, we could not generate testes having consistent induction of Zfh1, nor having a robust stem cell tumor phenotype (see Addendum). We therefore had to turn to direct overexpression of Zfh1 in the cyst lineage. Even though in the past this approach uncovered a number of key principles about Zfh1 and CySCs (42), the approach was not robust enough for my purpose, as too many testes did not exhibit a strong enough phenotype (see Addendum).

We did not know exactly why the penetrance of stem cell tumor phenotype using UAS-Zfh1 was low. One reason could be that the genomic insertion site for this particular transgene site did not allow high enough expression. To obtain flies with a

59

more consistent phenotype, we generated our own UAS-Zfh1 transgenic lines. We also chose to epitope tag the protein. This would be beneficial since we could then use commercially available ChIP-grade anti-epitope tag antibodies if necessary.

- **Generating epitope-tagged UAS-Zfh1**

In order to generate epitope-tagged UAS-Zfh1, we first needed to know which Zfh1 isoforms were normally expressed in testes. When we began with this approach, two isoforms of Zfh1 had been reported in *Drosophila* embryos (Flybase, Fig.3). Zfh1-PB was a longer isoform than Zfh1-PA, and contained two additional zinc fingers and a polyQ region at the N-terminus (Fig.3). To test for the presence of transcripts encoding the two isoforms in testes, we performed 5' RLM-RACE (RNA Ligase Mediated Rapid Ampilification of cDNA Ends) and RT-PCR (Reverse Transcription PCR) experiments using isolated RNAs. We found evidence for Zfh1-RB and an alternative form of Zfh1-RA in wildtype testes (Fig.3). The variant of Zfh1-RA had a different first exon, but the same functional domains as Zfh1-PA. Thus, both Zfh1 isoforms were present in testes.

As stated above, an advantage of tagged UAS-Zfh1 was to use anti-epitope tag antibodies for ChIP. But one caveat here was that the epitope tag may interfere with the function of Zfh1 protein. Thus to investigate whether tagging at the N- or C-terminal was the best, we made constructs with the tag at either end. We also chose HA and Myc as the tags, because ChIP-grade antibodies are available against these two epitopes. Using Gateway Cloning, we successfully generated tagged UAS-Zfh1-RB plasmids. For the short isoform, we used UAS-Zfh1-RA-1×Flag-1×HA, a construct from BDGP (Berkeley Drosophila Genome Project). However, since transgenic flies with Zfh1-RA-1×Flag-1×HA expression did not cause stem cell tumor phenotype in testes (see Addendum), below I will focus on the tagged UAS-Zfh1-RB lines.

- **N-terminally 3×HA-tagged UAS-Zfh1-RB gives rise to stem cell tumor phenotype at 100% penetrance and with high expressivity**

We successfully generated several transgenic lines with epitope-tagged UAS-Zfh1-RB. To investigate whether the transgene could be expressed well *in vivo*, we first induced the ectopic proteins in epithelial cells of embryos using Patch-Gal4, a driver expressed in a pattern of stripes. We observed this ectopic pattern using antibodies against either the epitope tag or Zfh1 (Fig.4B, B', C, C'). We also noticed that embryos with tagged Zfh1-RB did not survive to larval stage. These embryos appeared to be disorganized (Fig.4A, B, C), and many cells with ectopic Zfh1 expression exhibited bright DNA staining, suggesting the death of cells (data not shown). Since the mammalian homologue of Zfh1 activates an epithelial to mesenchymal transition, we thought ectopic expression of Zfh1 in epithelium cells may change cell fate, thus causing the patterning defect.

To test whether the tagged Zfh1 could cause stem cell tumor phenotype in testes, we overexpressed the transgene in cyst lineage. The extent of phenotype varied among different transgenic lines (see Addendum Fig.3). But one N-terminally 3×HA tagged UAS-Zfh1-RB line gave rise to ectopic CySCs and GSCs at 100% penetrance and with high expressivity (Fig.5B). Different from sibling controls, these overexpression testes appeared to be bigger and fatter under light microscope (data not shown). This may be due to a plethora of extra cells filling the overexpression testes. Ectopic *zfh1* expression cells could be identified throughout the testes using antibodies against either Zfh1 or HA (Fig.5B', D). These extra Zfh1+ cells were functional CySCs, as excess GSCs marked by dotted fusomes were also induced in the overexpression testes (Fig.5B"). Thus, we chose to use this N-terminally 3×HA tagged UAS-Zfh1-RB line for the ChIP experiment.

Do we have a ChIP-grade antibody for Zfh1?

Now we had an N-terminally 3×HA tagged UAS-Zfh1-RB line suitable for ChIP, we could apply the commercial ChIP-grade antibody against HA for our experiment. In addition, we tested the various antibodies directly against Zfh1. Since anti-HA and anti-Zfh1 recognized different epitopes, we thought overlapping ChIP results obtained from these different antibodies would be more likely to reflect real Zfh1 targets. However, we could not get ChIP to work using anti-Zfh1 antibodies (data not shown). Therefore, below I will discuss the anti-HA antibody.

- **The commercially available anti-HA antibody can IP tagged Zfh1 protein, but we do not know for sure whether it works for ChIP**

We took a systematic strategy to assess whether the ChIP could be successful using anti-HA. We first detected ectopic Zfh1 proteins in whole cell lysates using an antibody against HA raised in rat. We observed a dominant band with the size similar to that predicted for Zfh1-PB in protein lysates isolated from overexpression testes (Fig.6A, arrow). This finding allowed us to track the tagged protein during each step of the ChIP protocol. To investigate whether we can IP the tagged Zfh1, we carried out the IP experiment by following the ChIP protocol and using a commercial ChIP-grade anti-HA antibody developed in rabbit. We analyzed results from each step of the procedure by Western Blot. We could detect tagged Zfh1 in the experimental and not control samples (Fig.6B, arrow). Most importantly, we reproducibly saw enriched Zfh1 proteins in IP'ed sample (Fig.6C). This demonstrated that the rabbit anti-HA can pull down tagged Zfh1.

One difference in the IP protocol above, and that which would be used in the true ChIP experiment is that testes used above were not treated with formaldehyde to cross-link chromatin and protein. We did perform a similar experiment using cross-linked chromatin. In this case, instead of a sharp band, we observed smears after Western Blot in the size range of Zfh1 both before and after IP (data not shown). We believe it is reasonable to assume that this is due to the cross-linking. Alternatively, it could reflect

some other problems with the procedure, and should be followed up in the future if necessary.

Can we carry out ChIP in our lab?

- **Predicting target genes of Zfh1**

For ChIP-qPCR, we selected three genes as putative targets of Zfh1: *eya*, *mys*, and *shg*. The rationale for choosing each gene is stated below.

The gene *eya* is expressed in differentiating cyst cells, but not CySCs. Previous work in our lab showed that expression of *eya* in CySCs is repressed by Zfh1, as CySCs mutant for *zfh1* started to express *eya* and differentiated directly rather than remaining as CySCs (42). We hypothesized that *eya* might be directly regulated by Zfh1 through cis-regulatory regions. To identify potential binding regions of Zfh1, we examined the expression pattern of two lacZ reporter lines for *eya* (Figure 7) (101). The expression of C1-LacZ recapitulated the Eya testis pattern, exhibiting expression in later, differentiating cyst cells (Fig.7A). In contrast, the A3-LacZ reporter exhibited precocious expression, now in CySCs in addition to later differentiating cyst cells (Fig.7B). These two regions might contain Zfh1 binding sites. In particular, since Zfh1 was predicted to act as a repressor, it might bind better to C1, which recapitulated the endogenous Eya pattern, compared to A3, which exhibited precocious expression in CySCs (where Zfh1 was expressed).

Another putative target that we selected was *mys*, which encodes βPS-integrin. It has been shown that integrin accumulated at the hub-CySC interface, and that integrin was necessary for the attachment of CySCs (47). Thus *mys* needed to be expressed in CySCs, however, its expression had to be maintained at a relatively low level at this interface; otherwise, CySCs would outcompete GSCs for position in the niche (47). Low level *mys* expression was achieved by repression due to JAK-STAT signaling in CySCs (47). Because Zfh1 was predicted to be a transcriptional repressor downstream of JAK-STAT activation, we hypothesized that Zfh1 controlled *mys* expression, and thus, selected *mys* as a potential positive control in our ChIP. A second reason for the selection of *mys* was that the White lab had generated a gene list from Zfh1 ChIP-chip using chromatin prepared from wildtype embryos (100). While the data from that experiment was not confirmed yet (see Discussion), *mys* was present on their list.

A third possible target of Zfh1 is *shg*, the *Drosophila* homologue of E-Cadherin. We chose this gene because ZEB1, the mammalian homologue of Zfh1, represses Cadherin directly. This seems also true in fruit fly testis development. During gonadogenesis, Zfh1 is initially expressed in all somatic gonad precursors (SGPs) (88). A subset of SGPs will then lose Zfh1 expression as they adopt hub cell fate, and these cells exhibt increased E-Cadherin expression (88, 102). Some of the remaining SGPs retain high Zfh1 expression and adopt CySC fate, and these cells exhibit relatively low level of E-Cadherin

62

expression (88, 102). This reciprocal expression pattern of Zfh1 and E-Cadherin is also observed in adult testes (Fig.7C). To further test the notion that Zfh1 repressed E-Cadherin, we expressed Zfh1 ectopically in the hub cells of adult testes. This greatly diminished the enrichment of E-Cadherin in hub cells (Lindsey Wingert, Fig.7D). Thus we concluded that Shg can be (genetically) suppressed by Zfh1. It was worth noting that *shg* also appeared on the embryo list made by the White lab.

Once we selected putative target genes, we narrowed down the genomic region for which qPCR primers will be designed. For *eya*, we already knew the sequence of A3 and C1, but the length of each fragment was more than 5kb. To further pinpoint the sub-region, we searched for Ebox sites in the two fragments. It has been shown that the zinc fingers of Zfh1 bind to the consensus Ebox sequence, CACCTG *in vitro* (91). We identified multiple Ebox sites in A3 and C1 fragments using the software DNASTAR (Fig.8). For *mys* and *shg*, we initially scanned the binding region from the embryo ChIP-chip data, but found no Ebox site in either (denoted as mys-772 and shg-346 in Fig.8). Thus we further searched regions downstream, and identified Ebox sites around the start codon of each gene (Fig.8). Thus, we designed qPCR primers flanking each EBox site, with the size of PCR fragment close to 100bp (Fig.8).

- **ChIP on H3K27me3 can be reproducibly carried out**

It is widely agreed that transcription factor ChIP is tough to achieve successfully, as the abundance of a particular transcription factor per cell is relatively low, and while antibodies might work well for Western Blot or immunolocalization, their behavior in the ChIP approach is usually uncertain. Thus to make sure that ChIP can be done effectively in our hands, we decided to also perform ChIP on post-translational histone marks, which comprise abundant epitopes, and for which ChIP-grade antibodies exist. Because Zfh1 was predicted to be a transcription repressor, we thought it would be useful if we chose H3K27me3, a repressive histone mark. If we were successful, the ChIP-qPCR results might then be compared for HA-Zfh1 and H3K27me3 as these might exhibit a positive correlation.

We have carried out multiple trials for the H3K27me3 ChIP-qPCR. It was clear that the histone mark ChIP was working, although with some variation among trials (Fig.9A). We reproducibly observed higher binding enrichment on all *eya* sites, compared to *mys* and *shg*. The enrichment at *eya* by H3K27me3 matched with our previous prediction, as Eya should be repressed in Zfh1 expressing cells. However, the potential situation for *shg* might be more complex. While we showed E-Cadherin expression in hub cells was suppressed by ectopic Zfh1 protein, it is known that E-Cadherin can still accumulate in Zfh1 overexpression testes (42). Thus, we must also consider the possibility that *shg* would actually not be repressed in *zfh1* expressing cells. The relative depletion on *shg* sites observed from H3K27me3 ChIP-qPCR was potentially consistent with the fact that E-Cadherin was present in Zfh1 overexpression testes.

63

- **IgG ChIP-qPCR results demonstrate low background**

As a negative control, IgG ChIP-qPCR was also carried out multiple times. Signals for IgG ChIP-qPCR were significantly lower than that for H3K27me3 and HA-Zfh1 ChIP (Fig.9A, B, C), suggesting low background in our experiments. Similar to the results for H3K27me3, we also observed variation in the absolute amount of target DNA precipitated comparing different trials. However, within each trial, the results for all the primer sets were very similar (Fig.9B). This matched with our expectation, as anti-IgG should pull down chromatin non-specifically.

- **ChIP on testes with tagged Zfh1**

The HA-Zfh1 ChIP-qPCR results were tricky to interpret. We felt confident to say that Zfh1 bound to *eya* and *shg* (Fig.9C, D). The binding also appeared more consistent on the *eya*A3 sites compared to *eya*C1, even though the genetics might have suggested stronger association with C1 compred to A3.

There are two ways to analyze ChIP-qPCR data. One is to express the data by calculating "% of Input", which compares results for ChIP'ed chromatin with the Input (un-ChIP'ed). The other is to express the data by "fold change", which calculates the signal of HA-Zfh1 ChIP relative to negative control (IgG) ChIP. We applied both methods to analyze our HA-Zfh1 ChIP data (Fig.9C, D). If the ChIP is performed successfully, an expected qPCR signal for a transcription factor is in the range of 0.05-0.3% of Input, and 5-fold change (PGFI ChIP-Seq Workshop). Thus we took 0.05% of Input, or a 5-fold change as a measure of significance when examining the plotted data. For primers of *eya*A3-5 and *shg*-346-1, we reproducibly observed an enriched signal in every trial no matter which analysis method was used. Thus we conclude that the binding on these two sites is real. For other primers applied, there was often variation among trials. But in general, the binding on *eya*A3 sites tended to be more consistent than *eya*C1 sites, which was opposite to what we expected (see Discussion). We took into account that signal differences observed in ChIP-qPCR might be due to biological variation within each batch of testes processed. But, if one focuses on the data within one trial, there were consistent results using different primer pairs representing the same gene fragement. For example, eyaA3-4 and eyaA3-5 were two different primer pairs targeting Ebox2 of *eya*A3. The results for using these two primers were pretty similar within each trial. This suggested strongly to us that each individual experiment was of good quality.

- **The anti-HA antibody used in HA-Zfh1 ChIP experiments is specific**

To investigate the specificity of the antibody against HA, we also performed ChIP-qPCR on Nanos>Upd testes, samples with the same phenotype as Zfh1 overexpression testes but lacking any HA epitope. We expected to see relatively reduced qPCR signals on these negative control testes. Given the signal variation in ChIP-qPCR experiments,

64

we compared results of experiments that were performed at a similar time. For anti-HA ChIP, signals on the negative control Nanos>Upd testes were often 4 times lower than those on the positive control EyaA3>3×HA-Zfh1 (Fig.9E). For ChIP controls in these experiments, anti-H3K27Me3 and anti-IgG ChIP, signals on Nanos>Upd samples were on the same order, and followed the same trend as EyaA3>3×HA-Zfh1 (Fig.9F, G). Thus, we concluded the rabbit anti-HA used in ChIP experiments is specific.

The size distribution of sequencing libraries prepared from ChIP'ed chromatin has an aberration

We have prepared libraries for the sequencing part of the project. We could reproducibly make libraries from Input (un-ChIP'ed) chromatin. As assayed by BioAnalyzer, the size distribution of such libraries was enriched for a single peak in the 200-300bp region (Fig.10A), which was perfect for sequencing. However, for libraries prepared from ChIP'ed chromatin, we often observed two peaks on the BioA graph (Fig.10B). The lower-sized peak was similar to what was observed in Input libraries, with the correct size and concentration for sequencing. The second peak, representing a higher molecular size, should not be present, and it may interfere with the sequencing. To address this problem, we discussed potential solutions with experts in the Functional Genomics Core. There were two possibilities for the nature of the DNA comprising the additional upper peak. The first was that it represents a pool of larger DNA fragments in the ChIP's samples. The ChIP protocol involves extensive sonication to reduce chromatin size. Perhaps the size distribution of our initial chromatin was too broad, and we had larger than desirable DNA size among the ChIP'ed chromatin. We therefore size-selected the already generated libraries. This method got rid of the additional upper peak (Fig.10C), but at the same time also unavoidably reduced the concentration of the sample below the minimum requirement for sequencing.

A second possibility was that the upper peak represented DNA concatamers assembled from multiple smaller (and appropriate) sized chromatin fragments. This can occur as one outcome of a PCR step during library preparation, where a low PCR primer concentration may cause the formation of concatamers. One way to bring concatemers back to individual chromatin was to re-do the PCR for two cycles with freshly added primers. We also tried this alternative trouble-shooting method. But the upper peak did not disappear in the subsequent BioA analysis (data not shown).

We have prepared enough samples using the first trouble-shooting method, and are waiting in the queue to have our samples sequenced.

Genetic modifier Screen for Zfh1

A modifier screen is a powerful genetic approach to identify suppressors and enhancers of the phenotype caused by sustained Zfh1 expression. Ideally, such a screen would involve reducing the gene dose for some factor necessary **for** Zfh1 to act, or to

65

antagonize Zfh1 function. Thus, to conduct a successful modifier screen, a sensitized background is preferred, where the extent of phenotype is likely to be manipulated by the dosage of genes. The testes used for ChIP-Seq purposefully had an extreme phenotype, as extra CySCs and GSCs filled the entire testis. Such a phenotype would not be ideal for a modifier screen, since a potential suppressor or enhancer may not be able to influence it. Thus we conducted a time course experiment to visualize the progression of the stem cell tumor phenotype caused by sustained Zfh1 expression. We hoped to identify a stage when the testes had a moderate phenotype. I will state our findings, and our screen plans below.

The stem cell tumor phenotype develops progressively from the tip of testes

In order to obtain the full blown stem cell tumor phenotype, crosses for generating flies with ectopic Zfh1 expression were set up at 18°C to avoid the lethality caused by Zfh1 overexpression during development. The suppression of Gal4-UAS system was achieved by the expression of a temperature sensitive allele of Gal80 (Gal80ts), which repressed the Gal4 function at the permissive temperature (18°C). Young flies that eclosed from the crosses were shifted to 29°C to inactivate Gal80ts function, and allow the expression of Gal4-UAS (and, thus Zfh1). 12 days after aging at 29°C, bright DNA staining, a marker for actively dividing cells, were observed throughout the entire testis, and the testes were enriched with extra CySCs and GSCs (Fig.11E).

In the time course experiment, we examined the presence of bright DNA staining in testes aged for various times at 29°C (Fig.11A). At 3 days after induction of Zfh1 bright DNA was still generally restricted to the testis tip, similar to samples prior to the temperature shift (Fig.11B, C); but at 6 days of Zfh1 expression, the bright DNA region had expanded to the middle of the testis tube (Fig.11D). We quantified the area of bright DNA staining using ImageJ (see Materials and Methods). As shown in Fig.11F, the fraction of testis filled with bright DNA increased steadily as testes were aged at 29°C for longer periods of time. We noted some variation of the phenotypic strength among testes grown under the same conditions and aged for the same period. However, this variation did not obscure the general trend (Fig.11G). Thus, we concluded that phenotypic progression depended on how long ectopic 3×HA-Zfh1 had been expressed.

Design and current progress of the screen

The results from the time course experiment suggested that testes aged at 29°C for 6 days were a better background in which to conduct the modifier screen. We hypothesized that by analyzing the fraction of testis filled with bright DNA, we could identify modifiers in either direction. For example, a suppressor or enhancer could either shrink or expand the region with bright DNA staining in 6-day testes, making those 6-day testes appear more like 3-day or 12-day samples, respectively. Note that a phenotypic

66

"suppressor" in this genetic experiment (where we are **reducing** gene dose) would encode a **positive** factor acting along with Zfh1.

To test this basis of our screen, we first carried out a pilot, using mutant alleles for genes predicted to play a role downstream of (or in collaboration with) Zfh1. Our previous results showed that Zfh1 was a transcriptional repressor in testes, and ectopic Zfh1 in cyst lineage initiated BMP ligand expression to guide GSC renewal. Thus genes chosen for the pilot screen included CtBP (a known co-repressor of Zfh1), Punt (a BMP receptor), and Med (a BMP transducer), Dally Dlp (BMP co-receptors). Results showed that with only one copy of *CtBP*, testes aged at 29°C for 6 days had a reduced fraction of bright DNA (Fig.12). This was consistent with what we expected, since CtBP was also required for CySC maintenance and Zfh1 function (42). We did not observe a change of phenotype when the dose of components of BMP pathway was reduced (Fig.12).

To conduct the modifier screen, we decided to use deficiency lines from Exelixis library. Each line has molecularly defined end-points, and collectively, the lines cover about 50% of genes on the 3rd chromosome (103). Thus, if any positives were identified, we should be able to easily test each of the annotated genes contained within the deficiency in order to identify the relevant gene. We have screened 26 lines so far. Df(3L)Exel6101 may be a potential hit (data not shown) but further experiments are needed to verify its candidacy.
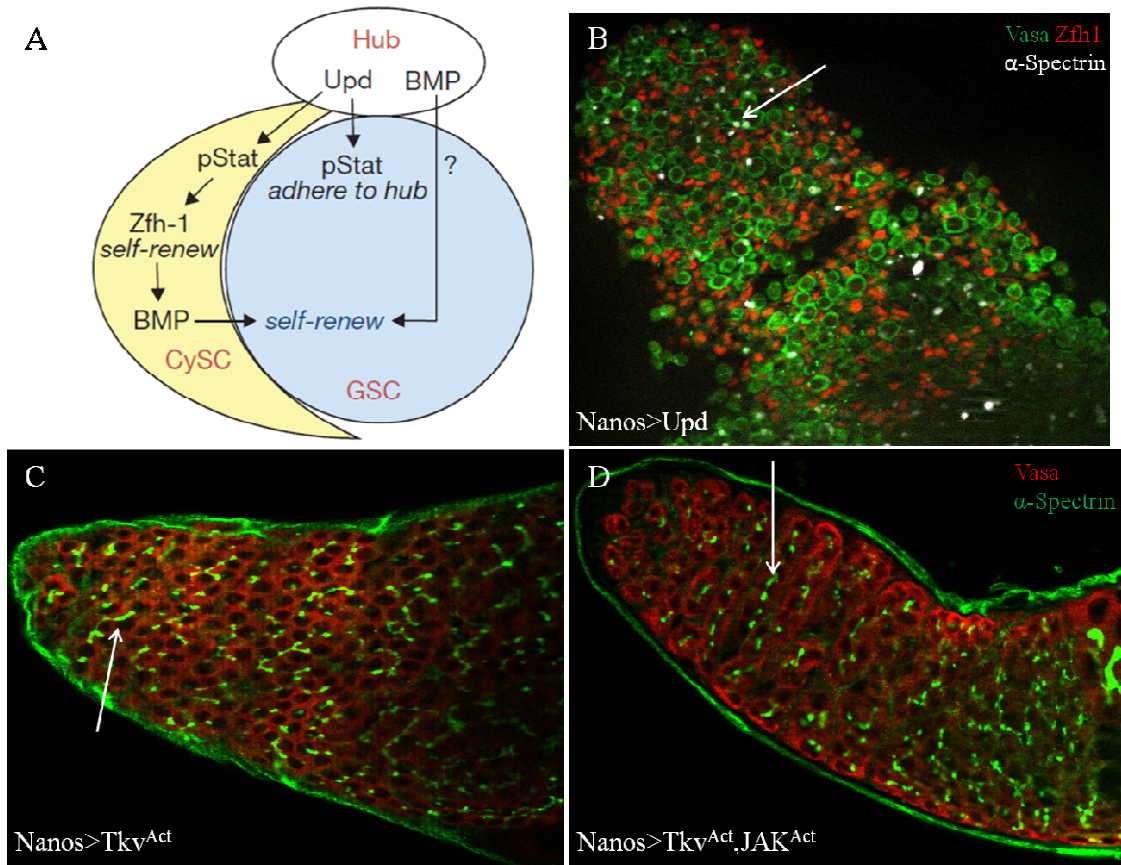
Figure 1. The self-renewal of GSCs is governed by CySCs via BMP pathway and other unknown signaling. (A) A model proposed based on the previous work in our lab (copied from Fig.4E in ref (40)). JAK-STAT is important for GSC anchorage to the hub, while BMP signals emanating from CySCs control GSC self-renewal. The expression of BMP ligands in CySCs is (genetically) induced by Zfh1, a transcription factor downstream of JAK-STAT activation. (B) When the JAK-STAT ligand Upd is ectopically provided (in this case, from germline cells), testis exhibits many extra GSCs with dotted fusome (α-Spectrin, white, arrow), as well as CySCs (Zfh1, red). (C) Ectopic BMP activation in the germline using a constitutively activated form of Type I receptor Tkv^{Act} does not result in extra stem cells, as the majority of germ cells exhibit branched fusomes (α-Spectrin, green, arrow). (D) Ectopic activation of both BMP and JAK-STAT in the germline also does not give rise to a stem cell tumor phenotype, as germ cells exhibit branched fusomes.
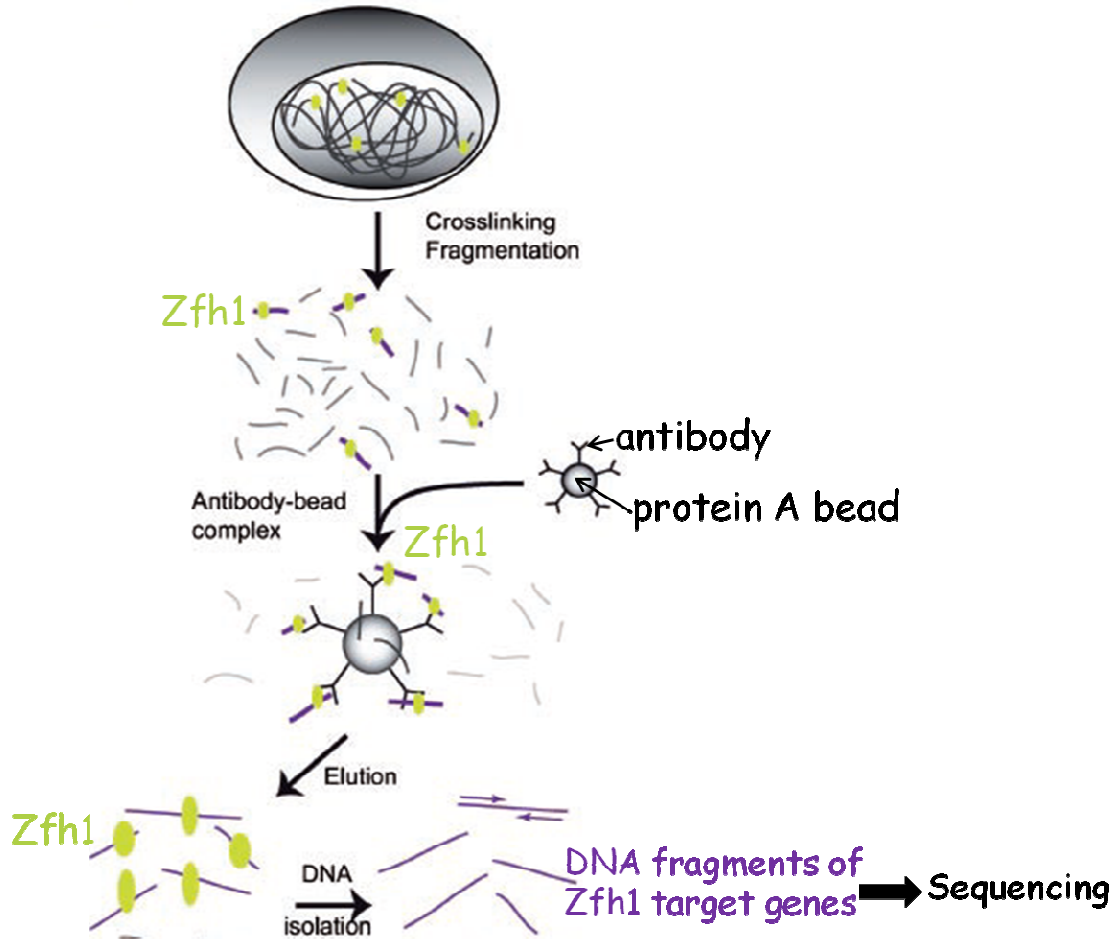
Figure 2. The general procedure of ChIP-Seq. First, cells of interest are enriched, and chromatin and protein are cross-linked using formaldehyde. Second, chromatin isolated from cell lysates are fragmented by sonication. Third, immunoprecipitation (IP) is performed on chromatin fragments using antibody-conjugated beads. Forth, pulled down chromatin-protein complexes are isolated, and the IP'ed chromatin is eluted by reversing the cross-linking. Finally, purified DNA fragments are assembled into a library and sequenced. This figure is modified from Fig.1A in ref (104).
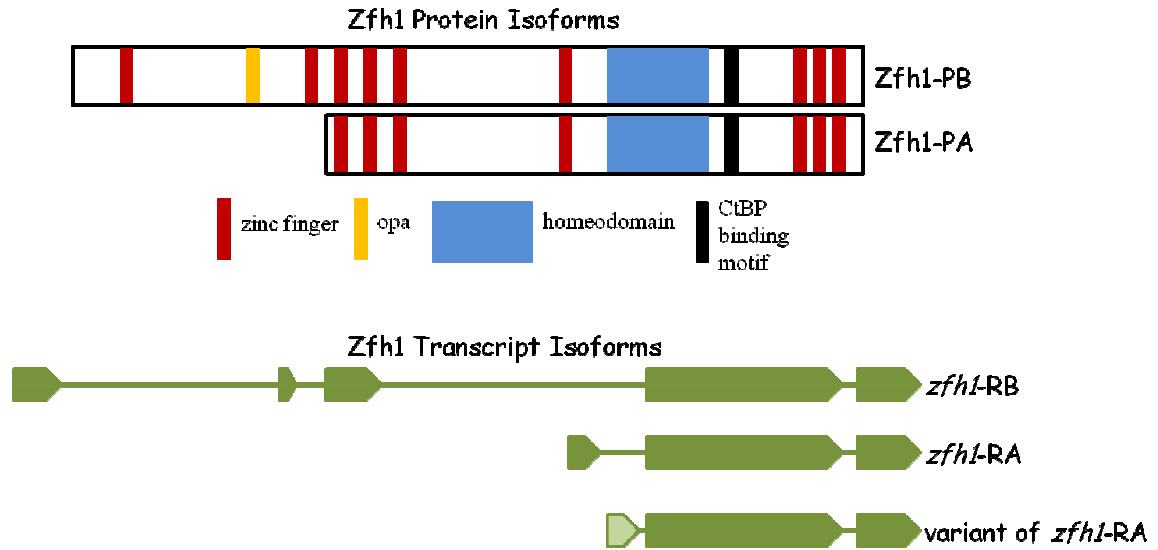
Figure 3. Isoforms of Zfh1 protein and transcript. There are two Zfh1 isoforms, each has an N-terminal zinc finger cluster, a homeodomain, a CtBP binding motif, and a C-terminal zinc finger cluster. Zfh1-PB is longer than Zfh1-PA, with two additional zinc fingers and a polyQ region towards the N-terminus. In *Drosophila* embryos, *zfh1*-RB and *zfh1*-RA are transcripts corresponding to the two protein isoforms respectively. In the testis, *zfh1*-RB and an alternative form of *zfh1*-RA were detected.
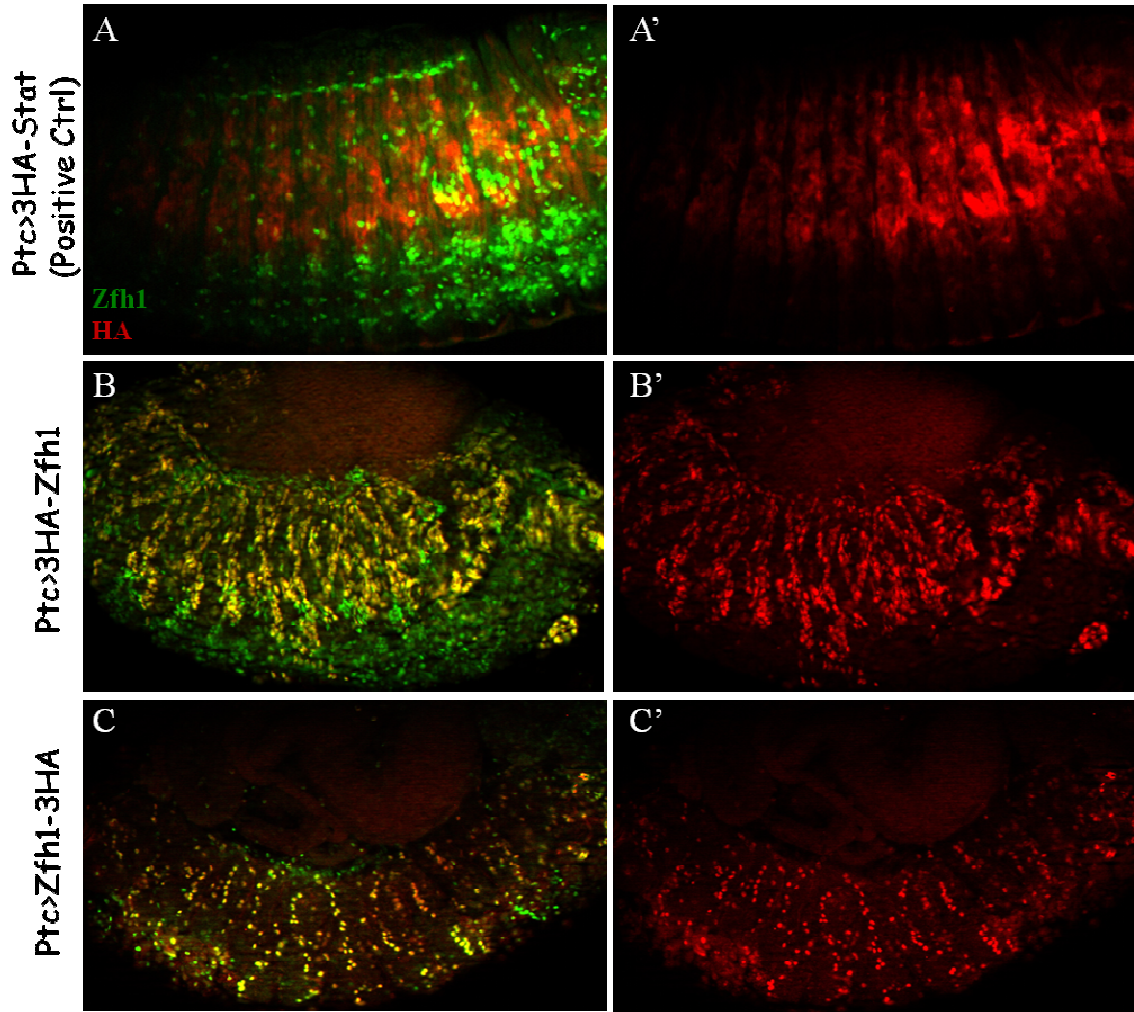
Figure 4. Tagged UAS-Zfh1-RB can be expressed properly in embryos. (A) A positive control line with N-terminally 3×HA tagged UAS-STAT was driven by Patch-Gal4, resulting in ectopic HA expression (red, A') in a pattern of stripes. Notice endogenous Zfh1 (green) was not predominantly expressed in HA+ region. (B, C) When driven by Patch-Gal4, either N- (B) or C- terminally (C) 3×HA tagged UAS-Zfh1-RB lines exhibited ectopic HA expression (red, B', C'). Antibodies against Zfh1 could also detect the ectopic protein (green), as Zfh1 staining now overlapped with HA (yellow). The patterning of embryos overepxressing Zfh1 appeared misorganized, the much smaller size of HA+ cells in C' indicated that these cells were undergoing apoptosis.
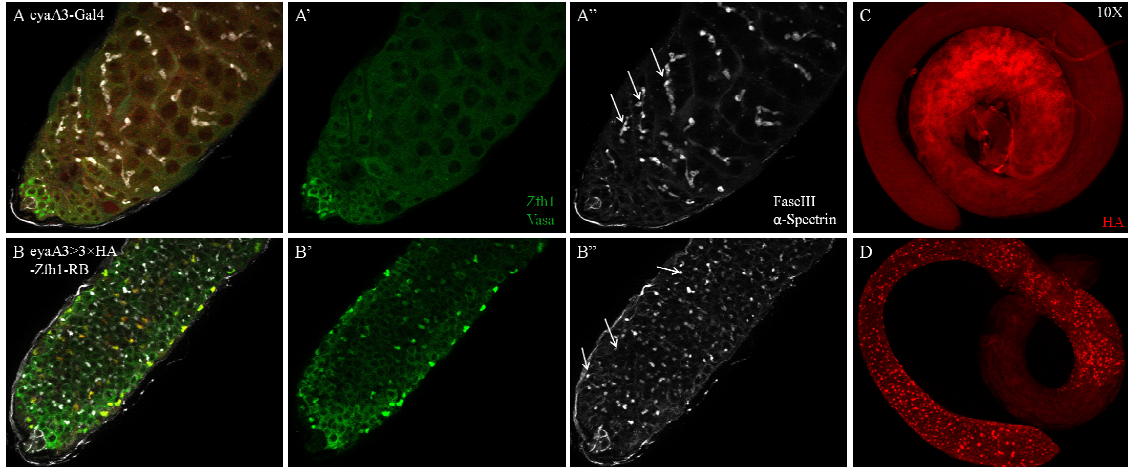
Figure 5. The N-terminally 3×HA tagged UAS-Zfh1-RB gives rise to ectopic GSCs and CySCs at 100% penetrance and with high expressivity. (A) The control testis with a cyst lineage Gal4 expression (eyaA3-Gal4) only had CySCs (Zfh1+ cells, A') and one tier of GSCs near the hub (FascIII, A"), with most germ cells (Vasa+, A') exhibiting branched fusomes (α-Spectrin, A", arrows). (B) When overexpressed in the cyst lineage, N-terminally 3×HA tagged UAS-Zfh1-RB caused ectopic CySCs (Zfh1+ cells, B') and GSCs (Vasa+ cells with dotted α-Spectrin staining, B', B", arrows) throughout the testis. The stem cell tumor phenotype was present in all testes scored (n=24). (C, D) Ectopic HA expression was detected in the entire testis with tagged Zfh1 expression (D), but not in Gal4 only control testis (C). Images of A and B were taken using 40x lens, whereas C and D were snapshots under 10x.

72

A WB: Rat anti-HA

Eva   Eva   w1118
HA-STAT HA-Zfh1 embryo

B IP: Rabbit anti-HA, WB: Rat anti-HA

8: pos ctrl (Eva HA-Zfh1 whole cell lysate)
9: neg ctrl (Gal4 or UAS only testes)
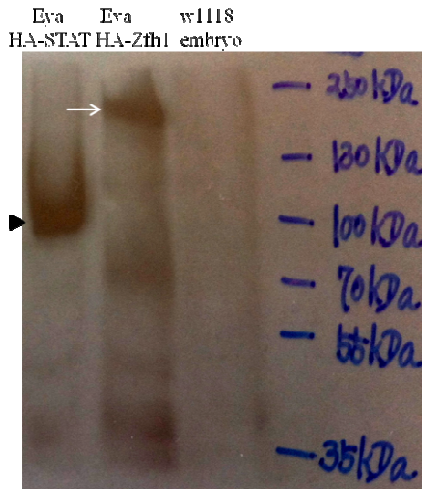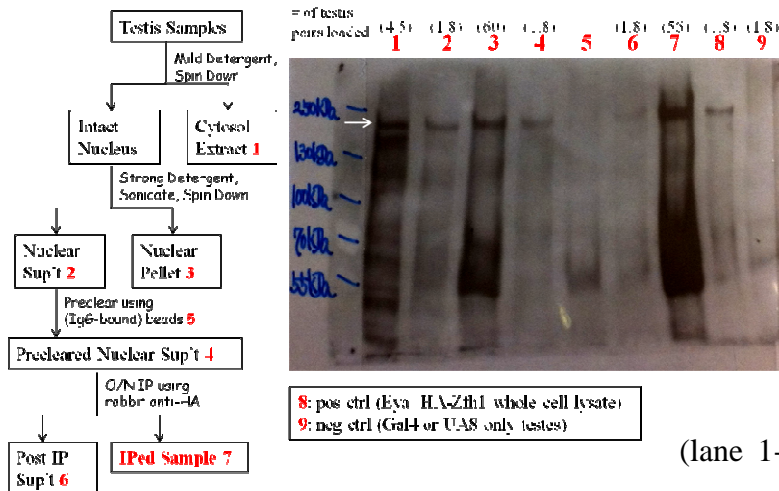
C IP: Rabbit anti-HA, WB: Rat anti-HA
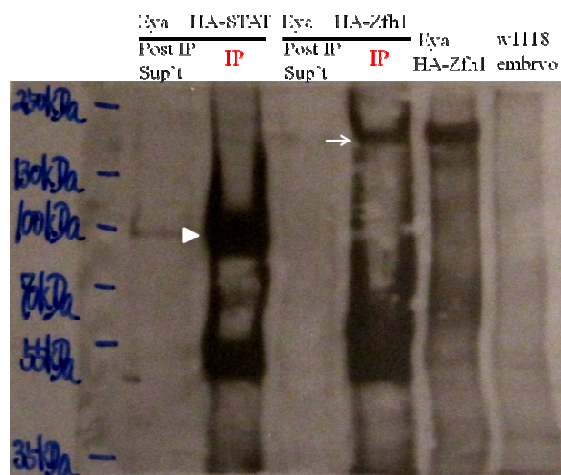
Figure 6. Rabbit anti-HA can immunoprecipitate (IP) tagged Zfh1-PB from testis lysates. (A) Using an antibody against HA developed in rat, a dominant band with the size similar to that predicted for Zfh1-PB was detected in whole cell lysates isolated from Zfh1 overexpression testes (arrow). A specific band also appeared for testis sample overexpressing tagged STAT (arrowhead), a positive control for the experiment. No band was detected in lysates isolated from w1118 embryos. (B) IP was performed following the ChIP protocol (the flow chart). Zfh1 overexpression testes were used, but they were not treated with formaldehyde to cross-link chromatin and protein. Using a commercial ChIP-grade anti-HA antibody raised in rabbit, the tagged Zfh1 could be pulled-down (lane 7). The tagged proteins could also be tracked during each step of the protocol (lane 1-6). (C) Results for another IP trial. The specific Zfh1 band was present in the IP'ed sample (arrow), but not in the post IP supernatant. For the positive control sample with tagged STAT overexpression, a band specific to STAT was also present in the IP'ed sample (arrowhead).

73
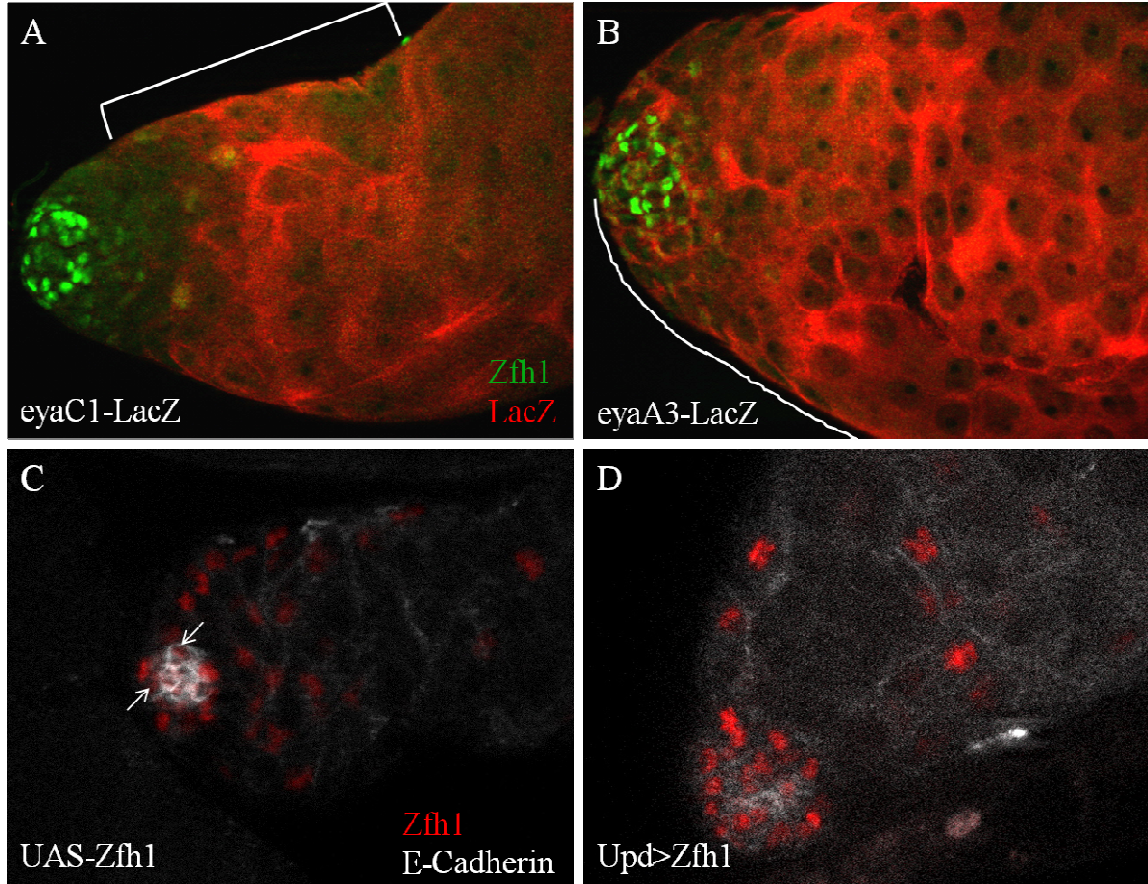
Figure 7. *eya* and *shg* (E-Cadherin) may be putative targets of Zfh1. (A, B) eyaC1-LacZ and eyaA3-LacZ were reporter lines of two regulatory fragments of *eya*. The expression of eyaC1-LacZ was restricted to differentiating cyst cells (A, red, bracket), but not in CySCs where Zfh1 was expressed (A, green). In contrast, eyaA3-LacZ was present in the entire cyst lineage, including Zfh1+ cells (B, green) and differentiating cyst cells (B, drawn white curved line). (C) E-Cadherin (white) was enriched in hub cells, where Zfh1 expression (red) was low (arrows). (D) When ectopic Zfh1 was expressed in the hub (red), the expression of E-Cadherin (white) was reduced.
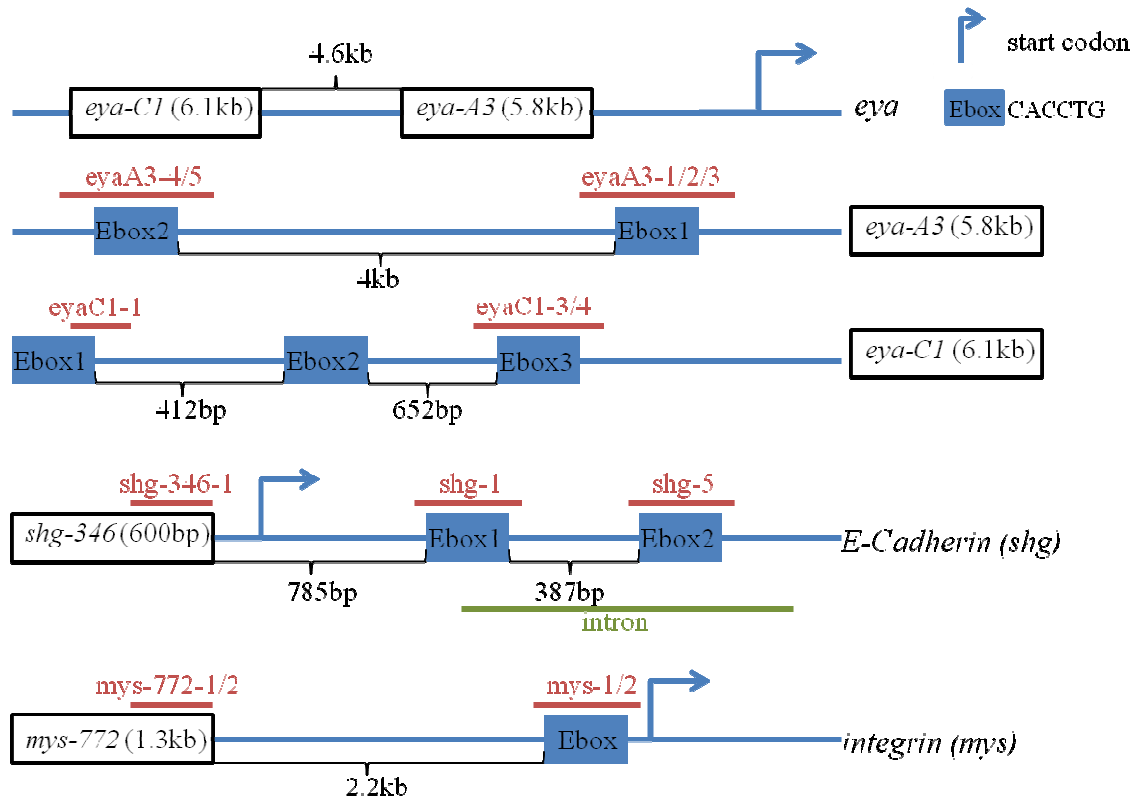
Figure 8. Primers designed for ChIP-qPCR. The sequences of eyaC1 and eyaA3 came from studies performed by Bonini *et al.* (101), and shg-346 and mys-772 were identified from a Zfh1 ChIP-chip experiment using wildtype embryos (100). Sequences downstream of shg-346 and mys-772 were from Flybase. The presence of Ebox site (CACCTG) to which Zfh1 binds was identified using DNASTAR. Predicted amplicons (red) derived from qPCR primers designed that flanked each EBox site, with the size of PCR fragment close to 100bp.

75

A

H3K27Me3 ChIP-qPCR

Legend: 1st trial, 2nd trial, 3rd trial, 4th trial, 5th trial

Y-axis: % Input

X-axis: eyaA3-1, eyaA3-2, eyaA3-3, eyaA3-4, eyaA3-5, eyaC1-1, eyaC1-3, mys-772-1, mys-772-2, mys-1, mys-2, shg-346-1, shg-5

B

IgG ChIP-qPCR

Y-axis: % Input

X-axis: eyaA3-1, eyaA3-2, eyaA3-3, eyaA3-4, eyaA3-5, eyaC1-1, eyaC1-3, mys-772-1, mys-772-2, mys-1, mys-2, shg-346-1, shg-5

C

HA-Zfh1 ChIP-qPCR

Y-axis: % Input

X-axis: eyaA3-1, eyaA3-2, eyaA3-3, eyaA3-4, eyaA3-5, eyaC1-1, eyaC1-3, mys-772-1, mys-772-2, mys-1, mys-2, shg-346-1, shg-5

D

HA-Zfh1 ChIP-qPCR

Y-axis: Fold Change

X-axis: eyaA3-1, eyaA3-2, eyaA3-3, eyaA3-4, eyaA3-5, eyaC1-1, eyaC1-3, mys-772-1, mys-772-2, mys-1, mys-2, shg-346-1, shg-5

Figure 9. ChIP-qPCR results. (A) The H3K27me3 ChIP-qPCR reproducibly showed higher binding enrichment on all eya sites, compared to mys and shg. (B) Signals in IgG ChIP-qPCR was much lower than either H3K27me3 or HA-Zfh1 ChIP (notice the different scales of the Y-axis). (C, D) Analysis of HA-Zfh1 ChIP-qPCR using two approaches: % of Input (C), and fold change (D). The minimum point of the Y-axis was set to either 0.05 (C) or 5 (D), an accepted cutoff threshold thought to represent successful ChIP-qPCR (PGFI ChIP-Seq Workshop). Signal enrichment was reproducibly observed for primers of eyaA3-5 and shg-346-1. In general, the binding on eyaA3 sites tended to be more consistent than eyaC1 sites. (E-G) Comparison of ChIP-qPCR results using either tagged Zfh1 overexpression testes (blue, red, and green bars) or JAK-STAT overexpression testis (black bar). For anti-HA ChIP, signals on Nanos>Upd testes were often 4 times lower than those on Zfh1 overexpression testes (E). For anti-H3K27Me3 and anti-IgG ChIP, signals on Nanos>Upd samples were on the same order, and followed the same trend as EyaA3>3×HA-Zfh1 (F, G).
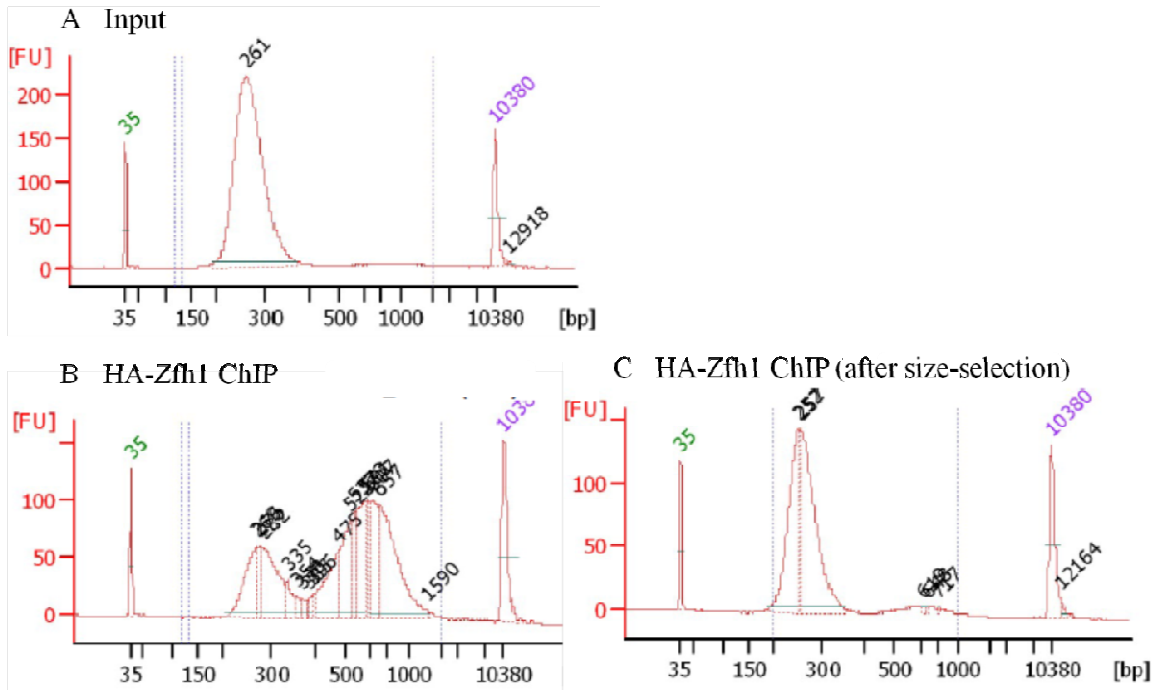
Figure 10. The size distribution of sequencing libraries prepared from ChIP'ed chromatin has an aberration. (A) Libraries prepared from Input (un-ChIP'ed) chromatin exhibited an enrichment in the 200-300bp region. This pattern of size distribution was perfect for sequencing. (B) Libraries generated from HA-Zfh1 ChIP'ed chromatin had two peaks on the BioA graph, with a second peak representing a higher molecular size. (C) After size-selection, the additional upper peak disappeared, but the concentration of the sample was also unavoidably reduced (data not shown).

78
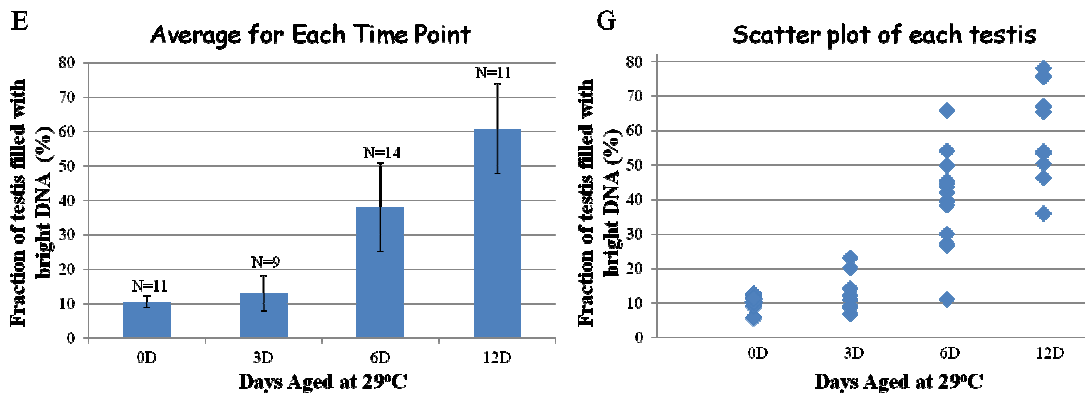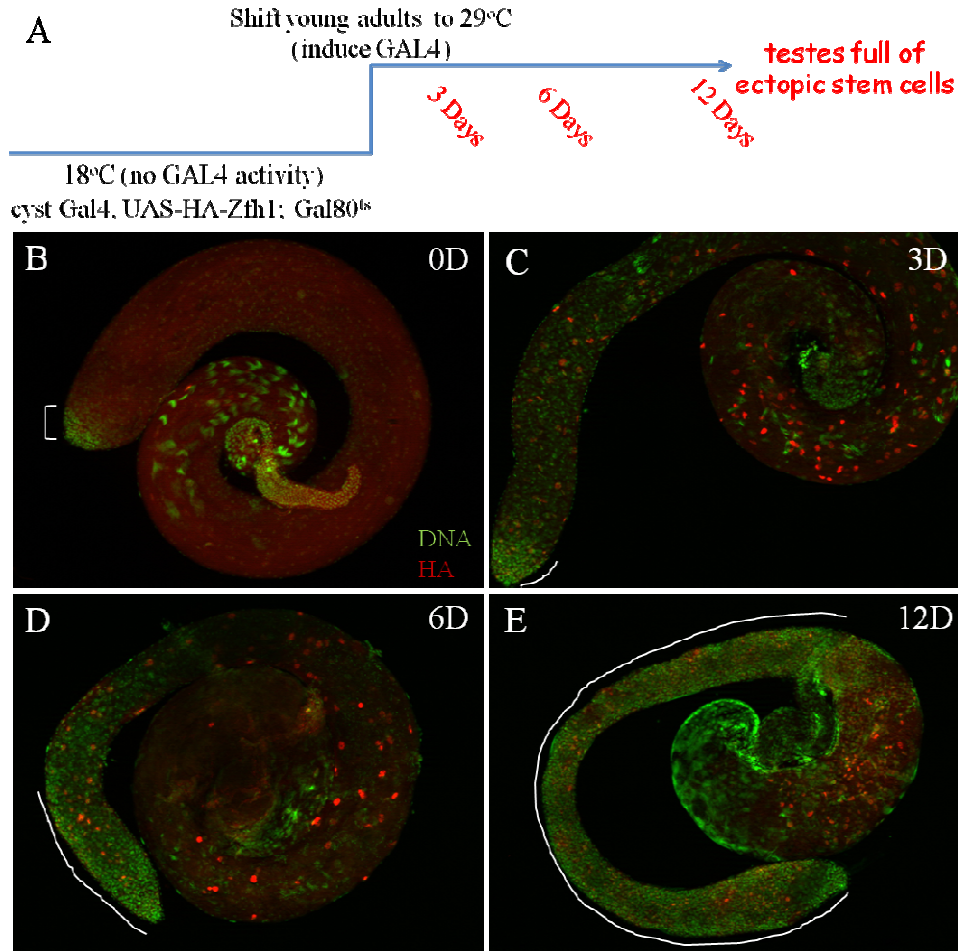
Figure 11. The stem cell tumor phenotype caused by Zfh1 overexpression develops progressively from the testis tip. (A) The schematic design of the time course experiment. (B-D) The bright DNA region (green) was expanded gradually from the tip of the testis (bracket, drawn white curved lines), as tagged ectopic Zfh1 (red) was sustained. (E) Statistical measurement of the fraction of testis filled with bright DNA at each time point. (F) A scatter plot of the measured bright DNA fraction for each testis in the time course experiment.
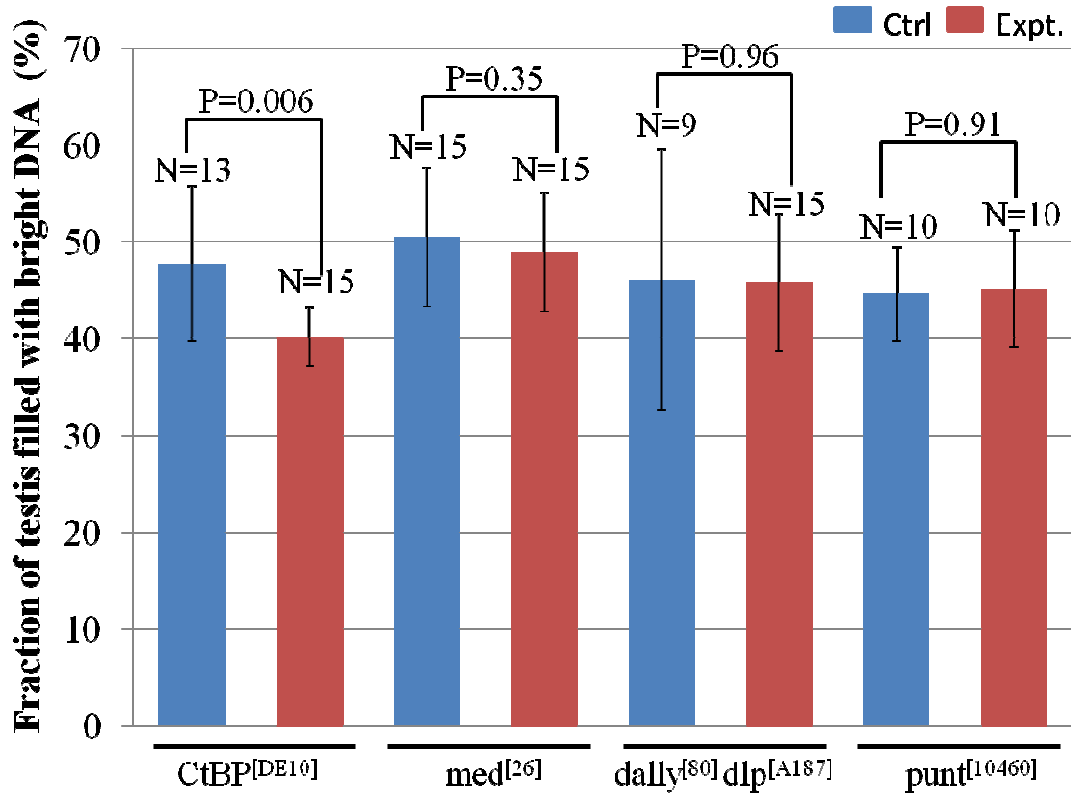
Figure 12. Results of Zfh1 pilot screen. Genes shown here are: CtBP (a known co-repressor of Zfh1), Punt (a BMP receptor), and Med (a BMP transducer), Dally Dlp (BMP co-receptors). Genotypes are: 3×HA-Zfh1/eyaA3-Gal4; +/tubulin-Gal80ts (Ctrl), and 3×HA-Zfh1/eyaA3-Gal4; mutant allele of selected gene/tubulin-Gal80ts (Experimental).

Discussion

The transcription factor Zfh1 is an important stem cell regulator in *Drosophila* testes (42). Here we attempt to identify target genes of Zfh1 using two complementary approaches, ChIP-Seq and a genetic modifier screen. We generated an N-terminally 3×HA tagged UAS-Zfh1-RB line, which proves to be an appropriate reagent for carrying out ChIP using anti-HA antibodies. Results from our preliminary ChIP-qPCR experiments showed that Zfh1 was enriched at sequences from the regulatory region near *shg* and *eya*. We also found that the ability of Zfh1 to cause a stem cell tumor was reduced under conditions where the co-repressor CtBP was impaired. These preliminary results demonstrate the feasibility of the two independent approaches.

How are excess stem cells induced in Zfh1 overexpression testes?

The stem cell tumor phenotype resulting from Zfh1 overexpression is dramatic. The development of ectopic stem cells (CySCs and GSCs) involves dedifferentiation, a process in which differentiated cells revert to stem cells. Understanding how dedifferentiation occurs *in vivo* will aid in elucidating the mechanism of tissue regeneration. In our experiments, ectopically produced Zfh1 protein was restricted to the cyst lineage. However, Zfh1 overexpression also influenced the neighboring germline lineage, as excess GSCs were induced. This non-autonomous effect of Zfh1 demonstrates that one type of stem cell can serve as a niche, producing factors to control the maintenance of another stem cell population. Studying signals that guide the behavior of the second stem cell lineage will further aid our understanding in stem cell-niche biology.

For these reasons it is intriguing to consider how the phenotype in Zfh1 overexpression testes is developed simply by manipulating the expression of a single gene. Albeit oversimplified, it is reasonable to dissect the question into three sub-questions: 1) which cell stage generates the *de novo* stem cells? 2) how do *de novo* stem cells proliferate to create the stem cell tumor? 3) and, what is the non-autonomous mechanism that induces GSCs? We do not have definitive answers to these questions. But observations made in the time course experiment may have given us some clues. Below I will discuss the three sub-questions respectively, and present some speculation.

We think the *de novo* cyst stem cells are generated by de-differentiation from early-stage cyst cells. The Gal4 driver used to express Zfh1 ectopically will drive Zfh1 expression in all cyst cells, even late-stage cyst cells normally associated with meiotic germ cells. In fact, epitope-tagged Zfh1 was visible throughout the entire testes, even after only 3 days of Zfh1 expression. However, the bright DNA signal, a marker for actively dividing cells, was initially restricted to the apical tip of the testis, where the endogenous proliferation center is located. Only after Zfh1 was expressed for longer periods, did the region of bright DNA gradually expand further down the testis. We conclude that not all somatic cells ectopically expressing Zfh1 are converted into stem cells. This, in turn, suggests that cells at different developmental stages of a lineage have

81

differential potential to change back to stem cells. Obviously here, cells closer to the endogenous pool of stem cells have stronger potential to become stem cells. Because all cyst cells, the differentiating progeny of CySCs, have exited from cell cycle, the fact that they re-initiate division suggests that they have regained some stemness properties. These potential candidates are also cells that are at an earlier stage of differentiation; for example, they have exited the cell cycle only very recently. This observation is consistent with previous findings in the field. It has been shown that early rather than late stage germ cells (spermatogonia) can dedifferentiate to become GSCs (49). Thus, in a similar manner, among cyst cells now expressing Zfh1 the early stage cells may be easier to convert back to CySCs.

As for the second sub-question, it is reasonable to think that the generation of the stem cell tumor is caused mainly by continuous proliferation of *de novo* stem cells. The newly formed stem cells as described above are constantly dividing. Normally, in the testis system, the division of stem cell is often asymmetric, as one daughter retains stemness, whereas the other starts to differentiate (32). However, in Zfh1 overexpression testes, since the CySC determinator is expressed in the entire lineage, the fate of a newly produced daughter cell should also be stem cell, and the progeny of this daughter cell retain the stemness too. Thus, their continued division in this manner can account for the tumor.

It is worth mentioning that we occasionally observed a small patch of cells exhbiting brightly staining DNA in the middle of the testes, spatially disconnected from the proliferating cells at the testis tip (data not shown). This suggests that occasionally late stage cyst cells can be converted back to CySCs, perhaps if Zfh1 expression has been maintained for long enough. In the future, this possibility should be examined more closely to determine whether late-stage dedifferentiation might contribute to tumor formation.

For the third sub-question, recall that the induction of new GSCs relies on the successful generation of new CySCs. Thus, it is reasonable to think that early cyst cells which are more prone to become CySCs play a role to coax nearby spermatogonia to dedifferentiate into new GSCs. We found that germ cells with dotted fusomes, a marker for GSCs, were not observed in excess in testes 3 or 6 days after Zfh1 induction (data not shown). Therefore, we think the dedifferentiating germ cells do not adopt GSC fate immediately. Rather, germ cells may first regain the property of division, producing more cells similar to them. As Zfh1 expression remains high in the neighboring somatic cells (now becoming CySCs), the actively dividing germ cells then gradually become *bona fide* GSCs. How this two-step (or even multi-step) conversion correlates with changes happening as cyst cells convert into true CySCs is unknown.

Can Zfh1 be a transcriptional activator?

82

The HA-Zfh1 ChIP-qPCR result shows that Zfh1 appeared enriched near *shg*, the gene encoding the *Drosophila* homologue of E-Cadherin. Since Zfh1 is predicted to be a transcriptional repressor, this binding suggests that E-Cadherin is suppressed in Zfh1 overexpression testes. However, in Zfh1-overexpressing testes, Judy Leatherman found that E-Cadherin actually accumulated in Zfh1+ cells. This is not consistent with the idea that Zfh1 is repressing E-Cadherin expression. In addition, H3K27me3, a repressive histone mark, also appears relatively depleted in *shg* regulatory region. Thus how do we explain the conflicting findings? One possible explanation is that Zfh1 is generally acting as a repressor in testes, but its binding near *shg* is not functional because other nuclear partners that would be required for effective repression are not recruited to the *shg* site. Therefore the expression of *shg* is not suppressed in spite of the binding of Zfh1. Another possibility is that Zfh1 may actually function as a transcriptional activator at some target genes, such as *shg*. One argument against this may be that E-Cadherin is suppressed by ectopic Zfh1 in hub cells. However, the presence of other DNA-binding proteins as well as transcription co-factors around the regulatory region of *shg* may be quite different in hub cells and CySCs, thus the effect of Zfh1 on *shg* in these two different cell types may be different. It has been shown that many transcription factors can work as both repressors and activators depending on promoter and cellular context, as well as availability of other proteins (105). Thus it is possible that Zfh1 may serve as a transcriptional activator for *shg* in CySCs.

The possibility that Zfh1 may be a transcriptional activator can also help to explain the perplexing results for *eya*A3 and *eya*C1. The expression of *eya*A3-LacZ is present in both CySCs and cyst cells, whereas *eya*C1-LacZ is only expressed in cyst cells. Since Zfh1 was originally thought to be a transcriptional repressor, we hypothesized Zfh1, normally enriched in CySCs, would bind more effectively to C1 than A3, accounting for C1 repression in CySCs. Therefore we expected that C1 would exhibit a higher relative enrichment than A3 in the Zfh1 ChIP. However, enrichment of HA-Zfh1 to A3 appeared to be more consistent than to C1. The confounding results can be explained if Zfh1 can also act as a transcription activator. Zfh1 can then bind to A3, and activate its expression in CySCs. The reciprocal expression pattern of C1 and Zfh1 may be explained as a coincidence, only indicating the possible binding. Nevertheless, previous genetic data show that Eya is suppressed in Zfh1+ cells, and my own H3K27me3 ChIP-qPCR support this idea. We think this can be explained by the fact that there exist multiple *eya* regulatory elements (101). Thus the regulation of *eya* expression may be complex, involving other elements and proteins, and is not dictated solely by A3 and Zfh1.

Another argument against the notion that Zfh1 may be a transcriptional activator is that reduced expression of CtBP, the co-repressor of Zfh1, dampens stem cell tumor phenotype. This observation can be explained by two possibilities. One is that CtBP may also instead function as a co-activator in Zfh1+ cells. In *Drosophila*, *in vitro* and *in vivo* experiments have demonstrated that monomers of CtBP activate some Wingless targets,

83

whereas dimers repress the expression of other genes (106). Thus CtBP can be a co-activator depending on its oligomeric state. The other possibility is that Zfh1 can serve as both an activator and a repressor in CySCs, depending on which gene it regulates, that is, on context of its binding sites, or of other regulatory factors involved. Recently, strong data from Eileen Furlong's lab has shown that *snail*, a well-established transcriptional repressor during *Drosophila* embryogenesis can also function as an activator for other target genes in the same type of cells (107). Thus, it is possible that Zfh1 may also play a dual role in CySCs.

Are there better approaches to identify direct targets of Zfh1?

The ChIP-qPCR experiment on H3K27me3 demonstrates that we can execute a ChIP experiment successfully, at least for relatively abundant histone marks. Our results on HA-Zfh1 ChIP-qPCR, while suggestive, have been somewhat inconclusive. The sequencing of libraries should provide us with more potential positive controls, and those can be used for further refining the experimental procedure to successfully carry out ChIP for Zfh1. Nevertheless, there exist two major limitations of the HA-Zfh1 ChIP-qPCR experiment, which may prevent us from obtaining successful and comprehensive ChIP-Seq results. First, it is intrinsically difficult to perform ChIP on a small number of cells, which is what we are attempting to do here. Second, the positive controls chosen for ChIP-qPCR come from a gene list generated by a Zfh1 ChIP-chip experiment conducted on wildtype embryos. This experiment was carried out in a large scale cis-regulatory annotation project, so the gene list has not been verified by those investigators using ChIP-qPCR and anti-Zfh1 (100). In addition, that work used an antibody against Zfh1, one that we have not been able to verify as working in our embryo ChIP (see Addendum). For these reasons, we cannot be certain that the genes we selected are definitively "positive controls". Because of these caveats to our current ChIP-Seq experiment, it is worthwhile thinking about alternative approaches to identify direct targets of Zfh1.

A modified version of ChIP is to FACS sort *zfh1* expressing CySCs and conduct ChIP starting from a pure population of cells. In the current ChIP-qPCR experiments, testis samples are used, therefore, a lot of cells without Zfh1 expression also go into the ChIP. The high amount of chromatin from these cells may interfere with the specific binding of the antibody. In contrast, the FACS method can produce an enriched pool of *zfh1* expressing cells. This would allow the antibody to have a higher chance of recognizing the correct epitope during ChIP. We have generated flies with tagged UAS-Zfh1 and UAS-GFP. This reagent will be useful for performing the GFP-based FACS before ChIP.

An alternative approach to identify direct targets of Zfh1 is DamID (DNA adenine methyltransferase identification). DNA adenine methylation is widely present in bacterial genomes, but not in eukaryotes. When the Dam enzyme is fused to a transcription factor, and expressed in eukaryotic cells, DNA near the binding site of the transcription factor

will be modified by the tethered Dam (108). The detection of the modification can be achieved by Methyl PCR. A specific antibody against the transcription factor is not required in DamID, thus the method is not restricted by the quality of an antibody reagent. We have obtained the UAS construct to make Dam fused with Zfh1, and it should not be straight-forward for us to try this alternative approach.

Speculation on whether the short isoform of Zfh1 can also cause excess stem cells

In the course of our work, we discovered that two Zfh1 isoforms are present in testes, and these have different lengths. Here we showed that the long isoform can cause stem cell tumor phenotype. Due to a complication (see Addendum), we do not know whether the short isoform can also generate extra stem cells. However, there is indirect evidence to suggest that it can. We have detected the expression of both isoforms in testes overactivated for the JAK-STAT pathway, which are full of extra CySCs and GSCs (data not shown). Furthermore, using RNA-Seq, Gan *et al.* have shown that the short and long transcripts of *zfh1* are expressed at similar levels in *bam* mutant testes, which are enriched with early stage germ cells including GSCs (109). These data demonstrate that the short isoform is indeed present in stem cell-enriched testes, and suggest that it might contribute to the phenotype. We have generated new UAS constructs for the short isoform. Thus we can use these newly synthesized tools to directly test the capability of the short isoform to induce stem cells. Because the short isoform misses two additional zinc fingers and a polyQ region at the N-terminus compared to the long isoform, the result would suggest us whether those protein motifs play a role in the Zfh1 overexpression experiment.

Material and methods
Fly strains

Fly lines used were: FRT82B *zfh1*[65.34], FRT82B zfh1[75.26], and UAS-*stat*-HA (Erika Bach, New York University, USA), MARCM 82B, and *upd*-Gal4 (Erika Matunis, John Hopkins University, USA), UAS-*hop*[tumL] (Norbert Perrimon, Harvard University), *nanos*-Gal4:VP16 (Erica Selva, University of Delaware, USA), *CtBP*[DE10] (Ken Cadigan, University of Michigan, UAS). All other stocks were provided by the Bloomington Stock Center or generated in this study. Flies were grown at 25ºC unless noted.

For Zfh1 genetic modifier screen, 215 lines from Exelixis deficiency library were ordered. Since multiple crosses were needed to generate the appropriate fly stock for the screen, we further cut down the number of deficiency lines to 188 by excluding lines with smaller deletion and nested in those with bigger deletion.

Plasmids

The construct of UAS-Zfh1-RA-1×Flag-1×HA came from BDGP (Berkeley Drosophila Genome Project). To make plasmids with tagged version of UAS-Zfh1-RB,

85

we sequenced the cDNA constructs from BDGP (Berkeley Drosophila Genome Project), and identified two point mutations and a 586bp deletion in exon4. Using site-directed mutagenesis (Agilent Technologies), we corrected the point mutation. Using restriction enzyme digestion and ligation, we repaired the deletion with a fragment from another *zfh1* cDNA construct. The flawless *zfh1-RB* sequence was cloned into various pUAST destination vectors (developed by Terence Murphy, DGRC) using Gateway recombination methods (Invitrogen). Transgenic flies were produced using standard germline transformation techniques.

Immunostaining

Immunostaining for adult testes and embryos was performed as previously described except 1×PBS was substituted for Buffer B (Leatherman and DiNardo, 2010). The following antibodies were used: mouse anti-lacZ (1:10,000, Promega), rat anti-E-Cadherin (1:20, DSHB), goat anti-Vasa (1:400, Santa Cruz), mouse anti-FascIII (1:50, DSHB), rabbit anti-α-Spectrin (1:200, DSHB), chick anti-GFP (1:1000, Molecular Probes), rat anit-HA (1:200, Roche), mouse anti-Myc (1:500, Santa Cruz). For anti-Zfh1 staining, 1:5000 and 1:500 were usually used for adult testes and embryos, respectively. The following antibodies have been used to visualize Zfh1: rabbit anti-Zfh1 (Ruth Lehmann, New York University, USA), rabbit anti-Zfh1 (Kevin White, New York University, USA), guinea pig anti-Zfh1 (James Skeath, Washington University in St. Louis).

Imaging and imaging analysis

Images were captured with a Zeiss Axioplan 2 equipped with an apotome. Z-series were analyzed by the AxioVision 4.6 software. The quantification of bright DNA on testis snapshot was conducted using ImageJ (NIH) by following a procedure similar to previously described (110).

Western Blot

The Western Blot was performed as previously described except that testes were lysed using 2×SDS-PAGE sample buffer (111). Because the size of Zfh1-PB was predicted to be about 145kDa, 7.5% Tris-HCl gel (Bio-Rad) was used to better visualize the protein. Antibodies used were rat anti-HA (1:1000, Roche), and mouse anti-actin (1:1000, Invitrogen).

Immunoprecipitation

The IP protocol was similar to ChIP, except that 60 pairs of testes were used per IP, and the collected testes were often not cross-linked by formaldehyde.

ChIP

86

ChIP was conducted using EZ-Magna ChIP A-Chromatin Immunoprecipitation Kit (Millipore). 80 pairs of testes were used per ChIP.

qPCR

The qPCR experiment was performed using Brilliant SYBR Green QPCR Master Mix (Agilent Technologies). Primers were designed using DNASTAR and Primer3. Following the manufacturer's protocol, the qPCR fragment size was determined to be about 100bp. We tested primer pairs on Input (un-ChIP'ed) samples first, and then checked the product size on 2% agarose gel. The qPCR data was analyzed by Excel (Microsoft).

Library preparation for sequencing

Sequencing libraries were prepared using NEBNext DNA Library Prep Master Mix Set for Illumina (NEB).

Cell culture

Experiments related to cell culture were performed as previously described (111).

CHAPTER 4

Final Discussion

Summary

The *Drosophila* male germline system is an excellent model to study niche-stem cell biology. Extensive work in the field has demonstrated that signals provided by the niche play a crucial role in regulating the behavior of GSCs (44-46, 50-53). Among those identified signals, the JAK-STAT pathway has received most attention (44, 45). A model which involves a single niche has also been dominant in the field. The studies presented here as well as recent work in our lab emphasize the importance of another signaling pathway, BMP, and also modify the niche-stem cell model (40). We characterize the role of Magu as a novel BMP modulator specifically required for GSC maintenance. The function of Magu may also depend on its interaction with heparan sulfate proteoglycans. Previous work in the lab identified the transcription factor Zfh1 as a key regulator for both CySCs and GSCs (42). We have attempted to identify downstream targets of Zfh1 using two genome-wide approaches. Preliminary results suggest that Zfh1 can function as either a repressor or activator to control the expression of target genes. Together, these findings further reveal the complexity of the seemingly simple niche system in the fruit fly testis. Below I will discuss two interesting questions related to the Magu project. I will also address remaining questions and future experiments for the ongoing project on Zfh1.

How is BMP activity restricted to the stem cell niche?

The BMP signaling pathway is conserved in both invertebrates and vertebrates. Studies in various model organisms (*Drosophila*, *Xenopus*, and *Zebrafish*) have demonstrated that secreted BMP ligands are able to diffuse over a long distance across tissues (112). This diffusion usually builds a gradient of ligand concentration to guide tissue patterning (112). Contrary to this classical view, BMP activation in fruit fly testes is often restricted to within one cell diameter from the ligand source, near where the stem cell niche is located (50-52). In other words, BMP signals function over a short range to specifically regulate GSC self-renewal. The restriction of BMP activity is necessary in the testes, as expanded BMP activation blocks the differentiation of gonial cells (50-52). Therefore, studying how BMP activation is restricted in this niche can further enhance our understanding of how niche signals are controlled.

One possibility for signal restriction is that pathway activation may be localized to the niche-stem cell interface. Recently, Michel *et al.* developed a fluorescent reporter for the activation of BMP type I receptor Thickvein (63). Using this tool, they have demonstrated that BMP signals from the hub are specifically received at the hub-GSC interface, where adherens junctions are located (63). We have also found that when overexpressed in the germline in an otherwise wildtype background, Dally-like (Dlp), a co-receptor for BMP ligands, is enriched at the hub-GSC interface. This specific localization is disrupted in *magu* mutant testes, as Dlp appears more diffuse around the entire germ cell surface. Since BMP activation is impaired in *magu* mutant testes, it is

89

possible that Magu functions to concentrate Dlp at the hub-GSC interface, and that concentration is necessary for proper pathway activation. In the future, we can investigate the direct interaction between Magu and Dlp by testing whether these two proteins can be co-immunoprecipitated from testes.

Another possibility to explain restricted activation is that pathway activity may be also governed by other pathways. It has been shown in multiple systems that BMP signaling restricts stem cell activation by suppressing Wnt signaling (113, 114). Thus, it is reasonable to speculate that there may be unidentified signaling at the testis niche that antagonizes BMP activation and restricts its function to the niche. We think results coming from the Zfh1 project would reveal additional pathways important for GSC self-renewal. We can then test whether BMP activity is expanded when any of newly identified pathways is impaired.

Can *magu* be a target gene of Zfh1?

Previous work in our lab has suggested that BMP pathway is activated non-autonomously in GSCs by sustained Zfh1 expression in the cyst lineage (40). Since Magu is an extracellular protein required for BMP activation in GSCs, it is possible that Magu functions downstream of Zfh1 activation, and may be a target of Zfh1. Due to the limited resolution of *in situ* hybridization in fly testes, we cannot be certain whether *magu* is expressed in CySCs, where *zfh1* is expressed. Thus, whether *magu* is a direct target of Zfh1 remains unknown.

Since Zfh1 is expressed in many other tissues, there might be other occasions where Magu acts along with or downstream of Zfh1. For example, *magu* is expressed prominently in embryonic neuroblasts (data not shown). This expression pattern may overlap with *zfh1*, which is also expressed in neuroblasts (115). But further experiments with double staining are needed to determine whether the two genes are expressed in the same neuroblasts. Since, Zfh1 mutant embryos exhibit a defect in motor neuron projection (98), we should also investigate whether *magu* mutant embryos have a similar phenotype.

How to prioritize the gene list generated by HA-Zfh1 ChIP-Seq?

The sequencing of libraries prepared from the HA-Zfh1 ChIP experiment is currently underway. We expect the resulting gene list will be long, thus it is important to prioritize the results for follow-up analysis. We will first rank the genes using the relative level of Zfh1 enrichment. We will then search for regions containing Ebox sites, which are known motifs that Zfh1 binds to (91). After these *in silico* analysis, we will visualize the expression pattern of selected genes in testes. This attempt can be fulfilled by *in situ* hybridization, or by using antibodies in those cases where one exists, or analyzing an enhancer trap line for those genes that have one associated with them. Because our ChIP-qPCR experiments suggest that Zfh1 may function as either a transcriptional repressor or

90

activator, we will look for genes that either specifically expressed in CySCs (where Zfh1 is expressed) or in differentiating cyst or hub cells (where Zfh1 is not expressed). The efforts to prioritize putative Zfh1 targets will also be complemented by results coming from the ongoing modifier screen. We think candidates suggested by both approaches have a higher chance to be a real target.

What effectors would be Zfh1 targets?

Genome-wide approaches have been taken in studies of *Drosophila* testis. In a previous microarray experiment, we identified genes enriched in JAK-STAT overexpression testes. Such genes included Zfh1 and Magu (64). The Fuller lab conducted a gain-of-function screen by overexpressing individual genes in the germ cells using a set of transgenic lines, each capable of expressing a neighboring gene using the Gal4 system. Their analysis uncovered the role of the differentiation factor called Bam (51). Thus, in our lab's and the Fuller Lab's work, novel genes influencing early stages of spermatogenesis have been identified. Thus, whole-genome approaches in the testis can generate new insights on stem cell regulators. Below I will state possible effectors of Zfh1, based on its dual function and other information.

We think there are two groups of effectors downstream of Zfh1: one governs CySC fate intrinsically, and the other controls how CySCs act non-autonomously as niche cells for GSC self-renewal. For genes belong to the first group, when their normal function is disturbed, mutant CySCs would lose the stemness and differentiate. For the second group of effectors, they would be specifically required for GSC maintenance, but not in CySC stemness. Therefore, if effectors in the first group are impaired, Zfh1 overexpression testes will not exhibit ectopic stem cells, neither CySCs nor the GSCs that rely upon them. However, extra CySCs but not GSCs will still be induced if genes in the second group are mutated.

It is worth mentioning that since ectopic stem cells in Zfh1 overexpression testes undergo active division, we expect some targets of Zfh1 would be regulators of the cell cycle. In addition, it has been shown that ZEB1, the mammalian homolog of Zfh1, negatively regulates expression of stemness-inhibiting microRNAs (116, 117). Thus some effectors of Zfh1 may also be microRNAs. Recently, Kadaja *et al.* discovered that Sox9, a newly identified transcriptional regulator for hair follicle stem cells, binds to genes encoding extracellular factors that promote TGFβ/Activin signaling (118). Therefore, secreted signaling factors (for instance, ligands for BMP or any unknown pathway) may be Zfh1 effectors.

How to further investigate dedifferentiation in Zfh1 overexpression testes?

The excess stem cells induced by ectopic Zfh1 are likely generated through dedifferentiation. In the Discussion session of Chapter 3, I speculated on how the dedifferentiation process could occur based on current knowledge in the field. To

91

elucidate the process definitively in the future, the combined approaches of immunofluorescent staining on fixed tissue and time-lapsed imaging of live testes should be applied. According to the time course experiment for Zfh1 overexpression testes, dedifferentiating cyst cells regain the capacity of cell division, a property of CySCs. To further confirm the identity of these cells, markers of stem cells should be used. It has been shown that Hedgehog signaling is required for CySC self-renewal (46, 53). Thus we can use Hh readouts to check pathway activation in somatic cells under division. We can also stain testes with antibodies against Eya, a marker for differentiated cyst cells. Findings from these experiments can tell us the status of cyst cells when converting into CySCs. Similarly, for the germline lineage, we can further investigate the identity of dividing germ cells using the differentiation marker Bam as well as GSC marker Escargot. The previous time course experiment suggested that majority of dedifferentiating germ cells are not *bona fide* GSCs at 6 days after Zfh1 activation. Thus the time point we will focus on to observe the first onset of *de novo* GSCs may be later than 6 day.

While examination on fixed testes can tell us important characters of dedifferentiating cells, it is likely that the actual process of dedifferentiation can be quite dynamic, and some key features of the process may not be revealed using fixed samples. Thus live imaging is a complementary approach to study the generation of excess stem cells. As mentioned in Chapter 3, the morphology of differentiated cyst cells and spermatogonia has to be changed dramatically in order to revert to stem cells, thus I think reagents that mark cell outlines would be revealing tools for live imaging. We can drive UAS-membrane GFP using either cyst or germline lineage Gal4 to visualize the real-time behavior of cells. During dedifferentiation, cells would rearrange so that newly generated CySC and GSC can associate with each other. This process may involve cell movement. The motility of cells may be acquired through actin-based protrusions. Therefore, it may be also useful to visualize cell behavior using actin-based constructs.

How to test that Zfh1 is a transcriptional activator?

Results from our HA-Zfh1 ChIP-qPCR experiments suggest that Zfh1 may function as a transcriptional activator. This finding contradicts the stereotypical model of Zfh1, which describes it as a transcriptional repressor (91). To further test the capability of Zfh1 to activate transcription, several follow-up experiments are needed.

First, to investigate how the gene expression profile is controlled by Zfh1, a RNA microarray or RNA-Seq experiment should be performed. Ideal, this type of experiment would be conducted comparing wildtype to *zfh1* depleted testes. Since Zfh1 is an essential gene, we cannot use genetic mutants for such an experiment. I have tried to knock down Zfh1 in adult testes by RNAi, but without great success (see Addendum). Therefore, the only expression profile that can be obtained effectively is from comapring wildtype to *zfh1* overexpression testes. If the expression of a gene is positively regulated by Zfh1, then its expression should be increased dramatically in *zfh1* overexpression

92

testes compared to wildtype. If such gene also ranks high on the ChIP-Seq list, it is likely that its transcription is directly activated by Zfh1.

Second, to further confirm the direct activation of certain genes by Zfh1, we would use both *in vivo* and *in vitro* experiments. We can generate *zfh1* mutant clones in testes, and then visualize whether the expression of a putative target is lost in the mutant cell. It is likely that regulatory fragments of some putative targets have been identified by other work in the field, and certain regulatory sequence may overlap with the binding region identified from ChIP-Seq experiment. Thus to ascertain Zfh1's control to those regions, we can perform luciferase assay in *Drosophila* S2 cells using reporter constructs including such regulatory fragments. In the case that regulatory fragments do not already exist, we can generate the necessary constructs by PCR amplification guided by the region identified from the HA-Zfh1 ChIP-Seq. If Zfh1 controls gene expression positively, the activation level of the reporter line would be higher when co-transfected with Zfh1.

Third, to determine how Zfh1 controls transcription activation, its binding site needs to be verified. There are two types of DNA-binding motifs in Zfh1: zinc fingers and a homeodomain. It has been shown that zinc fingers of Zfh1 bind to Ebox site to suppress transcription, whereas the homeodomain may activate transcription via binding to the sequence GCTAATTG (94, 119-125). We have identified a putative binding sequence for the homeodomain within the *eya*A3 region but not in C1 (data not shown). This seems consistent with our conclusion that Zfh1 activates the A3 fragment rather than C1. To test the importance of the homeodomain binding site, we can mutate its sequence in A3 and examine whether that alters A3-lacZ expression pattern.

Another possibility for how Zfh1 acts as an activator is that it may bind to a *de novo* motif. Recent study from the Eileen Furlong lab has demonstrated that *snail*, a stereotypic transcriptional repressor, can directly activate expression of different genes in the same type of cells (107). They further demonstrated that the decision of repression or activation is encoded in the target gene sequence, as the presence of a novel motif that Snail binds to is essential for potentiating gene expression (107). Thus, we should also compare the regulatory region of genes either activated or repressed by Zfh1, and attempt to discover any novel, recurring motifs in them.

Lastly, to further elucidate the mechanism of transcriptional activation governed by Zfh1, we can try to identify nuclear partners interacting with Zfh1. ZEB1 is the mammalian homolog of Zfh1. It has been shown that ZEB1 can bind to transcriptional co-activators p300 and P/CAF, thereby promoting transcription as a complex (126, 127). Hence we can also test whether Zfh1 interacts with these co-activators by performing Co-IP experiments using *zfh1* overexpressing testes. Another way to identify proteins associated with Zfh1 is to conduct mass spectrometry analysis on protein samples IP'ed by antibodies against Zfh1 (128). Chromatin modifiers are another type of key player for transcriptional activation (105). Although transcription factors like Zfh1 may or may not

93

directly interact with chromatin-remodeling complex, the two parts are mechanistically linked (105, 128). Thus we think the mass spectrometry experiment can either identify chromatin modifiers with a direct physical link with Zfh1 or proteins mediating the connection between Zfh1 and chromatin-remodeling complex. In either case, the experiment would further enhance our understanding of how Zfh1 may act as a transcriptional activator.

CHAPTER 5

Magu Project Addendum

1. Additional efforts to investigate Magu's involvement in BMP

We attempted to demonstrate the involvement of Magu in BMP signaling pathway by multiple approaches. Although the results of the following experiments did not serve the initial purpose, they might be informative to future work in the lab, and thus are included here.

A. the effect of activation of Sog in *magu* mutants

Sog is an extracellular antagoniss of BMP signals. To test whether the overexpression of Sog in a *magu* mutant background would further reduce GSC numbers, we overexpressed Sog using *nanos-Gal4* in $magu^{e00439}/magu^{f00256}$. There was no discernible difference between $magu^{e00439}/magu^{f00256};nanos-Gal4/UAS-sog$ and $magu^{e00439}/magu^{f00256}$ (Addendum Table 1). However, since the activation of Sog failed to cause a phenotype in *magu* heterozygotes, it was unclear whether the overexpression of Sog had been achieved in this experiment.

B. Other read-outs of BMP activation in testes

Besides using pMad accumulation as a readout for the BMP pathway, the activation of two other proteins involved in BMP signaling was also tested. Medea is the protein that forms a complex with pMad. The Mad-Medea complex translocates into the nucleus, and regulates expression of target genes. Specific staining of Medea was observed in some wildtype testes (data not shown), but the accumulation was in hub cells, not GSCs. Medea also accumulated in late stage cyst cells. This is expected, as BMP signaling is activated in those cells as previously reported (62).

Dad is a target gene of BMP activation, and it negatively regulates BMP signaling. BMP signaling in the *Drosophila* wing disc is routinely monitored using Dad reporter lines, including Dad-LacZ, and a newer tool, Dad-RFP (129). Similar to Medea and pMad, there was no reliable LacZ detection in GSCs in testes with two copies of *dad-LacZ* (data not shown). It was unclear whether the GSC staining observed in 3rd instar larvae gonads was specific, since the signal was also present in spermatogonia (data not shown). For Dad-RFP, the staining was blazingly bright on certain big-size sheath cells (Appendum Fig.1A; these are pigment cells). The specific staining of Dad-RFP also appeared in hub cells (Addendum Fig.1A', arrowhead), and cyst cells (Addendum Fig.1A', arrow). Similar to *magu*frgII-LacZ (Fig.1B, Chapter 2), the expression in hub cells sometimes was not uniform, as only a fraction of hub cells had the RFP staining (Addendum Fig.1B, B').

Because none of these assays was sensitive enough to detect BMP activation in GSCs in wildtype adult testes, I did not proceed to use them as a way to test BMP reduction in *magu* mutants.

C. UAS-tor-Tkv UAS-tor-Punt, another BMP activation construct

96

Tkv and Punt are the Type I and II receptors of BMP signaling pathway in *Drosophila*. Two different transgenic lines of flies have been used to activate the BMP signaling pathway. The first is an amino acid change in Tkv, the type I receptor. All the Nanos>TkvA testes had overproliferation cysts (Addendum Fig.2A, arrow), an expected phenotype of ectopic BMP activation in testes (50, 52). The second transgenic setup overexpresses both the type I and type II receptors UAS-tor-Tkv UAS-tor-Punt (130). Both constructs have been shown to cause constitutive transducing activity in other tissues (130, 131). However, only one-third of the Nanos>tor-Tkv tor-Punt testes exhibited the phenotype of overproliferation cysts (data not shown). Therefore, I chose to rescue *magu* mutants using UAS-TkvA.

2. Additional comments on pMad staining

As a positive control for pMad staining, it is worth noting that pMad activation in germ cells was consistently detected in testes with ectopic BMP activation in the germline (Addendum Fig.2B). Still, we could never observe consistent GSC accumulation of pMAD in wildtype testes, nor among GSCs of Magu overexpression testes (*upd*>V5-*magu*, data not shown). The other situation where a nice pMad staining on GSCs was reproducibly observed was testes with either JAK-STAT activation or Zfh1 overexpression in the cyst lineage (data not shown). In both situations, the testes were full of ectopic GSCs and CySCs (see Chapter 3 for details).

Recently, Li *et al.* reported a protocol for better pMad staining in *Drosophila* wing disc (132). Different from ours, the protocol used twice higher formaldehyde in the fixation buffer and supplemented phosphatase inhibitor for each step. We applied this protocol on wildtype testes. We did observe pMad staining in GSCs in most testes scored (data not shown). Because germ cells could not be visualized well in this particular trial, we could not test whether the pMad staining was present in every GSCs. In addition, there were many nonspecific dots on the testes in the pMad channel, and we did not know what caused that.

3. Drifting hub phenotype due to UAS-*dlp*-GFP

When the activation of *dlp-GFP* was sustained in hub cells for a long time (12 days, 29 ^{o}C), we observed a hub drifting phenotype, in which the apically located hub cells appeared far away from the testis tip (Addendum Fig.3C, arrow). This phenotype occurred in all 9 control testes scored (*magu* heterozygotes). However, the drifting hub was also observed in 6 out of 10 UAS-*dlp*-GFP only testes, although the new position of the hub appeared closer to the tip compared with Gal4-UAS samples (Addendum Fig.3A). We do not know whether this phenotype was simply due to genetic background, or whether UAS-*dlp* was leaky; though I could detect no specific GFP staining in Gal4 only testes.

97

Addendum Table 1. The effect of activation of Sog in *magu* mutants

Condition	Genotype [a]	Median GSC #	IQR [b]	Min - Max [c]	P value [d]
aged at 29°C for 3 days [f]	*magu*[e] / *magu*[f] ; *nanos-Gal4* or *UAS-sog/MKRS*	3 (11) [e]	0 - 4	0 - 6	
	magu[e] / *magu*[f] ; *nanos-Gal4/UAS-sog*	3 (11)	1.5 - 4	0 - 6	>0.05
aged at 29°C for 13 days [g]	*magu*[e] or [f]/*CyO*; *nanos-Gal4* or *UAS-sog/MKRS*	5 (9)	5 - 5	3 - 8	
	magu[e] or [f]/*CyO*; *nanos-Gal4/UAS-sog*	6 (9)	4 - 6	3 - 10	>0.05

[a] Alleles used: [e]=[e00439]; [f]=[f02256].

[b] interquartile range = Quartile 3 - Quartile 1 (Q[3] - Q[1]), Q[3] = the 75th percentile, Q[1] = the 25th percentile.

[c] Minimum - Maximum, representing the spread of GSC numbers observed

[d] Calculated by Mann-Whitney test.

[e] Number of testes scored in parentheses

[f] Animals (0-3 days of age) raised at 25°C were shifted to 29°C for 3 days.

[g] Animals (0-6 days of age) raised at 25°C were shifted to 29°C for 13 days.
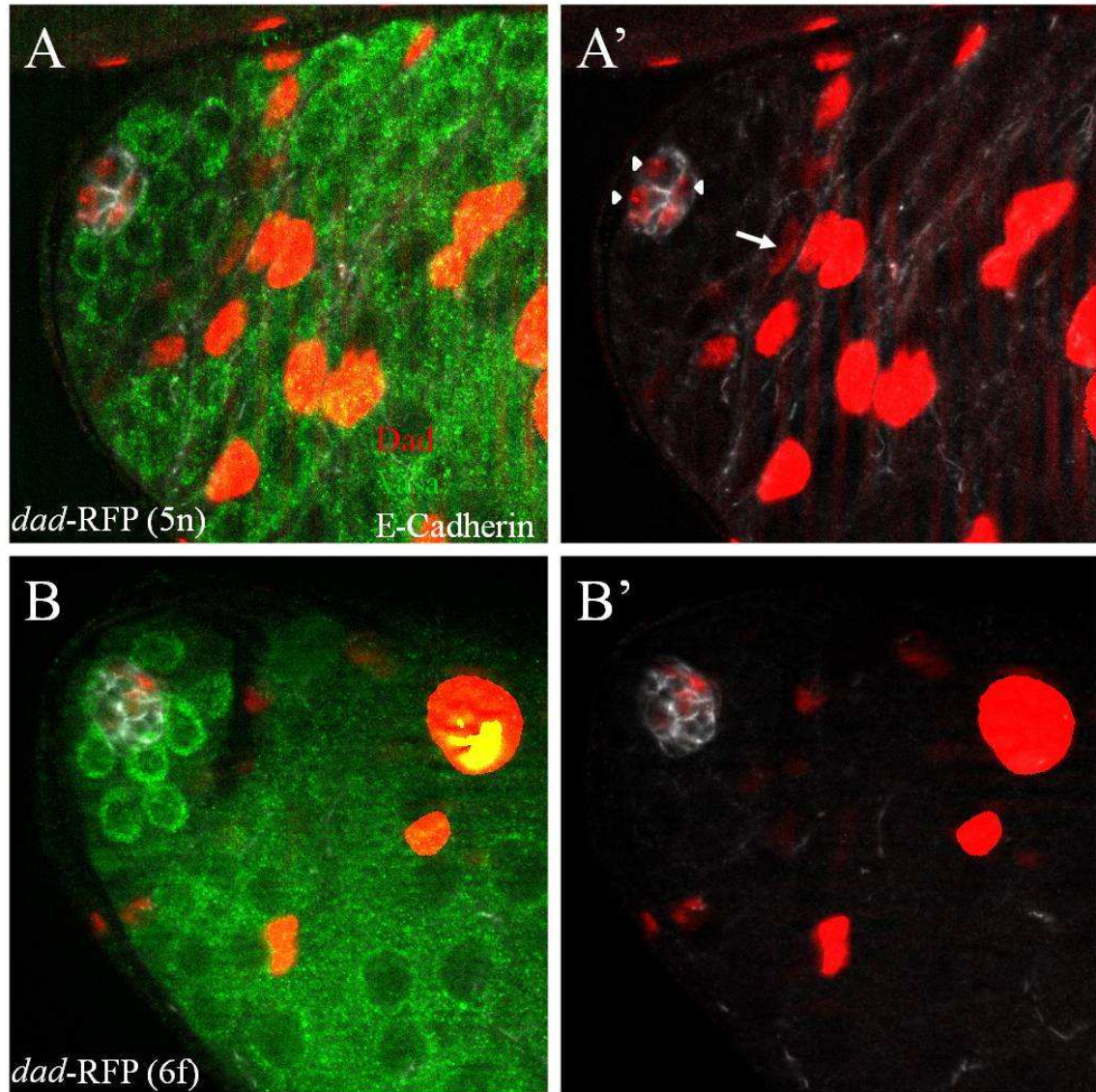
Addenudm Figure 1. *dad*-RFP does not exhibit expression in GSCs. (A) In one reporter line of *dad* (*dad*-RFP, 5n), the expression was present in hub cells (arrowheads), cyst cells (arrow), and big-size pigment cells on the testis sheath. (B) In the 6f line of *dad*-RFP, the expression in the hub (E-Cadherin, white) appeared restricted to a fraction of hub cells (B').
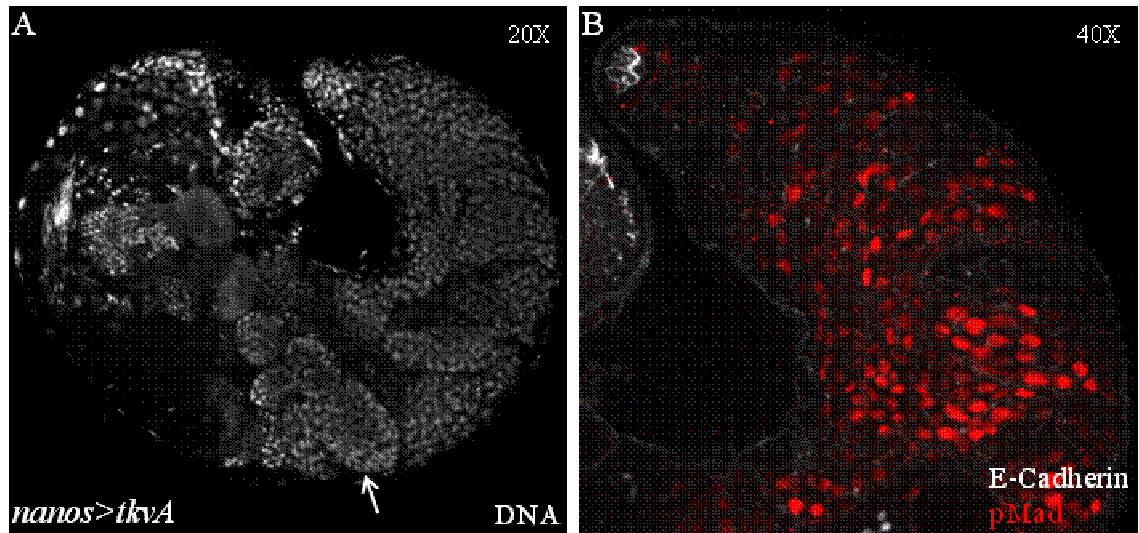
Addendum Figure 2. BMP signaling can be activated properly in the germline using a constitutively activated form of Type I receptor Thickvein. (A) When UAS-Tkv^{Act} was driven in the germline using *nanos*-Gal4, testes appeared to have overproliferation cysts with more than 16 spermatogonia (arrow). (B) The ectopic activation of BMP pathway could be detected by pMad staining (red) throughout the testis.
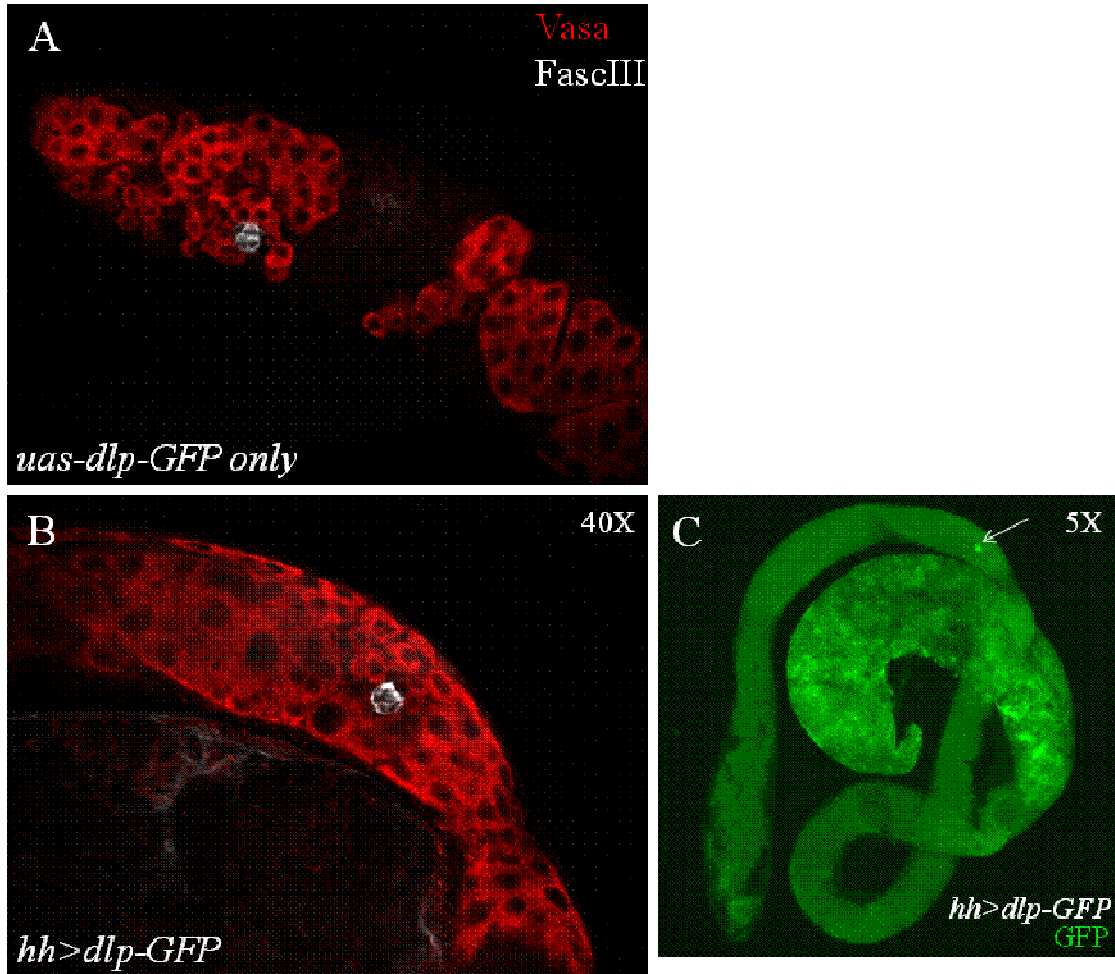
Addendum Figure 3. A drifting hub phenotype appears when UAS-*dlp*-GFP is expressed in hub cells using *hh*-Gal4 for 12 days. (A) In 6 out of 10 UAS-*dlp*-GFP only testes, the apically located hub cells (FascIII, white) exhibited away from the testis tip. (B) This phenotype had a higher penetrance in Gal4-UAS testes, present in all 9 testes scored. (C) The mislocalized hub in Gal4-UAS testes often appeared very far away from the apical tip, as visualized by anti-GFP under 5X.

CHAPTER 6

Zfh1 Project Addendum

1. Indirect activation of *zfh1* through JAK-STAT signaling pathway fails to generate a high fraction of testes enriched with functional CySCs (and extra GSCs)

There are two ways to activate JAK-STAT signaling in the cyst lineage. One is to overexpress an activated form of JAK (JAK^{Act}), the signal transducing kinase, using a cyst lineage Gal4; the other is to ectopically produce Upd, the secreted ligand, in the germ cells using Nanos-Gal4. Either of these approaches should generate testes with large number of *bona fide* CySCs, intermingled with many GSC-like cells (Addendum Fig.1B) (42). A previous postdoc in the lab took the first approach using EyaA3-Gal4, a commonly used cyst lineage driver. She used these JAK-STAT overactivation testes for the ChIP experiment. Her results suggested that we could successfully perform Zfh1 ChIP on testes. However, I could not repeat her data (data not shown), and, in re-examining her raw data, discovered some errors in the qPCR protocol and in analysis of qPCR results.

In addition, I examined EyaA3>JAK^{Act} testes in more detail. I found that the majority of testes did not have functional, ectopic CySCs, as suggested by the lack of extra GSCs (Addendum Fig.1A). In these testes, the *zfh1+* cells often formed patches, with the presence nearby of groups of spermatogonia and even spermatocytes (Addendum Fig.1C). To confirm this observation, I also tried to drive UAS-JAK^{Act} using two other cyst lineage drivers, c587-Gal4 and Tj-Gal4. Although the percentage of testis with excess CySCs and GSCs in those two overexpression samples was higher than the EyaA3>JAK^{Act} group, the stem cell tumor phenotype was far less than 100% penetrant (Addendum Fig.1A). I also scored functional CySCs phenotype in Nanos-Gal4 UAS-Upd testes. Similar to what had been reported, only half of the overexpression testes had extra GSCs (45). In summary, all these findings led us to conclude that indirectly activating *zfh1* through JAK-STAT pathway did not cause functional *zfh1+* cells in every testis, and this may be the reason why Zfh1 ChIP did not work when using such testes.

2. Direct activation of *zfh1* using untagged UAS-Zfh1-RB also does not cause enough extra *zfh1+* cells

We also tried to increase the number of *zfh1+* cells directly. There existed an untagged UAS-Zfh1-RB line generated by Postigo *et al*. The construct of this transgenic fly was made from *zfh1* cDNA plasmid prepared by Fortini *et al.* (Flybase) (91). When compared with information in Flybase, the originally published *zfh1* cDNA sequence has deletions in the polyQ region (opa) and another point mutation (120). It is unclear whether Postigo *et al*. corrected these sequence aberrations when generating the UAS-Zfh1-RB construct (Flybase) (91). Nevertheless, this UAS-Zfh1 line can supply normal Zfh1 function to rescue defects on glia cells in *zfh1* mutant embryos (97). We also used this line previously to demonstrate that sustained Zfh1 in the cyst lineage caused excess CySCs and GSCs.

103

I overexpressed Zfh1 using the Postigo's UAS-Zfh1 and various cyst lineage Gal4 drivers. As shown in Addendum Fig.1A, the percentage of testis with extra CySCs and GSCs was even lower than the JAK-STAT activation approach. This was similar to what we had noticed before (Judy Leatherman, personal communication). We do not know whether the sequence aberrations in the untagged UAS-Zfh1-RB decrease the ability of Zfh1 to generate excess stem cells, even thought the construct can rescue *zfh1* mutant phenotypes. Because of the low penetrance of the phenotype, I did not bother to try Zfh1 ChIP on testes expressing this form of Zfh1.

3. UAS-Zfh1-RA-1×Flag-1×HA fails to cause extra stem cells in testes

When the epitope tagged short isoform of Zfh1 was expressed in the cyst lineage using either EyaA3-Gal4 or c587-Gal4, we did not observe ectopic CySCs nor GSCs (Addendum Fig.2B). The testes did not have extra *zfh1+* cells, and the presence of branched fusomes in germ cells suggested normal spermatogenesis, just as in wildtype testes. This was in contrast to the positive control, which was the expression of untagged (Postigo's) UAS-Zfh1. In this case dotted fusomes accumulated at the tip of testis (Addendum Fig.2A).

Extensive efforts were made to trouble shoot this problem. We sequence verified the entire transgene for both the plasmid from BDGP and genomic DNA isolated from transgenic flies. To further test whether the transgene can be expressed *in vivo*, we overxpressed UAS-Zfh1-RA-1×Flag-1×HA using En-Gal4, a driver with a stripe pattern on embryos. We could only observe the ectopic expression using anti-Zfh1 (Addendum Fig.2C), but not using an antibody against the epitope tag (either Flag or HA, data not shown). Western Blot using anti-HA also did not detect the tagged Zfh1 in protein lysates isolated from En>Zfh1-RA-1×Flag-1×HA embryos (Addendum Fig.2D). This suggested that tagged Zfh1 proteins were not generated appropriately. Consistent with this idea, embryos expressing Zfh1-RA-1×Flag-1×HA looked morphologically normal (rather than disorganized, as embryos expressing Zfh1-RB, Fig.3 in Chapter 3), although they did not survive to the larval stage. We also attempted to visualize the ectopic expression *in vitro*, using transfection into cultured cells. However, S2R+ cells transfected by Ubi>Zfh1-RA-1×Flag-1×HA failed to show HA staining (data not shown). Together, these experiments suggested strongly that UAS-Zfh1-RA-1×Flag-1×HA could not be expressed properly, and it would not be useful for Zfh1 ChIP experiments.

We do not know why UAS-Zfh1-RA-1×Flag-1×HA is not expressed well. In the construct, there is an extra fragment between Zfh1-RA and 1×Flag-1×HA (Addendum Fig.2E. This fragment contains a stop codon and needs to be spliced out *in vivo*, to allow the in-frame expression of Flag and HA. We suspect that the splicing may not happen successfully. This may cause the misfolding of newly synthesized ectopic Zfh1 protein, or the improper translation of epitope tags.

4. Epitope-tagged UAS-Zfh1-RB lines cause stem tumor phenotype in various degrees

In Chapter 3, we reported that an N-terminally 3×HA tagged UAS-Zfh1-RB gave rise to stem cell tumor phenotype at 100% penetrance and high expressivity. We have also investigated other epitope-tagged UAS-Zfh1-RB lines. We found out that a C-terminally 3×HA tagged UAS-Zfh1-RB line only caused ectopic HA+ cells, but did not generate extra GSCs as shown by the presence of branched rather than dotted fusomes in germ cells (Addendum Fig.3A). For the N-terminally 6×Myc tagged UAS-Zfh1-RB line, ectopic Myc expression was present in every testis scored, but only the testis tip region exhibited a mild GSC tumor phenotype (Addendum Fig.3B). Similarly, although the penetrance of ectopic Myc+ cells was 100% for the C-terminally 6×Myc tagged UAS-Zfh1-RB line, only 36% of the testes examined had a mild GSC tumor phenotype at the tip region (Addendum Fig.3C). Additionally, testes looked thinner compared to the Gal4 only control testes.

The variation we observed among different tagged UAS-Zfh1-RB lines was expected. The genomic insertion sites of the transgenes were likely quite different from each other, and the identity and position of the tag could also pose an effect on the function of the ectopic protein.

5. Available antibodies against Zfh1 may not be useful for ChIP

Four labs had independently generated antibodies against Zfh1. These antibodies were mapped to a similar region of the protein (Addendum Fig.4). One of them, made by the Kevin White lab, was used for Zfh1 ChIP-chip on wildtype embryos (100), but the data from that experiment has not been confirmed yet. So it is unclear whether the available antibodies against Zfh1 were useful for ChIP. We performed immunofluorescent staining on embryos and testes using three of the four anti-Zfh1 antibodies (we did not use the one generated by the Lai lab). We determined that these three antibodies all recognized Zfh1 proteins nicely in the two tissues by immunofluorescence (data not shown). However, when we applied the antibodies developed by the labs of Ruth Lehmann and Kevin White for ChIP experiments on either embryo or testis samples, we did not observe a positive result (data not shown). Therefore, we concluded these anti-Zfh1 antibodies may not work for ChIP of Zfh1.

It is worth pointing out that the ChIP experiments described above all suffer from the fact that we may not have a *bona fide* positive control region to assay for successful ChIP (see Chapter 3 Discussion).

6. Antibodies generated by our group do not work

When we initially started the ChIP project, our idea was to carry out the ChIP using two different anti-Zfh1 sera. By focusing on regions common to both sera we would increase our chances of focusing on true *in vivo* targets of Zfh1, rather than spurious

105

enrichments. Based on this rationale, a former postdoc in the lab generated an antibody against a largely non-overlaping epitope as well as to a similar region as the other available Zfh1 antibodies (96). I made extensive efforts to test the fidelity of the new antibodies using immunofluorescent staining and Western Blot, but no positive results could be obtained (data not shown). Therefore, I went back to sequence the plasmids used for generating these antibodies. Unfortunately, the sequence of the epitopes was not present in the construct.

We also attempted to generate a monoclonal antibody against the same epitope as the anti-Zfh1 developed by the Ruth Lehmann lab. This work was outsourced by a company (Abmart). We received six tubes of ascites powder from the company. Each individual tube sample represented antibodies from an independent clone. While reconstituting the powder to obtain the original antibody-rich ascites fluid, we had trouble to get two of the six samples (C177 and C252) dissolved well. A summer college student working in the lab tested the remaining four clones by immunofluorescent staining, but we did not observe a specific staining on wildtype testes (Justin Sui, data not shown). I also tested the four clones on protein lysates isolated from EyaA3>3×HA-Zfh1 testes by Western Blot. The antibody generated from B100 clone seemed to detect a high molecular band with the size of Zfh1, but signal was low, and there was too much background signal to be confidant of this result (data not shown). The positive control (the polyclonal anti-Zfh1 generated by the Lehmann lab) exhibited a prominent Zfh1 band on the Western Blot (data not shown). Thus, we do not think the newly generated monoclonal anti-Zfh1 was useful.

7. Other negative controls for ChIP-qPCR experiment besides IgG ChIP

When performed ChIP-qPCR, we also carefully thought about negative controls. As described in the Results session, ChIP on IgG was used as a quality control for non-specific pull-down. We have also attempted to design negative control primers for the qPCR experiment. Since transcription factors usually do not bind to exonic regions, we thought primers targeted to that region may serve as negative controls for each selected gene. However, results showed that signals for these presumed negative control primers appeared indistinguiable from those targeted to regulatory regions of a gene (data not shown). We reasoned that because the size of the chromatin fragments that were going to be pulled down usually ranged from 100bp to 2kb, it is possible that the sequence of an exonic region may also be present in the IP'ed fragments, and thereby showed an enrichment in qPCR analysis.

8. Zfh1 cannot be knocked down efficiently using RNAi

An alternative way to identify Zfh1 targets was to compare gene expression in testes with *zfh1* knock-down to wildtype testes. Genes with differential expression profiles in the two testis samples were potential targets of Zfh1. Thus we have attempted to knock

down *zfh1* expression by RNAi. There existed two RNAi lines for *zfh1*. Using various cyst lineage Gal4 drivers, we found out that only the line generated from VDRC (Vienna Drosophila Rnai Center) could successfully suppress *zfh1* expression. However, the knock-down efficiency was low and the severity of the phenotype was variable. 80% of the 66 testes scored looked normal, similar to UAS-Zfh1-RNAi only control testes (Addendum Fig.5A). For the remaining 20% experimental testes, some had a reduced number of Zfh1+ cells at the tip (Fig.5B), while others did not have Zfh1+ somatic cells at all (Addendum Fig.5C). When testes were abolished for Zfh1+ cells, germ cells started to clump and occupy all the space around the hub (Addendum Fig.5C). It seemed that hub cells were now Zfh1 positive in these tests. This was likely a consequence of the shift to non-permissive temperature for Gal80ts, because hub cells often accumulated more Zfh1 when testes were grown at $29^{o}C$ for a long time. One other, perhaps odd, result was that in Zfh1 knock-down testes some germ cells also appeared to be Zfh1+ when genuine Zfh1 expressing cells were not present in the testes. We did not think this was real. There exists a low level of Zfh1 signal in germ cells in normal testes; perhaps this simply "appeared" brighter since there were no longer any *bona fide* Zfh1 cells. At a most severe situation of Zfh1 knocking-down, we did not observe any type of cells inside the testes (Addendum Fig.5D). We did see many bright Zfh1 stainings on the testis sheath, but we did not know whether they were real (Addendum Fig.5D).

9. Experiments to test whether N-terminally 3×HA tagged UAS-Zfh1-RB can rescue *zfh1* mutants

To investigate whether the newly generated 3×HA tagged UAS-Zfh1 line was functionally normal, we tried to use it to rescue *zfh1* mutants.

We first attempted to do the rescue experiment in testes. Since CySC clones mutant for *zfh1* were not maintained, and were not detectable even 2 days after clone induction (42), we decided to express tagged Zfh1 in the mutant clones, and test whether this would rescue clone loss 4 days after induction. The MARCM (Mosaic Analysis with a Repressible Cell Marker) flies used for this experiment failed to generate wildtype clones (data not shown), thus we obtained another MARCM stock from the Matunis lab (47). The MARCM tool from the Matunis lab was principally the same as what we had used to generate *zfh1* clones before. But the Matunis stock labeled clones with a membrane GFP, rather than a nuclear GFP. In our hands, this difference made it hard to assign the ownership of the GFP, since GSCs and CySCs were in direct contact with each other. Nevertheless, we did test this new MARCM stock thoroughly, and it could successfully generate both wildtype and *zfh1* mutant clones (data not shown). However, we could not definitively establish whether the UAS-HA-Zfh1 transgene was indeed being induced in the *zfh1* mutant cells by anti-HA (data not shown). We do not know exactly why. Maybe perdurance of Gal80 protein in the induced clone cells limited the amount of Gal4, so UAS-Zfh1 could not be activated. We are currently testing a 3rd MARCM stock.

The troubles experienced in testis rescue experiments made us refer to other tissues. Zfh1 plays a pleiotropic role during embryonic development. We determined that in embryos mutant for *zfh1* there was a significantly reduced number of SGPs (somatic gonad precursors) in the gonad. For one mutant allele, *zfh1*[65.34], the number of SGPs in homozygous embryos was only about one quarter of heterozygotes. We are currently performing experiments to rescue this phenotype by driving tagged UAS-Zfh1 using Six4-Gal4, a driver expressed in SGPs.

10. Verification of *zfh1* mutants

While performing the Zfh1 rescue experiment, we discovered aberrations in our *zfh1* mutant stocks. Thus we obtained fresh stocks from the Bach lab and Bloomington Stock Center. To better assess the strength of these *zfh1* mutants, we put the mutant chromosome over a balancer chromosome with a novel fluorescent maker expressed in embryos (133). This allowed us to identify heterozygous and homozygous *zfh1* mutants unambiguously. We discovered that residual Zfh1 protein was present in *zfh1*[2] allele (data not shown), similar to what had been reported before (98). There existed two EMS-induced *zfh1* mutant alleles, *zfh1*[65.34] and *zfh1*[75.26]. Broihier *et al.* reported that anti-Zfh1 antibody did not recognize protein in *zfh1*[65.34] nor *zfh1*[75.26] embryos (96). However, in our hands, while *zfh1*[65.34] was protein null, *zfh1*[75.26] had residual Zfh1 proteins in some homozygous embryos with scattered staining pattern and less bright signal (data not shown).

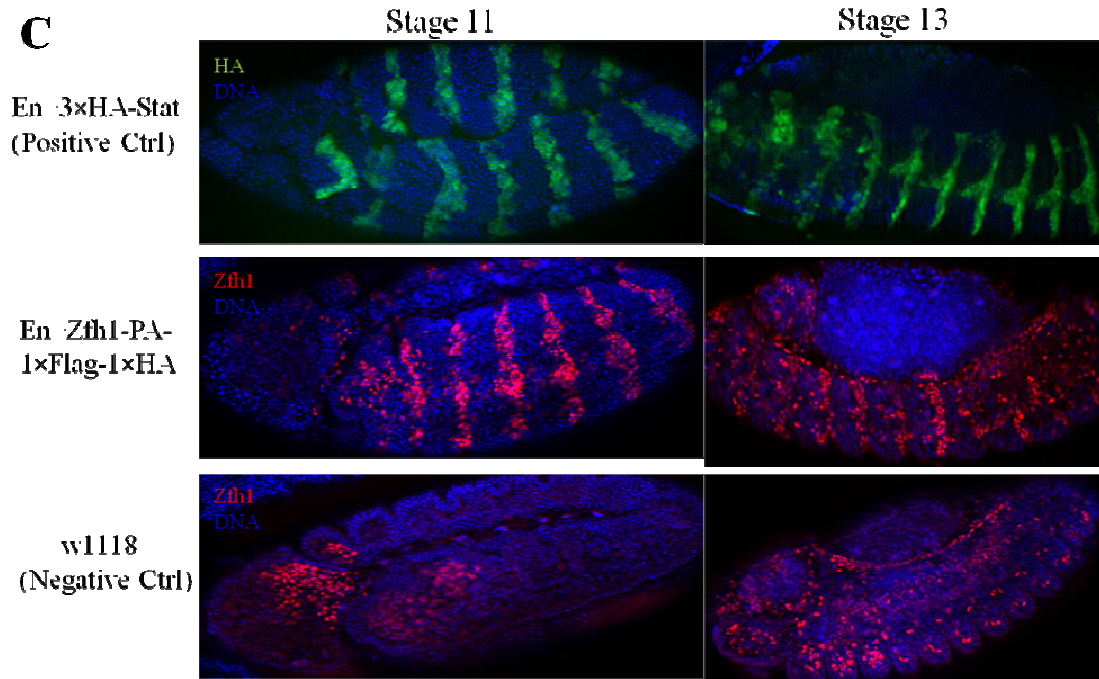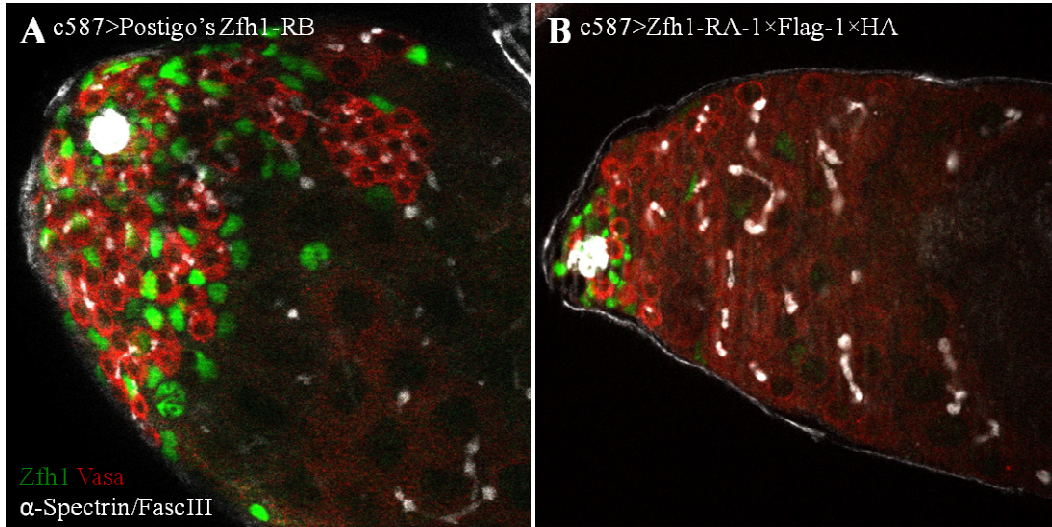## 11. Zfh1 ChIP experiments on wildtype embryos

Since the White lab Zfh1 ChIP embryo list was the only source for predicting Zfh1 targets (100), we initially decided to select putative positive control genes from the list, and confirm the enrichment of Zfh1 to these gene regions in our own preparations of embryo chromatin first. Then the positives from our embryo ChIP-qPCR experiment would be potential positive controls for our attempts to ChIP Zfh1 from testis chromatin. Based on this rationale, we also performed ChIP experiment using wildtype embryos. We could not get the Zfh1 ChIP worked out on embryos, even using the same antibody the White lab used to generate the embryo list (data not shown). However, we could successfully ChIP H3K27me3, the positive control (data not shown). We further read through protocols from other labs, and identified several steps that can be modified, for instance, the amount and stage of embryos collected, the concentration of formaldehyde used for cross-linking. We applied these modifications on our embryo ChIP experiments. The signal for H3K27me3 was dramatically increased, but still, the Zfh1 ChIP on wildtype embryos seemed not working (data not shown).
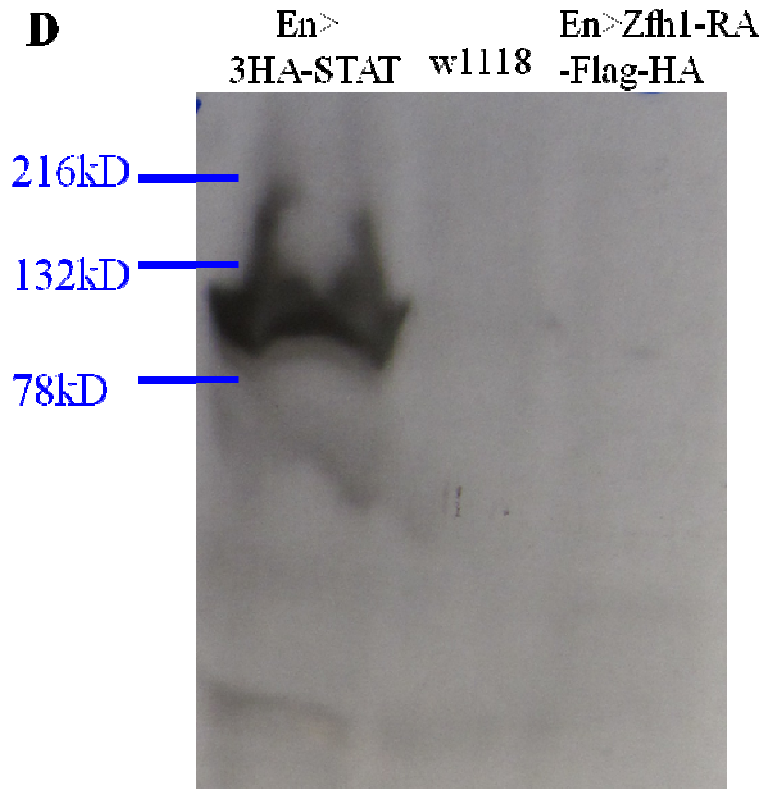
Gal4-UAS Scheme	% of testis w/excess CySCs & GSCs	Growth Condition
Eya-A3> HopTumL	9% (n=46)	young adults aged at 29degree for 16D
c587> HopTumL	65% (n=63)	young adults aged at 29degree for 10.5D
Tj> HopTumL	24% (n=33)	young adults aged at 29degree for 10.5D
Nanos>Upd	48% (n=99) 53% (n=106)	young adults aged at 25degree for 2 or 3 weeks
Eya-A3> Zfh1	14% (n=37)	young adults aged at 29degree for 10D
Eya-A3> Zfh1	8% (at the tip only, n=26)	young adults aged at 29degree for 16D
c587> Zfh1	10% (at the tip only, n=52)	young adults aged at 29degree for 5D
Tj> Zfh1	0% (n=18)	young adults aged at 29degree for 11.5D
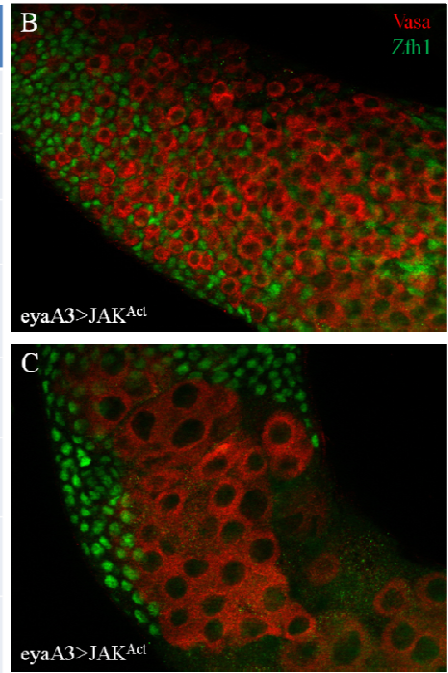
Addendum Figure 1. Either indirect activation of *zfh1* through JAK-STAT signaling pathway, or direct activation of *zfh1* using untagged UAS-Zfh1-RB, does not generate enough functional *zfh1+* cells (CySCs). (A) Statistical measurement of % of testis with excess CySCs and GSCs in various Gal4-UAS conditions. (B) An example of JAK-STAT overactivation testis with extra CySCs (Zfh1+, green) and GSCs (individual Vasa+ cell with small size, red). (C) In some testes overexpressing the constitutively activated form of JAK (JAK[Act]), *zfh1+* cells formed patches (green), surrounding groups of spermatogonia (interconnected Vasa+ cells with big size, red).

A c587>Postigo's Zfh1-RB

B c587>Zfh1-RA-1×Flag-1×HA

Zfh1 Vasa
α-Spectrin/FascIII

C

	Stage 11	Stage 13

En -3×HA-Stat
(Positive Ctrl)

HA
DNA

En -Zfh1-PA-
1×Flag-1×HA

Zfh1
DNA

w1118
(Negative Ctrl)

Zfh1
DNA

D

En>
3HA-STAT w1118 En>Zfh1-RA
-Flag-HA

216kD —
132kD —
78kD —

E structure of tagged UAS-Zfh1-RA-1×Flag-1×HA

stop codon
spliced out — 1×Flag-1×HA

Addendum Figure 2. UAS-Zfh1-RA-1×Flag-1×HA does not cause extra stem cells in testes, and cannot be expressed properly *in vivo*. (A) Ectopic CySCs (Zfh1+, green) and GSCs (Vasa+ cells with dotted α-Spectrin staining, white) were accumulated in testis overexpressing an untagged form of Zfh1-RB. (B) Only endogenous CySCs and GSCs near the hub (FascIII, white blot at the testis tip) could be observed in Zfh1-RA overexpression testis. (C) When driven by En-Gal4 in embryos, the tagged UAS-Zfh1-RA exhibited a pattern of stripes only detectable by anti-Zfh1 (red), but not using an antibody against the epitope tag (data not shown). In positive control embryos, the ectopic expression of tagged STAT protein could be visualized by anti-HA (green). (D) Consistent to observations shown by immunofluorescent staining, tagged Zfh1 in embryo lysates could not be detected by Western Blot using anti-HA, whereas the positive control protein (STAT) was visible. (E) A schematic structure of the tagged UAS-Zfh1-RA construct. A fragment between Zfh1-RA and 1×Flag-1×HA was supposed to be spliced out *in vivo* to allow proper expression of the tags.

111
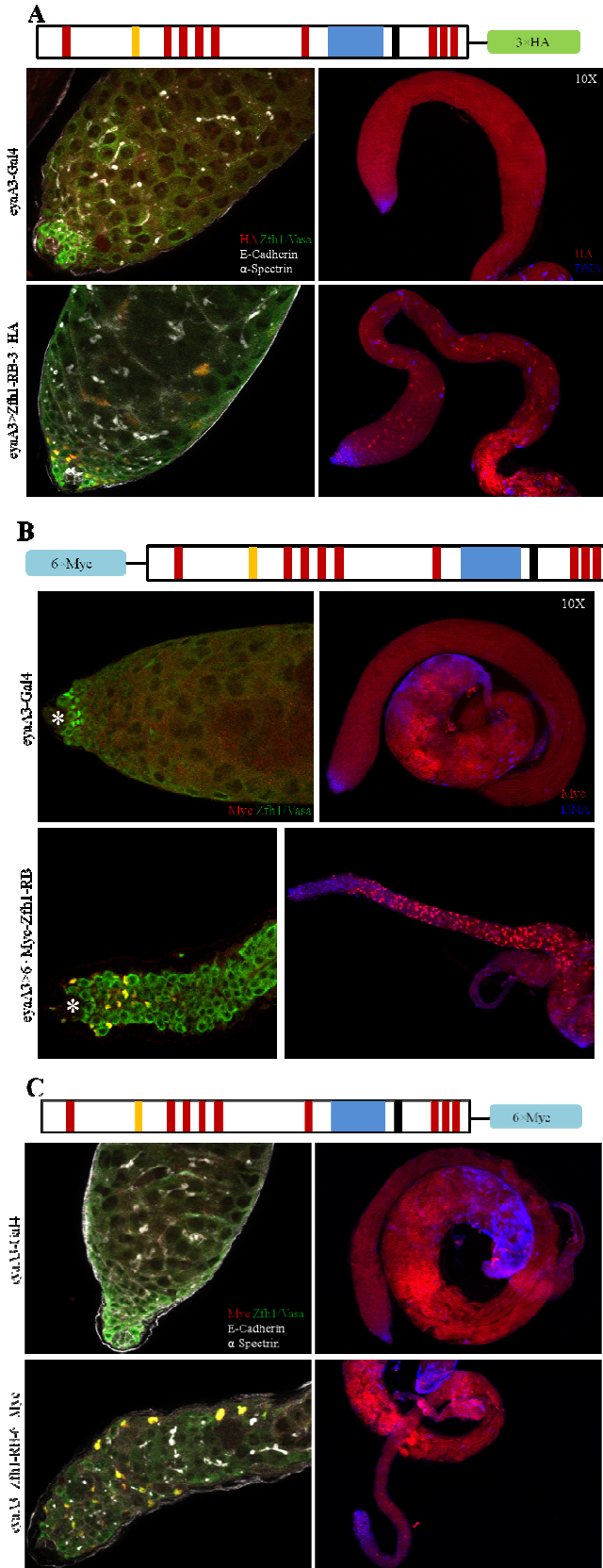
Addendum Figure 3. Epitope-tagged UAS-Zfh1-RB lines cause stem tumor phenotype in various degrees. (A) A C-terminally 3×HA tagged UAS-Zfh1-RB line caused ectopic HA+ cells (red), but did not generate extra GSCs as shown by the presence of branched rather than dotted fusomes (α-Spectrin, white) in germ cells (Vasa, green) (n=34). (B) An N-terminally 6×Myc tagged UAS-Zfh1-RB line had ectopic Myc expression (red) in every testis scored (n=14), but only the testis tip region exhibited a mild GSC tumor phenotype. (C) The mild GSC tumor phenotype was also present in a C-terminally 6×Myc tagged UAS-Zfh1-RB line, with a 36% penetrance (n=22).
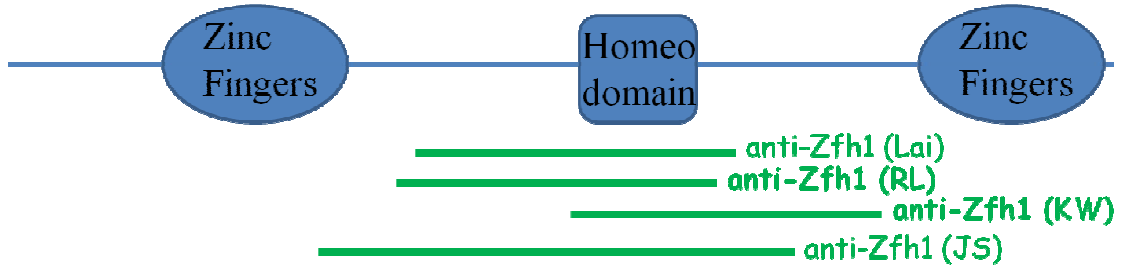
Addendum Figure 4. Various antibodies against Zfh1 generated by different labs. There existed four different antibodies against Zfh1, each mapped to a similar region of the protein crossing the homeodomain. Antibodies generated by the labs of Ruth Lehmann (RL), Kevin White (KW), and James Skeath (JS) could recognize Zfh1 proteins nicely in embryos and testes (we did not test the antibody generated by Lai *et al.*) We tried anti-Zfh1 (RL) and anti-Zfh1 (KW) for ChIP experiment.
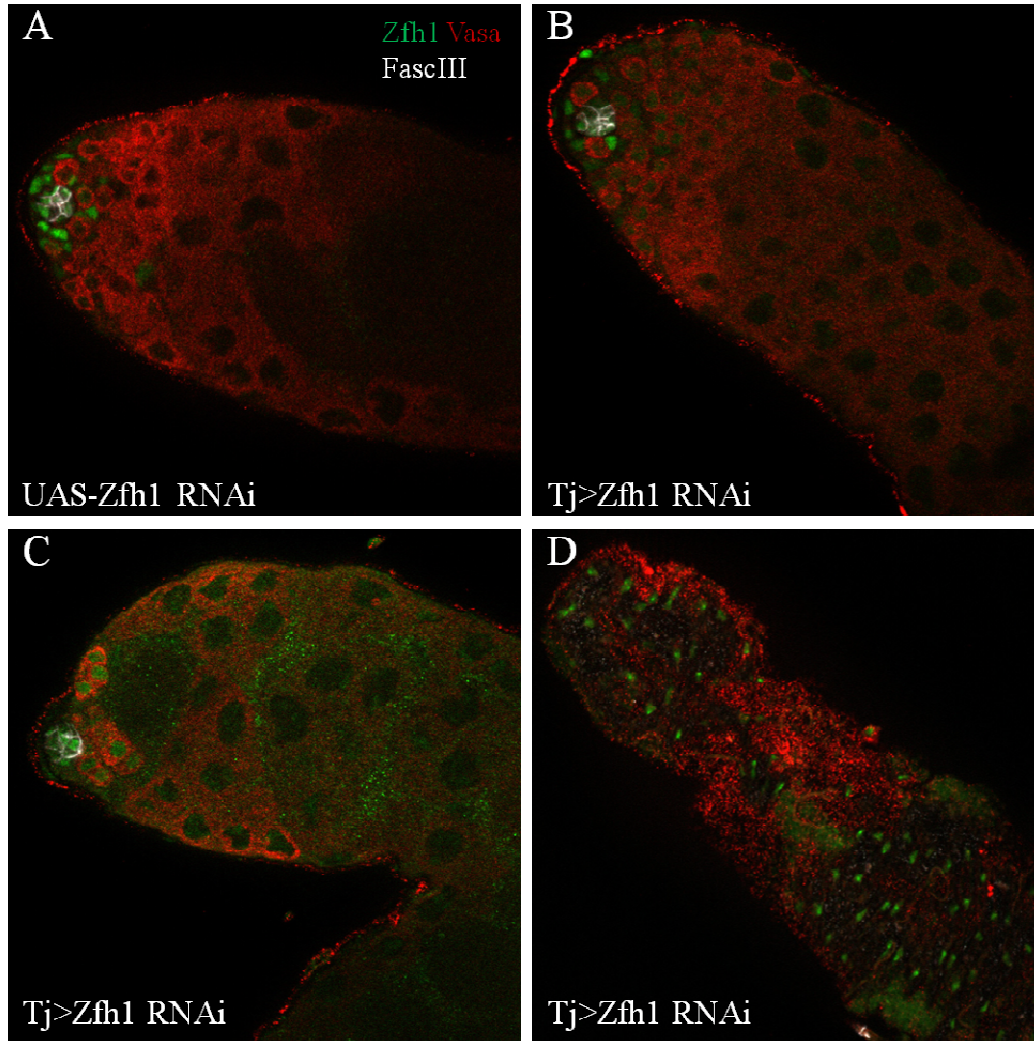
Addendum Figure 5. Zfh1 cannot be knocked down efficiently using RNAi. (A) About 20 Zfh1+ cells (green) were clustered around the hub (FascIII, white) in UAS-Zfh1-RNAi only control testes. 80% of Tj>Zfh1 RNAi testes scored (n=66) exhibited a similar phenotype. (B-D) Remaining 20% Tj>Zfh1 RNAi testes appeared to have various phenotypes. Some had a reduced number of Zfh1+ cells at the tip (B), whereas others did not have Zfh1+ somatic cells at all (C, D). See text for detailed phenotype analysis.

CHAPTER 7

References

References

1. Morrison SJ, Spradling AC. Stem cells and niches: Mechanisms that promote stem cell maintenance throughout life. Cell. 2008 Feb 22;132(4):598-611.

2. Jopling C, Boue S, Izpisua Belmonte JC. Dedifferentiation, transdifferentiation and reprogramming: Three routes to regeneration. Nat Rev Mol Cell Biol. 2011 Feb;12(2):79-89.

3. Bianconi E, Piovesan A, Facchin F, Beraudi A, Casadei R, Frabetti F, et al. An estimation of the number of cells in the human body. Ann Hum Biol. 2013 Nov-Dec;40(6):463-71.

4. Klein AM, Simons BD. Universal patterns of stem cell fate in cycling adult tissues. Development. 2011 Aug;138(15):3103-11.

5. Gomez-Lopez S, Lerner RG, Petritsch C. Asymmetric cell division of stem and progenitor cells during homeostasis and cancer. Cell Mol Life Sci. 2014 Feb;71(4):575-97.

6. Yamashita YM. Cell adhesion in regulation of asymmetric stem cell division. Curr Opin Cell Biol. 2010 Oct;22(5):605-10.

7. Zimdahl B, Ito T, Blevins A, Bajaj J, Konuma T, Weeks J, et al. Lis1 regulates asymmetric division in hematopoietic stem cells and in leukemia. Nat Genet. 2014 Mar;46(3):245-52.

8. Sheng XR, Brawley CM, Matunis EL. Dedifferentiating spermatogonia outcompete somatic stem cells for niche occupancy in the drosophila testis. Cell Stem Cell. 2009 Aug 7;5(2):191-203.

9. Salzmann V, Inaba M, Cheng J, Yamashita YM. Lineage tracing quantification reveals symmetric stem cell division in drosophila male germline stem cells. Cell Mol Bioeng. 2013 Dec;6(4):441-8.

10. Nakagawa T, Sharma M, Nabeshima Y, Braun RE, Yoshida S. Functional hierarchy and reversibility within the murine spermatogenic stem cell compartment. Science. 2010 Apr 2;328(5974):62-7.

11. Doupe DP, Klein AM, Simons BD, Jones PH. The ordered architecture of murine ear epidermis is maintained by progenitor cells with random fate. Dev Cell. 2010 Feb 16;18(2):317-23.

12. Clayton E, Doupe DP, Klein AM, Winton DJ, Simons BD, Jones PH. A single type of progenitor cell maintains normal epidermis. Nature. 2007 Mar 8;446(7132):185-9.

13. Klein AM, Nakagawa T, Ichikawa R, Yoshida S, Simons BD. Mouse germ line stem cells undergo rapid and stochastic turnover. Cell Stem Cell. 2010 Aug 6;7(2):214-24.

14. Snippert HJ, van der Flier LG, Sato T, van Es JH, van den Born M, Kroon-Veenboer C, et al. Intestinal crypt homeostasis results from neutral competition between symmetrically dividing Lgr5 stem cells. Cell. 2010 Oct 1;143(1):134-44.

15. Shenghui H, Nakada D, Morrison SJ. Mechanisms of stem cell self-renewal. Annual Review of Cell and Developmental. 2009;25:377-406.

16. Kai T, Spradling A. Differentiating germ cells can revert into functional stem cells in drosophila melanogaster ovaries. Nature. 2004 Apr 1;428(6982):564-9.

17. van Es JH, Sato T, van de Wetering M, Lyubimova A, Nee AN, Gregorieff A, et al. Dll1+ secretory progenitor cells revert to stem cells upon crypt damage. Nat Cell Biol. 2012 Oct;14(10):1099-104.

18. Tata PR, Mou H, Pardo-Saganta A, Zhao R, Prabhu M, Law BM, et al. Dedifferentiation of committed epithelial cells into stem cells in vivo. Nature. 2013 Nov 14;503(7475):218-23.

19. Kimble J, Seidel H. C. elegans germline stem cells and their niche. In: StemBook. Cambridge (MA): Judith Kimble and Hannah Seidel; 2008.

20. Kimble J, White J. On the control of germ cell development in< i> caenorhabditis elegans. Dev Biol. 1981;81(2):208-19.

21. Nystul T, Spradling A. An epithelial niche in the drosophila ovary undergoes long-range stem cell replacement. Cell Stem Cell. 2007 Sep 13;1(3):277-85.

22. O'Reilly AM, Lee HH, Simon MA. Integrins control the positioning and proliferation of follicle stem cells in the drosophila ovary. J Cell Biol. 2008 Aug 25;182(4):801-15.

23. Ehninger A, Trumpp A. The bone marrow stem cell niche grows up: Mesenchymal stem cells and macrophages move in. J Exp Med. 2011 Mar 14;208(3):421-8.

24. Song X, Zhu CH, Doan C, Xie T. Germline stem cells anchored by adherens junctions in the drosophila ovary niches. Science. 2002 Jun 7;296(5574):1855-7.

25. Jin Z, Kirilly D, Weng C, Kawase E, Song X, Smith S, et al. Differentiation-defective stem cells outcompete normal stem cells for niche occupancy in the< i> drosophila ovary. Cell Stem Cell. 2008;2(1):39-49.

26. Grassinger J, Haylock DN, Storan MJ, Haines GO, Williams B, Whitty GA, et al. Thrombin-cleaved osteopontin regulates hemopoietic stem and progenitor cell functions

through interactions with alpha9beta1 and alpha4beta1 integrins. Blood. 2009 Jul 2;114(1):49-59.

27. Potocnik AJ, Brakebusch C, Fassler R. Fetal and adult hematopoietic stem cells require beta1 integrin function for colonizing fetal liver, spleen, and bone marrow. Immunity. 2000 Jun;12(6):653-63.

28. Schreiber TD, Steinl C, Essl M, Abele H, Geiger K, Muller CA, et al. The integrin alpha9beta1 on hematopoietic stem and progenitor cells: Involvement in cell adhesion, proliferation and differentiation. Haematologica. 2009 Nov;94(11):1493-501.

29. Kanatsu-Shinohara M, Takehashi M, Takashima S, Lee J, Morimoto H, Chuma S, et al. Homing of mouse spermatogonial stem cells to germline niche depends on β1-integrin. Cell stem cell. 2008;3(5):533-42.

30. Hardy RW, Tokuyasu KT, Lindsley DL, Garavito M. The germinal proliferation center in the testis of drosophila melanogaster. J Ultrastruct Res. 1979 Nov;69(2):180-90.

31. Gonczy P, DiNardo S. The germ line regulates somatic cyst cell proliferation and fate during drosophila spermatogenesis. Development. 1996 Aug;122(8):2437-47.

32. Yamashita YM, Jones DL, Fuller MT. Orientation of asymmetric stem cell division by the APC tumor suppressor and centrosome. Science. 2003 Sep 12;301(5639):1547-50.

33. Fuller MT. Genetic control of cell proliferation and differentiation in< i> drosophila spermatogenesis. Seminars in cell & developmental biology; Elsevier; 1998.

34. Cheng J, Tiyaboonchai A, Yamashita YM, Hunt AJ. Asymmetric division of cyst stem cells in drosophila testis is ensured by anaphase spindle repositioning. Development. 2011 Mar;138(5):831-7.

35. Okegbe TC, DiNardo S. The endoderm specifies the mesodermal niche for the germline in drosophila via delta-notch signaling. Development. 2011 Apr;138(7):1259-67.

36. Kitadate Y, Kobayashi S. Notch and egfr signaling act antagonistically to regulate germ-line stem cell niche formation in drosophila male embryonic gonads. Proc Natl Acad Sci U S A. 2010 Aug 10;107(32):14241-6.

37. Papagiannouli F, Lohmann I. Shaping the niche: Lessons from the drosophila testis and other model systems. Biotechnol J. 2012 Jun;7(6):723-36.

38. Bonilla E, Xu EY. Identification and characterization of novel mammalian spermatogenic genes conserved from fly to human. Mol Hum Reprod. 2008 Mar;14(3):137-42.

39. Leatherman J. Stem cells supporting other stem cells. Frontiers in genetics. 2013;4.

118

40. Leatherman JL, Dinardo S. Germline self-renewal requires cyst stem cells and stat regulates niche adhesion in drosophila testes. Nature cell biology Aug;12(8):806-11.

41. Issigonis M, Matunis E. The drosophila BCL6 homolog ken and barbie promotes somatic stem cell self-renewal in the testis niche. Dev Biol. 2012 Aug 15;368(2):181-92.

42. Leatherman JL, Dinardo S. Zfh-1 controls somatic stem cell self-renewal in the drosophila testis and nonautonomously influences germline stem cell self-renewal. Cell stem cell. 2008 Jul 3;3(1):44-54.

43. Flaherty MS, Salis P, Evans CJ, Ekas LA, Marouf A, Zavadil J, et al. Chinmo is a functional effector of the JAK/STAT pathway that regulates eye development, tumor formation, and stem cell self-renewal in drosophila. Dev Cell. 2010 Apr 20;18(4):556-68.

44. Kiger AA, Jones DL, Schulz C, Rogers MB, Fuller MT. Stem cell self-renewal specified by JAK-STAT activation in response to a support cell cue. Science. 2001;294(5551):2542-5.

45. Tulina N, Matunis E. Control of stem cell self-renewal in drosophila spermatogenesis by JAK-STAT signaling. Science. 2001;294(5551):2546-9.

46. Amoyel M, Sanny J, Burel M, Bach EA. Hedgehog is required for CySC self-renewal but does not contribute to the GSC niche in the drosophila testis. Development. 2013 Jan 1;140(1):56-65.

47. Issigonis M, Tulina N, de Cuevas M, Brawley C, Sandler L, Matunis E. JAK-STAT signal inhibition regulates competition in the drosophila testis stem cell niche. Science. 2009 Oct 2;326(5949):153-6.

48. Tarayrah L, Herz HM, Shilatifard A, Chen X. Histone demethylase dUTX antagonizes JAK-STAT signaling to maintain proper gene expression and architecture of the drosophila testis niche. Development. 2013 Mar;140(5):1014-23.

49. Brawley C, Matunis E. Regeneration of male germline stem cells by spermatogonial dedifferentiation in vivo. Science. 2004 May 28;304(5675):1331-4.

50. Kawase E, Wong MD, Ding BC, Xie T. Gbb/bmp signaling is essential for maintaining germline stem cells and for repressing bam transcription in the drosophila testis. Development. 2004 Mar;131(6):1365-75.

51. Schulz C, Kiger AA, Tazuke SI, Yamashita YM, Pantalena-Filho LC, Jones DL, et al. A misexpression screen reveals effects of bag-of-marbles and TGF beta class signaling on the drosophila male germ-line stem cell lineage. Genetics. 2004 Jun;167(2):707-23.

52. Shivdasani AA, Ingham PW. Regulation of stem cell maintenance and transit amplifying cell proliferation by tgf-beta signaling in drosophila spermatogenesis. Curr Biol. 2003 Dec 2;13(23):2065-72.

53. Michel M, Kupinski AP, Raabe I, Bokel C. Hh signalling is essential for somatic stem cell maintenance in the drosophila testis niche. Development. 2012 Aug;139(15):2663-9.

54. Kiger AA, White-Cooper H, Fuller MT. Somatic support cells restrict germline stem cell self-renewal and promote differentiation. Nature. 2000 Oct 12;407(6805):750-4.

55. Sarkar A, Parikh N, Hearn SA, Fuller MT, Tazuke SI, Schulz C. Antagonistic roles of rac and rho in organizing the germ cell microenvironment. Curr Biol. 2007 Jul 17;17(14):1253-8.

56. Tran J, Brenner TJ, DiNardo S. Somatic control over the germline stem cell lineage during drosophila spermatogenesis. Nature. 2000 Oct 12;407(6805):754-7.

57. Parrott BB, Hudson A, Brady R, Schulz C. Control of germline stem cell division frequency--a novel, developmentally regulated role for epidermal growth factor signaling. PLoS One. 2012;7(5):e36460.

58. Schulz C, Wood CG, Jones DL, Tazuke SI, Fuller MT. Signaling from germ cells mediated by the rhomboid homolog stet organizes encapsulation by somatic support cells. Development. 2002 Oct;129(19):4523-34.

59. Li L, Xie T. Stem cell niche: Structure and function. Annu Rev Cell Dev Biol. 2005;21:605-31.

60. Fuller MT, Spradling AC. Male and female drosophila germline stem cells: Two versions of immortality. Science (New York, N Y. 2007 Apr 20;316(5823):402-4.

61. Fabrizio JJ, Boyle M, DiNardo S. A somatic role for eyes absent (eya) and sine oculis (so) in drosophila spermatocyte development. Dev Biol. 2003 Jun 1;258(1):117-28.

62. Matunis E, Tran J, Gonczy P, Caldwell K, DiNardo S. Punt and schnurri regulate a somatically derived signal that restricts proliferation of committed progenitors in the germline. Development. 1997;124(21):4383-91.

63. Michel M, Raabe I, Kupinski AP, Perez-Palencia R, Bokel C. Local BMP receptor activation at adherens junctions in the drosophila germline stem cell niche. Nat Commun. 2011 Aug 2;2:415.

64. Terry NA, Tulina N, Matunis E, DiNardo S. Novel regulators revealed by profiling drosophila testis stem cells within their niche. Dev Biol. 2006 Jun 1;294(1):246-57.

65. Li Y, Tower J. Adult-specific over-expression of the drosophila genes magu and hebe increases life span and modulates late-age female fecundity. Mol Genet Genomics. 2009 Feb;281(2):147-62.

66. Vuilleumier R, Springhorn A, Patterson L, Koidl S, Hammerschmidt M, Affolter M, et al. Control of dpp morphogen signalling by a secreted feedback regulator. Nat Cell Biol. 2010 Jun;12(6):611-7.

67. Thomas JT, Canelos P, Luyten FP, Moos M,Jr. Xenopus SMOC-1 inhibits bone morphogenetic protein signaling downstream of receptor binding and is essential for postgastrulation development in xenopus. J Biol Chem. 2009 Jul 10;284(28):18994-9005.

68. Sheng XR, Posenau T, Gumulak-Smith JJ, Matunis E, Van Doren M, Wawersik M. Jak-STAT regulation of male germline stem cell establishment during drosophila embryogenesis. Dev Biol. 2009 Oct 15;334(2):335-44.

69. Khalsa O, Yoon JW, Torres-Schumann S, Wharton KA. TGF-beta/BMP superfamily members, gbb-60A and dpp, cooperate to provide pattern information and establish cell identity in the drosophila wing. Development. 1998 Jul;125(14):2723-34.

70. Bangi E, Wharton K. Dpp and gbb exhibit different effective ranges in the establishment of the BMP activity gradient critical for drosophila wing patterning. Dev Biol. 2006 Jul 1;295(1):178-93.

71. Ray RP, Wharton KA. Context-dependent relationships between the BMPs gbb and dpp during development of the drosophila wing imaginal disk. Development. 2001 Oct;128(20):3913-25.

72. Cook O, Biehs B, Bier E. Brinker and optomotor-blind act coordinately to initiate development of the L5 wing vein primordium in drosophila. Development. 2004 May;131(9):2113-24.

73. Chen D, McKearin DM. A discrete transcriptional silencer in the bam gene determines asymmetric division of the drosophila germline stem cell. Development. 2003 Mar;130(6):1159-70.

74. Guo Z, Wang Z. The glypican dally is required in the niche for the maintenance of germline stem cells and short-range BMP signaling in the drosophila ovary. Development. 2009 Nov;136(21):3627-35.

75. Hayashi Y, Kobayashi S, Nakato H. Drosophila glypicans regulate the germline stem cell niche. J Cell Biol. 2009 Nov 16;187(4):473-80.

76. Blair SS. Wing vein patterning in drosophila and the analysis of intercellular signaling. Annu Rev Cell Dev Biol. 2007;23:293-319.

77. Ben-Zvi D, Pyrowolakis G, Barkai N, Shilo BZ. Expansion-repression mechanism for scaling the dpp activation gradient in drosophila wing imaginal discs. Curr Biol. 2011 Aug 23;21(16):1391-6.

78. Hamaratoglu F, de Lachapelle AM, Pyrowolakis G, Bergmann S, Affolter M. Dpp signaling activity requires pentagone to scale with tissue size in the growing drosophila wing imaginal disc. PLoS Biol. 2011 Oct;9(10):e1001182.

79. Lin X. Functions of heparan sulfate proteoglycans in cell signaling during development. Development. 2004 Dec;131(24):6009-21.

80. Serpe M, Umulis D, Ralston A, Chen J, Olson DJ, Avanesov A, et al. The BMP-binding protein crossveinless 2 is a short-range, concentration-dependent, biphasic modulator of BMP signaling in drosophila. Dev Cell. 2008 Jun;14(6):940-53.

81. Mihelic M, Turk D. Two decades of thyroglobulin type-1 domain research. Biol Chem. 2007 Nov;388(11):1123-30.

82. Brekken RA, Sage EH. SPARC, a matricellular protein: At the crossroads of cell-matrix communication. Matrix Biol. 2001 Jan;19(8):816-27.

83. Vannahme C, Smyth N, Miosge N, Gosling S, Frie C, Paulsson M, et al. Characterization of SMOC-1, a novel modular calcium-binding protein in basement membranes. J Biol Chem. 2002 Oct 11;277(41):37977-86.

84. Vannahme C, Gosling S, Paulsson M, Maurer P, Hartmann U. Characterization of SMOC-2, a modular extracellular calcium-binding protein. Biochem J. 2003 Aug 1;373(Pt 3):805-14.

85. Wang X, Harris RE, Bayston LJ, Ashe HL. Type IV collagens regulate BMP signalling in drosophila. Nature. 2008 Sep 4;455(7209):72-7.

86. Liu P, Pazin DE, Merson RR, Albrecht KH, Vaziri C. The developmentally-regulated Smoc2 gene is repressed by aryl-hydrocarbon receptor (ahr) signaling. Gene. 2009 Mar 15;433(1-2):72-80.

87. Maier S, Paulsson M, Hartmann U. The widely expressed extracellular matrix protein SMOC-2 promotes keratinocyte attachment and migration. Exp Cell Res. 2008 Aug 1;314(13):2477-87.

88. Sinden D, Badgett M, Fry J, Jones T, Palmen R, Sheng X, et al. Jak-STAT regulation of cyst stem cell development in the drosophila testis. Dev Biol. 2012 Dec 1;372(1):5-16.

89. Chang YJ, Pi H, Hsieh CC, Fuller MT. Smurf-mediated differential proteolysis generates dynamic BMP signaling in germline stem cells during drosophila testis development. Dev Biol. 2013 Nov 1;383(1):106-20.

122

90. Parks AL, Cook KR, Belvin M, Dompe NA, Fawcett R, Huppert K, et al. Systematic generation of high-resolution deletion coverage of the drosophila melanogaster genome. Nat Genet. 2004 Mar;36(3):288-92.

91. Postigo AA, Ward E, Skeath JB, Dean DC. Zfh-1, the drosophila homologue of ZEB, is a transcriptional repressor that regulates somatic myogenesis. Mol Cell Biol. 1999 Oct;19(10):7255-63.

92. Liu M, Su M, Lyons GE, Bodmer R. Functional conservation of zinc-finger homeodomain gene zfh1/SIP1 in drosophila heart development. Dev Genes Evol. 2006 Nov;216(11):683-93.

93. Sellin J, Drechsler M, Nguyen HT, Paululat A. Antagonistic function of lmd and Zfh1 fine tunes cell fate decisions in the twi and tin positive mesoderm of drosophila melanogaster. Dev Biol. 2009 Feb 15;326(2):444-55.

94. Su MT, Fujioka M, Goto T, Bodmer R. The drosophila homeobox genes zfh-1 and even-skipped are required for cardiac-specific differentiation of a numb-dependent lineage decision. Development. 1999 Jun;126(14):3241-51.

95. Lai ZC, Rushton E, Bate M, Rubin GM. Loss of function of the drosophila zfh-1 gene results in abnormal development of mesodermally derived tissues. Proc Natl Acad Sci U S A. 1993 May 1;90(9):4122-6.

96. Broihier HT, Moore LA, Van Doren M, Newman S, Lehmann R. Zfh-1 is required for germ cell migration and gonadal mesoderm development in drosophila. Development. 1998 Feb;125(4):655-66.

97. Ohayon D, Pattyn A, Venteo S, Valmier J, Carroll P, Garces A. Zfh1 promotes survival of a peripheral glia subtype by antagonizing a jun N-terminal kinase-dependent apoptotic pathway. EMBO J. 2009 Oct 21;28(20):3228-43.

98. Layden MJ, Odden JP, Schmid A, Garces A, Thor S, Doe CQ. Zfh1, a somatic motor neuron transcription factor, regulates axon exit from the CNS. Dev Biol. 2006 Mar 15;291(2):253-63.

99. Postigo AA, Dean DC. ZEB represses transcription through interaction with the corepressor CtBP. Proc Natl Acad Sci U S A. 1999 Jun 8;96(12):6683-8.

100. Negre N, Brown CD, Ma L, Bristow CA, Miller SW, Wagner U, et al. A cis-regulatory map of the drosophila genome. Nature. 2011 Mar 24;471(7339):527-31.

101. Bonini NM, Leiserson WM, Benzer S. The< i> eyes absent gene: Genetic control of cell survival and differentiation in the developing drosophila eye. Cell. 1993;72(3):379-95.

102. Le Bras S, Van Doren M. Development of the male germline stem cell niche in drosophila. Dev Biol. 2006 Jun 1;294(1):92-103.

103. Cook RK, Christensen SJ, Deal JA, Coburn RA, Deal ME, Gresens JM, et al. The generation of chromosomal deletions to provide extensive coverage and subdivision of the drosophila melanogaster genome. Genome Biol. 2012;13(3):R21,2012-13-3-r21.

104. Barski A, Zhao K. Genomic location analysis by ChIP-seq. J Cell Biochem. 2009 May 1;107(1):11-8.

105. Ma J. Crossing the line between activation and repression. Trends Genet. 2005 Jan;21(1):54-9.

106. Bhambhani C, Chang JL, Akey DL, Cadigan KM. The oligomeric state of CtBP determines its role as a transcriptional co-activator and co-repressor of wingless targets. EMBO J. 2011 May 18;30(10):2031-43.

107. Rembold M, Ciglar L, Yanez-Cuna JO, Zinzen RP, Girardot C, Jain A, et al. A conserved role for snail as a potentiator of active transcription. Genes Dev. 2014 Jan 15;28(2):167-81.

108. Orian A, Abed M, Kenyagin-Karsenti D, Boico O. DamID: A methylation-based chromatin profiling approach. Methods Mol Biol. 2009;567:155-69.

109. Gan Q, Schones DE, Ho Eun S, Wei G, Cui K, Zhao K, et al. Monovalent and unpoised status of most genes in undifferentiated cell-enriched drosophila testis. Genome Biol. 2010;11(4):R42,2010-11-4-r42. Epub 2010 Apr 15.

110. Lawlor KT, Ly DC, DiNardo S. Drosophila dachsous and fat polarize actin-based protrusions over a restricted domain of the embryonic denticle field. Dev Biol. 2013 Nov 15;383(2):285-94.

111. Franklin-Dumont TM, Chatterjee C, Wasserman SA, Dinardo S. A novel eIF4G homolog, off-schedule, couples translational control to meiosis and differentiation in drosophila spermatocytes. Development. 2007 Aug;134(15):2851-61.

112. Yan D, Lin X. Shaping morphogen gradients by proteoglycans. Cold Spring Harb Perspect Biol. 2009 Sep;1(3):a002493.

113. He XC, Zhang J, Tong WG, Tawfik O, Ross J, Scoville DH, et al. BMP signaling inhibits intestinal stem cell self-renewal through suppression of wnt-beta-catenin signaling. Nat Genet. 2004 Oct;36(10):1117-21.

114. Haramis AP, Begthel H, van den Born M, van Es J, Jonkheer S, Offerhaus GJ, et al. De novo crypt formation and juvenile polyposis on BMP inhibition in mouse intestine. Science. 2004 Mar 12;303(5664):1684-6.

115. Lai ZC, Fortini ME, Rubin GM. The embryonic expression patterns of zfh-1 and zfh-2, two drosophila genes encoding novel zinc-finger homeodomain proteins. Mech Dev. 1991 Jun;34(2-3):123-34.

116. Burk U, Schubert J, Wellner U, Schmalhofer O, Vincan E, Spaderna S, et al. A reciprocal repression between ZEB1 and members of the miR-200 family promotes EMT and invasion in cancer cells. EMBO reports. 2008 Jun;9(6):582-9.

117. Wellner U, Schubert J, Burk UC, Schmalhofer O, Zhu F, Sonntag A, et al. The EMT-activator ZEB1 promotes tumorigenicity by repressing stemness-inhibiting microRNAs. Nature cell biology. 2009 Dec;11(12):1487-95.

118. Kadaja M, Keyes BE, Lin M, Pasolli HA, Genander M, Polak L, et al. SOX9: A stem cell transcriptional regulator of secreted niche signaling factors. Genes Dev. 2014 Feb 15;28(4):328-41.

119. Clark SG, Chiu C. C. elegans ZAG-1, a zn-finger-homeodomain protein, regulates axonal development and neuronal differentiation. Development. 2003 Aug;130(16):3781-94.

120. Fortini ME, Lai ZC, Rubin GM. The drosophila zfh-1 and zfh-2 genes encode novel proteins containing both zinc-finger and homeodomain motifs. Mech Dev. 1991 Jun;34(2-3):113-22.

121. Postigo AA, Ward E, Skeath JB, Dean DC. Zfh-1, the drosophila homologue of ZEB, is a transcriptional repressor that regulates somatic myogenesis. Molecular and cellular biology. 1999 Oct;19(10):7255-63.

122. Vogler G, Urban J. The transcription factor Zfh1 is involved in the regulation of neuropeptide expression and growth of larval neuromuscular junctions in drosophila melanogaster. Dev Biol. 2008 Jul 1;319(1):78-85.

123. Ikeda K, Kawakami K. DNA binding through distinct domains of zinc-finger-homeodomain protein AREB6 has different effects on gene transcription. Eur J Biochem. 1995 Oct 1;233(1):73-82.

124. Remacle JE, Kraft H, Lerchner W, Wuytens G, Collart C, Verschueren K, et al. New mode of DNA binding of multi-zinc finger transcription factors: deltaEF1 family members bind with two hands to two target sites. EMBO J. 1999 Sep 15;18(18):5073-84.

125. Verschueren K, Remacle JE, Collart C, Kraft H, Baker BS, Tylzanowski P, et al. SIP1, a novel zinc finger/homeodomain repressor, interacts with smad proteins and binds to 5'-CACCT sequences in candidate target genes. J Biol Chem. 1999 Jul 16;274(29):20489-98.

126. Postigo AA, Depp JL, Taylor JJ, Kroll KL. Regulation of smad signaling through a differential recruitment of coactivators and corepressors by ZEB proteins. EMBO J. 2003 May 15;22(10):2453-62.

127. Postigo AA. Opposing functions of ZEB proteins in the regulation of the TGFbeta/BMP signaling pathway. EMBO J. 2003 May 15;22(10):2443-52.

128. Oh H, Slattery M, Ma L, Crofts A, White KP, Mann RS, et al. Genome-wide association of yorkie with chromatin and chromatin-remodeling complexes. Cell Rep. 2013 Feb 21;3(2):309-18.

129. Wartlick O, Mumcu P, Kicheva A, Bittig T, Seum C, Julicher F, et al. Dynamics of dpp signaling and proliferation control. Science. 2011 Mar 4;331(6021):1154-9.

130. Nellen D, Burke R, Struhl G, Basler K. Direct and long-range action of a DPP morphogen gradient. Cell. 1996 May 3;85(3):357-68.

131. Brummel TJ, Twombly V, Marques G, Wrana JL, Newfeld SJ, Attisano L, et al. Characterization and relationship of dpp receptors encoded by the saxophone and thick veins genes in drosophila. Cell. 1994 Jul 29;78(2):251-61.

132. Li Z, Zhang Y, Han L, Shi L, Lin X. Trachea-derived dpp controls adult midgut homeostasis in drosophila. Dev Cell. 2013 Jan 28;24(2):133-43.

133. Le T, Liang Z, Patel H, Yu MH, Sivasubramaniam G, Slovitt M, et al. A new family of drosophila balancer chromosomes with a w- dfd-GMR yellow fluorescent protein marker. Genetics. 2006 Dec;174(4):2255-7.